ESTIMATION OF VAPOUR PRESSURE AND SOLAR RADIATION IN SOUTH AFRICA

by

ROBERT DOUGLAS CHAPMAN

Submitted as the dissertation component in partial fulfillment of the requirement for the degree of Master of Science, Hydrology in the School of Bioresources Engineering and Environmental Hydrology, University of KwaZulu-Natal

Pietermaritzburg
2004

PREFACE

The analytical work described in this dissertation was conducted at the School of Bioresources Engineering and Environmental Hydrology, University of KwaZulu-Natal, Pietermaritzburg from February 2002 to March 2004 under the supervision of Professor Roland Edgar Schulze.

These studies represent original work by the author and have not otherwise been submitted in any form for any degree to diploma to any university. Where use has been made of the work of others it is duly acknowledged in the text.

Robert Douglas Chapman

ACKNOWLEDGMENTS

I wish to thank and express my sincere appreciation to the following persons and institutions for their contribution to the work presented in the dissertation:

Prof. R.E. Schulze, Professor of Hydrology, School of Bioresources Engineering and Environmental Hydrology (BEEH), University of KwaZulu-Natal, Pietermaritzburg, for the provision of funding for this project, supervision and logistical support throughout this project;

The National Research Foundation and Water Research Commission for the funding of this project;

Prof. M.J. Savage, Discipline of Agricultural Meteorology, School of Applied Environmental Sciences, University of KwaZulu-Natal, Pietermaritzburg; Steven Lynch, ESRI, Redlands, California, USA (formerly employed at the School of BEEH, University of KwaZulu-Natal); Karl Monnik, Bureau of Meteorology, Canberra DC, Australia (formerly employed by the ARC-ISCW, Pretoria) and Dr. Colin Everson, CSIR, University of KwaZulu-Natal for advice on, and development of some of the theory contained in this dissertation;

Manjulla Maharaj of the School of BEEH, University of KwaZulu-Natal, Pietermaritzburg, for the construction of the vapour pressure, vapour pressure deficit, relative humidity and solar radiation maps;

Mark Horan, Valerie Taylor, Cynthia O' Mahoney, Suzanne Kunz and Shaun Thornton-Dibb, all of the School of BEEH, University of KwaZulu-Natal, for their technical assistance.

ABSTRACT

Vapour pressure (interchangeably referred to as atmospheric humidity) and solar radiation data are, for different reasons, difficult data to obtain in South Africa. Relative humidity measuring instruments (from which vapour pressure values can be obtained) require constant maintenance, while solar radiation can only be measured electronically. Data from both of these variables are, however, required as inputs to the Penman-Monteith equation, which has become the internationally accepted reference for the estimation of potential evaporation. It is necessary, therefore, to produce estimates of vapour pressure and solar radiation over South Africa from more common surrogates, e.g. rainfall and temperature data.

Several methods of estimating vapour pressure and solar radiation from the literature are reviewed in this dissertation. Considerably greater attention is focused on models of vapour pressure than solar radiation, as less literature exists on this subject. In general, the methods involved in estimating vapour pressure tend to be relatively rudimentary. The FAO 56 documentation advises using saturated vapour pressure at minimum air temperature as an estimate of vapour pressure, yet the implicit assumptions of using this approach can fail in many circumstances, particularly in the more arid regions.

It was found that *monthly* vapour pressure at any given location in South Africa could be estimated from geographical (invariate) data alone. It was also found that the most influential factor affecting *daily* vapour pressure at a given location within a given time frame (less than one month) was "air masses". Air masses proved too complicated to model from surrogate data of temperature and rainfall, however, and were thus omitted from the final model. Daily values of vapour pressure and vapour pressure deficit were estimated by holding vapour pressure for a given month constant, but varying temperature on a daily basis.

It was found that this method produced acceptable results for both elements throughout South Africa.

The need for estimating solar radiation has existed for considerably longer than for vapour pressure. Professions other than agriculture, principally architecture and civil engineering, have long required solar radiation data/values. For this reason the art of estimating solar radiation values is better established and more models were available in the literature.

Several suitable and recently developed solar radiation models, which use surrogate data (temperature and rainfall), were identified from the literature survey. These models were then applied *in situ* and the results were compared with observed values. It was found that the majority of models produced similar output to one another. However, the Liu and Scott (2001) model, which is an enhancement of the Bristow and Campbell (1984) model, was found to be the best available model of those tested, particularly in the more humid locations of South Africa. Verification analyses revealed that the Liu and Scott (2001) model could be used to interpolate solar radiation where a sparse network of solar radiation measuring stations exists, e.g. in the arid locations of South Africa. The structure of the Liu and Scott (2001) model, however, prevented it from being employed in a subsequent exercise on mapping solar radiation over South Africa. For this purpose, the Hunt *et al.* (1998) model was employed.

The estimation of two elements, vapour pressure and solar radiation, was improved upon, and the Penman-Monteith equation can thus now be more confidently applied throughout South Africa. Of these two elements, it is vapour pressure, which, because of a paucity of research to date on the subject, lends itself to expansive research in the future.

TABLE OF CONTENTS **Page**

LIST OF TABLES **Page**

Chapter 1

INTRODUCTION

Solar radiation and vapour pressure are essential environmental driving variables for many land surface processes including potential evaporation, maximum potential soil water evaporation, and transpiration and actual evaporation. These processes are rarely referred to in subsequent chapters, yet their estimation forms the context of this dissertation. The elements of solar radiation and vapour pressure are fundamental to the understanding and estimation of these processes. Despite this, throughout the world, systematic measurements of solar radiation and vapour pressure are relatively scarce compared to measurements of temperature and precipitation (Running *et al.* 1987).

Vapour pressure is an important parameter in ecological and hydrological research as it strongly influences the transfer of moisture between the surface and atmosphere and hence the water balance at local to regional scales (Kimball *et al.*, 1997). Relative humidity, hereafter RH, is required as a variable for predictions of, for example, pathogen outbreaks, potential evaporation, vapour pressure deficit, hereafter VPD, and the emissivity of the atmosphere. Meteorologists generally agree that atmospheric moisture is the most difficult of the common weather elements to measure consistently and accurately over time. Moreover, Sadler and Evans (1989) state that the varied manner in which vapour pressure deficit is measured and reported leads to errors in calculating the potential evaporation. Sadler and Evans (1989) further state that modern technology compounds the problem by averaging the humidity related data, which are used to estimate vapour pressure over a given time span. Once the data are stored in an averaged form, they are not easily convertible to any other form. These problems underscore the need for efficient, indirect methods of estimating vapour pressure over large regions in support of regional to global scale ecological modelling efforts (Kimball *et al.*, 1997).

In this dissertation, the term "actual vapour pressure" comes to the fore as the pre-eminent atmospheric moisture status term on which the subsequent literature survey and research is to be focussed. Actual vapour pressure is established as the one term that can be easily interchanged with other terms and methods of describing atmospheric moisture status. Owing to a dearth of literature available on this subject, efforts in this dissertation are to be focused on factors affecting daily vapour pressure. Thereafter, alternative methods of estimating daily vapour pressure and vapour pressure dependent variables, (RH and vapour pressure deficit) are to be sought.

Solar radiation data can only be accurately measured by electronic means. Compared to temperature and rainfall records, solar radiation records in South Africa tend to be scarce. Spatially accurate solar radiation estimates are difficult to produce (Bristow and Campbell, 1984; Boisvert *et al.*, 1990; Thornton and Running, 1998; Liu and Scott, 2001). Running *et al.* (1987), working during the mid-1980s in the US state of Montana, noted that accurate, long term records that include solar radiation data were available, at that time, only from major airports. Until recently, in South Africa, many of the detailed solar radiation data which existed, usually did so as a result of experimental work by individual researchers. Little spatial coverage of long term data therefore existed. Moreover, researchers' records would typically run for approximately 18 months.

Owing to the fact that a considerably greater volume of literature on solar radiation estimation exists than on vapour pressure, less research on factors that influence daily solar radiation over South Africa is required. The literature survey (Chapter 3) also briefly focuses on the rapidly growing method of establishing solar radiation at ground level by employing satellite derived solar radiation information. This methodology, however is not pursued in subsequent sections. Simulation models, (which form the focus of this dissertation) are considered to be more relevant to local conditions and are less resource demanding than satellite derived information. Several solar radiation models are selected and are analysed using local daily temperature and rainfall data

(Chapter 8) whereafter further analyses are performed to determine the ability to interpolate values from the models at locations with similar climates (Chapter 8).

Thornton and Running (1998) state that the accuracy of solar radiation models can be improved if humidity data are also used in models. They further state that for greatest utility, estimations of solar radiation and humidity should be made simultaneously. An understanding of the RH regime (a derivative of the vapour pressure regime) is essential when estimating solar radiation, for water vapour not only attenuates incident solar radiation, but is also an indicator of cloud cover, the single most important influence on solar radiation. It is for these reasons, that the section on vapour pressure precedes that of solar radiation both in the literature review (Chapters 1 to 3) and the analyses parts of this dissertation (Chapters 5 to 8). An attempt is therefore also made to upgrade the current solar radiation models by including a vapour pressure term in it.

A "roadmap" (page 5) has been prepared for readers of this dissertation, which contains not only the problem statement and the broad objectives, but also the specific objectives of this study, in each case with chapter references. The introductory chapter, therefore, is followed in Chapter 2, by definitions relating to, and factors affecting, both vapour pressure and solar radiation. A review of literature on models of estimating vapour pressure and solar radiation is provided in Chapter 3. Chapter 4 details the methods employed in Chapters 5 to 9. Chapter 5 provides more detail into those factors affecting daily vapour pressure that were described in Chapter 2. An equivalent investigation for solar radiation is considered unnecessary, since the need for, and the science of estimating daily solar radiation, is considerably older than it is for vapour pressure. The methods thereof, are better established. Chapters 6 and 8 describe the estimation of vapour pressure and solar radiation respectively. Both chapters contain verification sections on the newly identified methods. Chapters 7 and 9 are primarily to display maps of vapour pressure and solar radiation respectively. Finally in Chapter 10 conclusions and recommendations are presented for further research on the estimation of vapour pressure and solar radiation.

For clarity and ease of understanding, the "roadmap" is repeated at the beginning of each major section of this dissertation, *viz.* definitions and factors (Chapter 2), methods and methodologies (Chapter 4), vapour pressure estimation (Chapter 5) and solar radiation estimation (Chapter 8).

Problem Statement: In order to estimate daily reference potential evaporation using the Penman-Monteith equation, values of daily vapour pressure and solar radiation are required

Objectives: To review current literature on current models for the estimation of daily vapour pressure and solar radiation, thereafter to employ and improve upon current method and models of estimating vapour pressure and solar radiation

Problem Statement

Broad Objectives	Literature Survey	Methods and Methodologies	Vapour Pressure Estimation	Solar Radiation Estimation	Conclusions and Recommendations
Specific Objectives	i) Introduction (Chapter 1) ii) Definitions relating to and factors affecting, vapour pressure and solar radiation (Chapter 2) iii) Review of literature on current methods of estimating daily vapour pressure (Chapter 3) iv) Review of literature on current methods of estimating daily solar radiation (Chapter 3)	i) Methods and methodologies employed in Chapters 5 to 9 (Chapter 4)	i) Characterisation of the vapour pressure regime in South Africa (Chapter 5) ii) Development of new models and methodologies of estimating vapour pressure (Chapter 6) iii) Verification of new methods of estimating vapour pressure (Chapter 6) iv) Mapping of vapour pressure, relative humidity and vapour pressure deficit over South Africa (Chapter 7)	i) Factors affecting solar radiation at ground level (Chapter 8) ii) Development of new models and methodologies of estimating solar radiation (Chapter 8) iv) Verification of new methods of estimating solar radiation (Chapter 8) iv) Mapping of solar radiation over South Africa (Chapter 9)	i) Conclusions and recommendations for future research (Chapter 10)

Chapter 2

DEFINITIONS OF AND FACTORS RELATING TO VAPOUR PRESSURE AND SOLAR RADIATION

What follows are definitions of terms associated with vapour pressure and solar radiation. These definitions are provided since confusion often arises from the use of similar terms in the literature, which may however, have different scientific connotations. The context of the observation usually defines which term is to be used. For convenience, the terms are listed alphabetically. As the definitions have been gleaned from standard textbooks, no specific references are given. Following on the sections on definitions, factors affecting vapour pressure and solar radiation are discussed.

2.1 Definitions Relating to Vapour Pressure

Absolute humidity (usually expressed in g/m^3) is the mass of water vapour in a given volume of air, i.e. it is the density of water vapor in a given parcel of air.

Actual vapour pressure Since water in the gaseous state (i.e. water vapour) exerts a pressure (kPa), it can be defined as the partial pressure exerted by the water vapour present in a parcel of air.

Condensation is the phase change of a gas to a liquid. In the atmosphere it is the change of water vapour to liquid water.

Dew point temperature (°C) is the temperature to which air has to be cooled in order for saturation to occur. The dew point temperature assumes that there is no change in air pressure or absolute humidity.

Relative humidity (%) is the amount of water vapour in the air divided by the maximum amount of water vapour the air is capable of holding, i.e. it is the ratio of actual to saturated vapour pressure.

Saturation of air is the condition under which the amount of water vapour in the air is the maximum possible at an existing temperature and pressure. Condensation, or sublimation, will begin if the temperature falls or water vapour is added to the air.

Saturated vapour pressure (kPa) is the maximum partial pressure that water vapour molecules would exert if the air were saturated with vapour at a given temperature. Saturation vapor pressure is related exponentially to temperature.

Specific humidity (g/kg) is the mass of water vapour in a parcel of air, divided by the total mass of the air in the parcel, including the water vapour.

Vapour pressure deficit (kPa) is the difference between the actual vapour pressure and the saturated vapour pressure in a given parcel of air.

Water vapour mixing ratio is the mass of water vapour in a given parcel of air, divided by the mass of the dry air in the parcel (not including the water vapour).

Wet bulb temperature (^{0}C) is the lowest temperature that can be obtained by evaporating water into the air at constant pressure. The name derives from the technique of placing a wet cloth over the bulb of a mercury thermometer and then blowing air over the cloth until the water evaporates. Since any evaporating surface absorbs heat from the environment, the thermometer will cool to a lower temperature than a thermometer with a dry bulb at the same time and place. Wet bulb temperatures can be used along with the dry bulb temperature to calculate dew point temperature or relative humidity.

2.2 Definitions Relating to Solar Radiation

Aerosols, excluding water vapour and clouds, consist of any microscopic particles that tend to stay in the air, such as smoke, dust, salt and pollen particles. Aerosols range in diameter from 10^{-3} µm to 20 µm (NASA, 2002).

Albedo (dimensionless) is the fraction of light that is reflected by a body or surface in a certain band of wavelength.

Atmospheric clearness index (dimensionless) is the ratio of solar radiation at ground level to exterrestrial solar radiation.

Atmospheric transmissivity (dimensionless) is the ratio of the directly transmitted light, after passing through one unit of a participating medium (consisting of the atmosphere, dust or fog), to the amount of light that would have passed the same distance through a vacuum.

Atmospheric turbidity (dimensionless) is the haziness in the atmosphere due to aerosols such as dust. If turbidity is zero, the atmosphere contains no dust.

Direct solar irradiance (W/m^2/day or MJ/m^2/day) is the measure of the rate of solar energy arriving at the earth's surface from the sun's direct beam, on a plane perpendicular to the beam.

Extraterrestrial solar radiation, Q_{ext} (W/m^2/day or MJ/m^2/day) is the radiation at the top of the atmosphere. It is estimated from the equation:

$$Q_{ext} = 14.9158(h.\sin\phi.\sin\delta + \cos\phi.\cos\delta.\sinh/r^2$$

where
- Q_{ext} = extraterrestrial solar radiation (MJ/m^2/day)
- r = the sun's radius vector
- δ = $0.409\cos[0.017(173-D)]$
- h = $\arccos(-\tan\phi.\tan\delta)$
- ϕ = latitude (radians)

Global solar irradiance (W/m^2) is the measure of the rate of total incoming solar energy (both direct and diffuse) on a horizontal plane at the Earth's surface.

Insolation (MJ/m^2/day) is the solar radiation that is received at the earth's surface per unit area. It is related to the solar constant, duration of daylight, the altitude of the sun, and the latitude of the receiving surface.

Irradiance (W/m^2) is the amount of radiant flux upon a given surface.

Solar constant is the rate per unit area at which solar radiation reaches the outer margin of the earth's atmosphere and has the value of approximately 1360 W/m^2.

Solar hour angle of a celestial body is the angular distance, expressed in hours, minutes, and seconds (one hour equals 15 degrees).

2.3 Factors Affecting Vapour Pressure

In Section 2.1, several terms are defined that are used to describe atmospheric moisture status, e.g. actual vapour pressure, relative humidity, mixing ratio etc. In this section and in all subsequent sections the term "vapour pressure" is used as the descriptor of atmospheric moisture status. The reason for this is that this term can be used interchangeably with the others.

Three mesoclimatic and macroclimatic factors described in Section 2.1, *viz.* continentality, seasonality and topography, singularly influence the vapour pressure regime at any given point on the earth's surface. Other interlinked factors, e.g. rainfall regimes (summer as opposed to winter), air masses and latitude, influence not only each other, but are themselves also influenced by the factors described below.

Continentality refers to the extent to which any place on the earth's surface is influenced by a land mass and the proximity to the sea. A high annual temperature range, hence a high annual vapour pressure range, characterises a continental climate. Since the influence of continentality increases with latitude, some climatologists measure continentality by dividing the temperature range by the sine of the latitude (NASA, 2002).

Seasonality refers to the annual variation of a given variable with time of the year. All weather variables are affected by seasonality. A clearly understood example of seasonality is the variation of monthly rainfall throughout the year, e.g. high in summer and low in winter in a summer rainfall climate. Average daily and monthly vapour

pressures are, therefore likely to be affected by seasonality, generally being higher in summer (higher temperatures) and lower in winter (lower temperatures).

Topography influences vapour pressure by being one of the principal mechanisms of removing moisture from the atmosphere. If a given parcel of air moving horizontally is suddenly forced to rise as a consequence of encountering a topographical feature (e.g. mountain range) the pressure of that parcel of air, and therefore its temperature, will decline, often causing the air mass to attain saturation (precipitation). When the same parcel of air returns to a similar altitude, its vapour pressure is considerably lower as a result of the preceding precipitation process. Conversely, if a given parcel of air moving horizontally decends in altitude, vapour pressure increases with increasing atmospheric pressure. Adiabatic heating therefore results.

2.4 Factors Affecting Solar Radiation

The following section is devoted primarily to those characteristics of the atmosphere that determine incident solar radiation at any given site. The celestial variables, i.e. solar altitude, solar declination, extraterrestrial solar radiation and hour angle have been excluded because they relate to seasonality of solar radiation and precise values are obtainable from formulae and tables.

Aerosols: The greater the concentration of aerosols in the atmosphere, the greater the degree of reflection of the incoming solar radiation. Aerosols also form condensation nuclei for water droplets and, therefore, have a direct influence on cloud formation, which is the single most important attenuating factor of solar radiation.

Altitude: The higher one ascends into the atmosphere, the shorter the length of the solar beam, hence the fewer aerosols in the path of the radiant beam. This means that with higher altitudes, solar radiation undergoes less attenuation. The well-known association between altitude and sunburn index is a result of a shortened radiant beam length.

Cloud cover: This factor is the single biggest attenuator of solar radiation. The extent of cloud cover and cloud morphology also influence solar radiation. For example, cirrus clouds are often translucent, whereas stratoform clouds tend to reflect radiation back into space more uniformly than for example, cumulus clouds. The latter are not only less even in shape, but especially in the later stages of development, they transmit considerably less radiation through to ground level as a result of their greater vertical extent.

Radiant beam length is the length of path through the atmosphere taken by incident radiation. The greater the path length, the more attenuation the beam experiences.

Seasonality is a function of latitude (distance from the equator) and solar declination. The maximum possible declination occurs in mid-winter. At that time of the year, path length which the incident beam has to pass through the atmosphere before reaching ground level is at its longest. Maximum atmospheric extinction therefore occurs at this time of the year.

Turbidity is a measure of the relative extinction of direct sunlight (solar radiation) due to aerosol scattering as the radiation passes through the atmosphere. Turbidity measurements allow researchers to determine information such as ozone, water and aerosol compositions in the atmosphere (National Renewable Energy Laboratory, 2002).

In this chapter, certain definitions of, and factors affecting vapour pressure and solar radiation have been given by way of background. In Chapter 3, which follows, a review is given of currently used methods and models of estimating daily vapour pressure and solar radiation.

CHAPTER 3

LITERATURE REVIEW ON MODELS OF VAPOUR PRESSURE AND SOLAR RADIATION ESTIMATION

In Chapter 2, several factors which affect daily vapour pressure and solar radiation were described. Not all factors described in Chapter 2 are employed in Chapter 3. The reader needs, however, to be aware of them. In this chapter, models of vapour pressure and solar radiation are reviewed.

3.1 Vapour Pressure Models

Many descriptions of the water vapour content of air (*cf.* Section 2.1) are expressed by the broad term of humidity. The principal methods of estimating humidity are the use of dew point temperature as well as actual and saturated vapour pressure values. Relative humidity, for example, is defined as

$$RH = e_d/e_s$$

where e_d = actual vapour pressure (kPa) and

e_s = saturated vapour pressure (kPa).

Bristow and Campbell (1984) and Running *et al.* (1987) both used the above relationship to estimate vapour pressure for evaporation studies (*cf.* Figure 3.1). It was, however, Bristow (1992) who formally stated the relationship:

$$T_d \equiv T_{mn}$$

where T_d = dew point temperature and (°C)

T_{mn} = minimum temperature (°C)

T_{mx} = maximum temperature (°C)

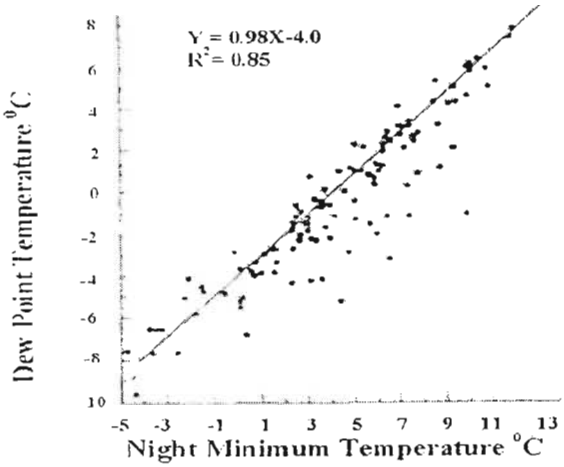

Figure 3.1 The relationship between dew point temperature and minimum temperature for Lubrecht Experimental Research Station, 1983 (Running *et al.*, 1987).

The above relationship depends on two assumptions, *viz.* that minimum temperature is always going to reach dew point temperature and secondly, that for a given day there is little diurnal variation in vapour pressure. Bristow (1992) conceded that, while this method was accurate in the humid tropical and sub-tropical regions, if one moved to semi-arid and arid regions, minimum temperatures often failed to reach dew point. Secondly, Bristow (1992) and Kimball *et al.* (1997) noted a significant variation in daytime vapour pressures in the arid regions. Kimball *et al.* (1997) devised another strategy of including a ratio "***EF***", of daily potential evapotranspiration, $I_{Ep,day}$, to annual precipitation, $I_{p,\ ann}$. This ratio was used as a daily index of evaporative demand at each station location. The empirical model in its final form appears as:

$$T_{d,est} = T_{mn}\,[-0.127+1.121(1.003-1.444EF+12.312EF^2 - 32.766EF^3) + 0.0006(T_{mx}-T_{mn})]$$

where $T_{d,est}$ = estimated dew point temperature

T_{mn} = minimum temperature (°C)

T_{mx} = maximum temperature and (°C)

EF = the ratio of daily potential evapotranspiration, $I_{Ep,day}$, to annual precipitation, $I_{p,\,ann}$

Kimball *et al.* (1997) claimed that this new method of estimating T_d reduced the error of estimating vapour pressure by up to 80%.

3.2 Solar Radiation Models

Scientists have been developing models for the estimation of solar radiation for many decades. The context of the research has, however, changed. Initially mainly meteorologists, architects and engineers required solar radiation information. With the exponential population growth of the previous century, greater demands are now being placed of food and water resources. This implies that a wider spectrum of environmental researchers such as hydrologists, biologists, animal scientists and, in particular, crop scientists share a common interest in their need to estimate solar radiation. However, the context within which they use solar radiation information is vital to understanding which model should be used. A model developed for crop yield simulation cannot necessarily be used for data patching. Conversely, and assuming one has access to reliable temperature and rainfall data, a data patching equation for solar radiation could be used for crop yield modelling.

A list of selected solar radiation models is given in Table 3.1. Certain models have been excluded on the basis of variables employed, notably one by Cengiz *et al.* (1981), who employed RH as a variable in their equation. The employment of RH as a variable to account for cloud cover an indicator of cloud cover is an obvious choice in any regression model on solar radiation models. Cengiz *et al.* (1981) claimed that the R^2 of their model was increased from 0.76 to 0.85 by the inclusion of RH. In spite of this, there are problems associated with RH measurements, as discussed in the introduction. It was for these reasons that Clemence (1992) and Hunt *et al.* (1998), who were aware of the Cengiz *et al.* (1981) equation, declined to use it. Instead of RH, those authors rather used daily temperature range as a surrogate variable to account for cloud cover.

Table 3.1. A selection of solar radiation models

Author and Year	Objective	Equation
Bristow and Campbell (1983)	Not stated	$Q_t=aQ_{ext}(1-exp(-b(D)^c)$
Richardson (1985), quoted by Liu and Scott (2001)	Crop yield modelling	$Q_t=aQ_{ext}(T_{mx}-T_{mn})^{0.5}$
Hargreaves *et al.* (1985), quoted by Hunt *et al.* (1998)	Crop yield modelling	$Q_t=aQ_{ext}(T_{mx}-T_{mn})^{0.5}+b$
Ratkowsky (1990), quoted by Hunt *et al.* (1998)	Crop yield modelling	$Q_t=aQ_{ext}(1-exp(-b(T_{mx}-T_{mn})^{0.5}-c(T_{mx}-T_{mn})-d(T_{mx}-T_{mn})^2))$
McCaskill (1990a)	Data infilling; risk analysis	$Q_t=aQ_{ext}+bR_{t-1}+cR_t+dR_{t+1}$
McCaskill (1990b)	Crop yield modeling	$Q_t=a+\sum_{J=1}^{n}[b\cos(\theta)+c\sin(\theta)]+\sum_{k=\lambda}^{m}df(R_{n+k})$ *(Note, owing to the complexity of this model, symbols and their units are described separately, cf. following page).*
Clemence (1992)	Crop yield modeling; Data infilling	$Q_t=0.04184(1.233Q_{ext}(T_{mx}-T_{mn}))+10.593T_{mx}-0.713T_{mx}(T_{mx}-T_{mn})+16.548$
De Jong and Stewart (1993)	Crop yield modeling	$Q_t=aQ_{ext}D^b(1+cP+P^2)$
*Donatelli and Campbell (1998)	Not stated	$Q_t=Q_{ext}Q_{t,mx}(1-exp(-a\ X\ D^2Y))$ *(Note, owing to the complexity of this model, symbols and their units are described separately, cf. following page).*
Hunt *et al.* (1998)	Crop yield modelling	$Q_t=aQ_{ext}(T_{mx}-T_{mn})^{0.5}+bT_{mx}+cP+dP^2+e$
*Thornton *et al.* (2000)	Environ-mental research	$Q_t=Q_{ext}Q_{t,mx}Q_{f,mx}$ *(Note, owing to the complexity of this model, symbols and their units are described separately, cf. following page).*
Liu and Scott (2001)	Crop yield modelling	$Q_t=aQ_{ext}(1-exp(-bD)^c)(1+dR_{t-1}+eR_t+fR_{t+1})+g$
Liu and Scott (2001)	Crop yield modelling	$Q_t=aQ_{ext}(1-exp(-bD)^c))+dR_{t-1}+eR_t+fR_{t+1}+g$
*Winslow *et al.* (2001)	Environ-mental research	$Q_t=T_{cf}G[1-0.877(e_s(T_{mn})/e_s(T_{mx}))]$ *(Note, owing to the complexity of this model, symbols and their units are described separately, cf. following page).* P.T.O.

Table 3.1 continued

where

Q_t = solar radiation estimated on a given day (MJ/m^2/day)

Q_{ext} = extraterrestrial solar radiation (MJ/m^2/day)

$Q_{t,mx}$ = maximum (cloud free) daily total transmittance at a location with a given elevation (fraction)

a to *h* = regression coefficients

T_{mx} = maximum temperature (°C)

T_{mn} = minimum temperature (°C)

$_{t, t-1, t+1}$ = measurements of subject element on previous, current and following day

R = transformed rainfall data (1 for a rainday and 0 for a non-rainday).

D = T_{mx}- $(T_{mn(t)}+T_{mn(t+1)})/2$ (°C)

P = total precipitation on a given day (mm).

For MacCaskill 1990b

θ = day number converted to a radian form (radians)

a to λ = determined by the regression analysis

f = a function of rainfall

R_{n+k} = rainfall on day $_{(n+k)}$

For the Donatelli and Campbell (1998) model

$X = 0.017exp(exp(-0.053D))$

$Y = exp(T_{mn}/b).$

For the Thornton *et al.* (2000) model

$$Q_{t,mx} = [\sum_{s=sr}^{ss} Q_{ext} \vartheta^{(Pz/Po)m2} / \sum_{s=s}^{ss} Q_{ext}] + (\varsigma e_d)$$

P.T.O

ϑ = the instantaneous transmittance at sea level, at nadir, for a dry atmosphere (unitless)

Po = surface air pressure at sea level. (Pa)

Pz = surface air pressure at elevation z. (Pa)

m = the optical air mass at solar zenith angle 2 (Pa)

S = solar time

sr = sunrise time

ss = sunset time

ς = a parameter describing the effect of vapour pressure on $Q_{t,mx}$ (Pa^{-1})

e_d = actual vapour pressure (kPa)

$Q_{f,mx}$ = the proportion of $Q_{t,mx}$ realised on a given day

$= 1.0 - 0.9exp(-B(T_{mx}-T_{mn}))$

where

$B = j+k(exp(-I.\Sigma(T_{mx}-T_{mn})/n))$

I = a parameter describing the effect of diurnal temperature range $T_{mx}-T_{mn}$ on daily total transmittance.

j to I = empirical parameters controlling the shape of the relationship between $\Sigma(T_{mx}-T_{mn})/n$ and B

n = number of observations of $(T_{mx}-T_{mn})$.

For the Winslow *et al.* (2001) model

$e_s(T_{mn})$ = saturated vapour pressure at minimum temperature (kPa)

$e_s(T_{mx})$ = saturated vapour pressure at maximum temperature (kPa)

T_{cf} = cloud free atmospheric transmissivity (≠ clear sky index)

= 0.67338 on a rainday, 0.774 on a non-rainday

G = $[1-(H-\pi/4^2)/2H^2]^{-1}$ (fraction)

H = half day length (hours)

Stochastic models were also excluded from Table 3.1. Stochastically generated values may be useful in explaining possible scenarios. Their values cannot be used for model verification and simulation analyses, however, as they do not match actual weather

conditions in an historical time sequence (Liu and Scott, 2001). Owing to the plethora of solar radiation models in the literature, only those models developed since 1980 have been included in Table 3.1.

3.3 Satellite Derived Solar Radiation Information

With the march of technology, the use of satellite data to estimate conditions on the earth's surface is becoming increasingly available to researchers. Nevertheless, at the time of writing, satellite data was still considered too expensive to be employed for the purposes of this dissertation. Section 3.3, which is not a comprehensive listing of available techniques, is nonetheless included to allow the reader to become aware of increasing availability of satellite derived data.

No standard methodology exists for the deriving of solar radiation information from satellite images. However, the methodologies described in this section are all variations of the same techniques, *viz.* those of Van Buskirk (2002) and the Australian Bureau of Meteorology (2002). Cloud and ground albedos first have to be estimated. These values are then subtracted from the irradiance at the top of the atmosphere. As with the irradiance models described in Section 3.2, the objectives of the researcher have to be taken into account.

Van Buskirk (2002) obtains a minimum image (clear sky index) from the Meteosat 7 satellite and uses it to determine surface albedos (*cf.* Figure 3.2). In this example, this is a single image of Eritrea, in a given month, on a cloud free day. Each pixel in Figure 3.2 represents an area of 6.25 km^2. The average image (a composite image) is taken to indicate change in surface albedo due to changing atmospheric turbidity and cloud cover (*cf.* Figure 3.2, middle). This composite image is the average of images taken over a given month. The cloud index is a measure of the cloud cover, hence cloud albedo (*cf.* Figure 3.2, right). This is also a composite image averaged for a whole month.

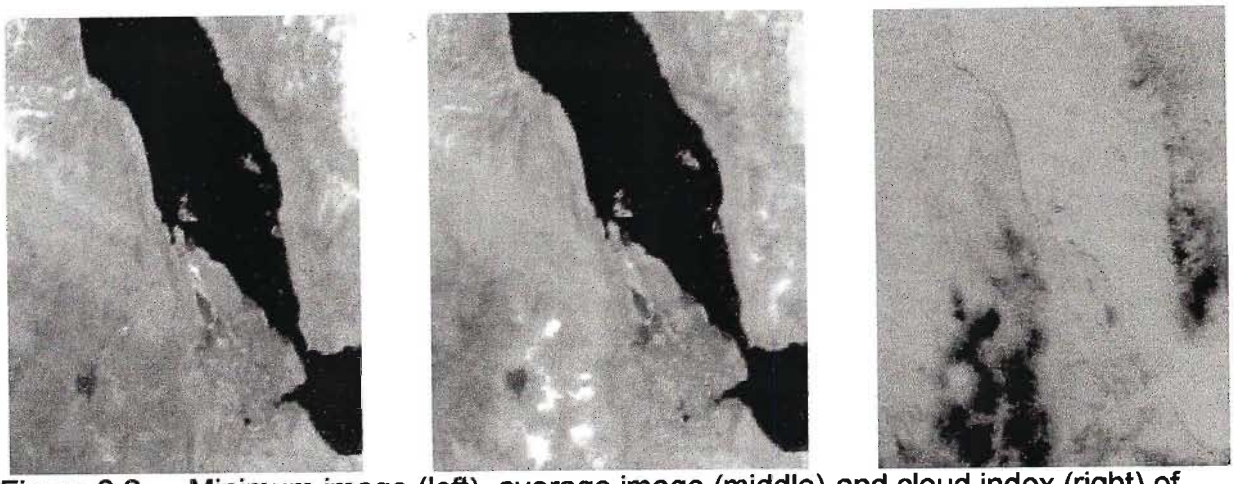

Figure 3.2 Minimum image (left), average image (middle) and cloud index (right) of Eritrea. All images are obtained from Tesfamicheal (2001).

The Australian Bureau of Meteorology (2002), in producing its daily solar radiation map, calculates its radiation values using the following simple model:

$$I_G = I_{TA} - I_{CA} - I_{SA} - I_{AA}$$

where I_G = irradiance at ground level (MJ/ m^2/day)

I_{TA} = extraterrestrial solar irradiance (MJ/ m^2/day)

I_{CA} = cloud albedo

I_{SA} = surface albedo and

I_{AA} = atmospheric absorption.

Irradiance at ground level can be calculated from irradiance at the top of the atmosphere, surface albedo, atmospheric absorption and cloud albedo (*cf.* Section 2.2, definitions and their units). Surface albedo is calculated from brightness of a satellite-derived pixel on a cloud free day, i.e. the darkest of a series of pixels on a given day. Pixel resolution is 36 km^2. Atmospheric absorption due to water vapour is calculated using radiosonde data. Other atmospheric absorption variables, e.g. Rayleigh scatter and ozone absorption, are ignored. Since surface albedo, atmospheric absorption and calculated irradiance at the top of the atmosphere can be estimated with reasonable accuracy, the difference between this value and irradiance at ground level can be

ascribed to cloud albedo. The error in solar radiation derived by this method is estimated at 7% under clear sky conditions and 20% under cloudy conditions (Australian Bureau of Meteorology, 2002).

3.4 Discussion and Conclusions

Owing to the widely differing methodologies and models described in Sections 3.1 (vapour pressure models), 3.2 (solar radiation models) and 3.3 (satellite derived solar radiation information), the discussions of these methods of estimating vapour pressure and solar radiation occur in separate sections.

3.4.1 Discussion and Conclusions: Vapour Pressure Models

Bristow (1992) and Kimball *et al.* (1997) noted the inadequacy of using minimum temperature to estimate dew point temperatures in arid regions. As already mentioned, Kimball *et al.* (1997) claimed that the method of including the ratio of potential evaporation to annual precipitation (***EF***) reduced the error of estimation of vapour pressure by up to 80%.

According to Thornton *et al.* (2000), humidity estimates showed an increase in mean absolute error and a positive bias at higher elevations in winter. However, it must be noted that Thornton *et al.* (2000) were working not only at high elevations (1400 m to 3100 m), but at high latitudes as well (central Europe), i.e. the conditions were considered dissimilar to South Africa.

While Bristow (1992) and Kimball *et al.* (1997) claimed that the relationship $T_{mn} \equiv T_d$ was inappropriate in arid and semi-arid regions. This method is nevertheless considered acceptable for the more humid, northern and eastern regions of South Africa, where the bulk of South Africa's population resides and agricultural production takes place.

As is the case with all other climate elements, climatologically homogeneous zones become a frame of reference for estimating vapour pressure and RH over a large area. Castellvi *et al.* (1997) concluded that in order to estimate vapour pressure deficit on a regional scale for areas where there is little or no meteorological information available, either mean vapour pressure or mean RH (the latter variable being more readily available) can be assumed to be relatively constant over the whole of a climatologically homogeneous zone.

The context of this research is the estimation of vapour pressure as an input to potential evaporation models. The Kimball *et al.* (1997) method of including the ratio of potential evapotranspiration to annual precipitation is, therefore, not acceptable for this purpose.

3.4.2 Discussion and Conclusions: Solar Radiation Models

Recent researchers have focused attention on their ability to transfer coefficients of solar radiation models from a point of determination to a nearby location, where no direct measurements are made, or to a location of similar climate. Hunt *et al.* (1998) tested several equations in order to obtain appropriate estimations of solar radiation for crop growth models (cf. Table 3.1). They found that one could transfer coefficients within a certain radius of the point of measurement. This radius depended on which equation was being used and the purposes for which the equation was intended, e.g. the Hunt *et al.* (1998) stated their model had a lower R^2 than the equation of Ratkowsky (1990), however, the root mean square error (RMSE) of the latter equation was greater. This implies that the operational radius (when using the same coefficients) for the Hunt *et al.* (1998) equation is greater. Hunt *et al.* (1998) did find that the RMSE increased as a linear function of distance between sites for all equations they tested.

Bezuidenhout (2002) who compared the output from the Clemence (1992) model to that of Hargreaves *et al.* (1985), Hunt *et al.* (1985), and Hook and McClendon (1992), ranked Clemence's (1992) model below the latter three models. Bezuidenhout (2002) therefore concluded that local calibration of a given model was preferable to a more global model of the type espoused by Clemence (1992).

Consideration should be given to the geographical locations where the equations were developed. For example, De Jong and Stewart (1993) as well as Hunt *et al.* (1998) developed their equations from data collected in central to western Canada. This is an area of relatively little topographical variation, but owing to the high latitudes (~50^0N) this region experiences very considerable seasonal variation of solar radiation. These are not environmental circumstances that are replicated in South Africa, (22^0-34^0 S latitude). Clemence (1992) used data from all the agricultural regions of South Africa. Similarly McCaskill (1990a), used data from every state in Australia.

The models of Thornton *et al.* (2000), Campbell and Donatelli (1998) and Winslow *et al.* (2001) differed from all the other models described in Table 3.1 in that all three groups of researchers incorporated another environmental variable, *viz.* a version of the "clear sky index". Winslow *et al.* (2001) refer to "cloud free atmospheric transmissivity". This term describes transmissivity on any cloud free day, without reference being made to, for example, haze or dust, whereas the "clear sky index" referred to by Thornton *et al.* (2000) and Campbell and Donatelli (1998) refers to the highest possible fraction of incoming solar radiation, i.e. atmospheric impediments to solar radiation are minimised on those particular days.

The models of Thornton *et al.* (2000) and Winslow *et al.* (2001) differed from the majority of the other models in that their models were constructed around atmospheric water vapour content. As has been stated in the introduction, and as subsequent chapters are going to attest, considerable difficulty surrounds the involvement of atmospheric water vapour in a given solar radiation model. The reason for this is the dearth of weather stations measuring RH. The modeller is therefore obliged to estimate the humidity of the atmosphere, and thereafter, to make a subsequent estimation of solar radiation from the estimated humidity.

Liu and Scott (2001) compared all of the equations in Table 3.1 except those by Clemence (1992), Campbell and Donatelli (1998), Thornton *et al.* (2000) and Winslow *et al.* (2001) and noted that if the researcher had access only to rainfall data, McCaskill's

(1990b) method worked best. With only temperature data available, the Bristow and Campbell (1984) model produced the best results. If, however, one had access to both temperature and rainfall data (and this is desirable), their own method (second last on Table 3.1) displayed the highest R^2. Liu and Scott (2001) also noted that transfer of coefficients could take place regardless of the distance between sites, provided the coefficients were developed in a similar climatic region.

3.4.3 Discussion and Conclusions: Satellite Derived Solar Radiation Information

Of the two methods described in Section 3.3, one must be aware of both the differing objectives of the respective researchers, and of the differing circumstances in regard to the availability of ground based instrumentation to verify model accuracy. As a result they developed differing methodologies. It was stated in the introductory paragraph to section 3.3 that this was not to be considered a comprehensive perusal of the literature on satellite derived solar radiation information, and was included to grant the reader some concept of the new methods.

The objective of Van Buskirk's (2002) satellite derived solar radiation estimation is to obtain average monthly irradiance for the purpose of solar heating for a third world country, *viz.* Eritrea. There is no reference to the calculation of, for example, atmospheric absorption or of Rayleigh scattering, nor is there any reference to error.

The objective of the Australian Bureau of Meteorology's (2002) satellite derived solar radiation information is meteorological research. The estimate of error is 7% under clear conditions and 20% in cloudy conditions as already stated. During cloudy conditions, however, less incident solar radiation is experienced at ground level, therefore, the overall magnitude of the error of the model is reduced to less than 10%.

The Australian Bureau of Meteorology's (2002) method is more comprehensive than Van Buskirk's (2002) and, therefore, any research on satellite derived solar radiation estimates would benefit from their greater accuracy. The availability of ground based

instruments, e.g. pyranometers or net radiometers and atmospheric observations (e.g. from radiosondes), means that their method is more accurate and relevant to a wider set of disciplines. Clearly, circumstance and availability of resources will determine which methods are to be used. Each method described has its own advantages and drawbacks. Should one require real-time or near real-time solar radiation estimates, then using satellite derived data is the best approach. This method, however, is likely to be costly.

This concludes the literature survey on established and currently employed methods of estimating vapour pressure and solar radiation. The objectives of this document are to develop new methods of estimating vapour pressure and solar radiation. Chapter 4 that follows (cf. the "Roadmap" on the next page) is a brief, but general, description of methods employed in subsequent analyses, where-after, each subsequent section shall present a brief description of the methods employed in that specific analysis.

Problem Statement: In order to estimate daily reference potential evaporation using the Penman-Monteith equation, values of daily vapour pressure and solar radiation are required

Objectives: To review current literature on current models for the estimation of daily vapour pressure and solar radiation, thereafter to employ and improve upon current method and models of estimating vapour pressure and solar radiation

Problem Statement

Broad Objectives	Literature Survey	Methods and Methodologies	Vapour Pressure Estimation	Solar Radiation Estimation	Conclusions and Recommendations
Specific Objectives	i) Introduction (Chapter 1) ii) Definitions relating to and factors affecting vapour pressure and solar radiation (Chapter 2) iii) Review of literature on current methods of estimating daily vapour pressure (Chapter 3) iv) Review literature on current methods of estimating daily solar radiation (Chapter 3)	i) Methods and methodologies employed in Chapters 5 to 9 (Chapter 4)	i) Characterisation of the vapour pressure regime in South Africa (Chapter 5) ii) Development of new models and methodologies of estimating vapour pressure (Chapter 6) iii) Verification of new methods of estimating vapour pressure (Chapter 6) iv) Mapping of vapour pressure, relative humidity and vapour pressure deficit over South Africa (Chapter 7)	i) Factors affecting solar radiation at ground level (Chapter 8) ii) Development of new models and methodologies of estimating solar radiation (Chapter 8) iii) Verification of new methods of estimating solar radiation (Chapter 8) iv) Mapping of solar radiation over South Africa (Chapter 9)	i) Conclusion and recommendations for future research (Chapter 10)

Chapter 4

METHODS AND METHODOLOGIES

Two climate elements, vapour pressure and solar radiation, are examined in this dissertation. Although the "Roadmap" (previous page) combines these two elements in this chapter, they are evaluated in separate sections. Since this dissertation contains a series of analyses, the methods of the individual analyses are described in detail in separate sections.

4.1 Vapour Pressure

In the sections on vapour pressure almost exclusive use was made of AWS data. As shall be observed in subsequent chapters, hourly data (which can only be obtained from an AWS) were employed to track the day-to-day variability in the vapour pressure regime. The RH measuring device employed at AWSs is considered to be more accurate than other RH measuring devices, e.g. thermohygrographs.

4.1.1 Data Sources

Temperature, rainfall and relative humidity data were obtained from countrywide networks of automatic weather stations (AWSs) operated by the South African Weather Service (SAWS). Data from stations operated by the South African Sugar Association's Experiment Station (SASEX) and the Agricultural Research Council's, Institute for Soil, Climate and Water (ARC-ISCW) were used where gaps in the SAWS station network existed, e.g. along the KwaZulu-Natal coastal belt and in the Northern Cape. Exceptions to the rule of applying only AWS data were made at, for example, Cedara in KwaZulu-Natal, which is a first order climate station, with three observations per day, and which employs the wet and dry bulb technique. A list and distribution map of all weather stations employed

in the vapour pressure analyses are presented in Table 4.1 and Figure 4.1 respectively, at the end of Section 4.1.3.

4.1.2 Methodologies and Models

Daily maximum and minimum temperature, daily maximum and minimum relative humidity and daily rainfall data were obtained from the South African Weather Service for 82 automatic weather stations countrywide. Means of daily vapour pressures were calculated using average vapour pressure at maximum and minimum temperatures respectively. The methodology used to calculate the aforementioned vapour pressures was obtained from the FAO 56 website (FAO 56, 2002). Saturated vapour pressure e_a (kPa) is calculated using the Teten's equations in which:

$$e_a \text{ (kPa)} = 0.6108.exp[17.27 \times T/(T+237.3)]$$

where T = temperature (^{0}C) at a given time.

Whenever actual vapour pressure e_d (kPa) was required, the calculated saturated vapour pressure was multiplied by the associated relative humidity (RH), itself expressed as a percentage, such that:

$$e_d \text{ (kPa)} = e_a \times (RH/100).$$

The altitude correction for actual vapour pressure is described as follows:

$$= e_d \times [(293-0.0065 \times z)/293]^{5.26}$$

where z = altitude (m)

4.1.3 Data Integrity

Having obtained daily temperature, relative humidity and rainfall data, these data were individually checked for extreme values. Where minimum RH data exhibited values of below 5%, then those data were regarded as suspicious. A

value of below 5% would not, however, be automatically rejected. Further values of RH below 5% were sought. In the event of several days (e.g. 5 days) in a given month with minimum RH below 5%, that entire month's record was rejected. For maximum RH, the data were scanned for values of greater than 96%. In arid locations, e.g. at Augrabies or Upington, it is possible in winter months for a whole month to pass without RH once approaching dewpoint. If a given month's maximum RH data did not include values greater than 96%, a decision was taken to either omit or include that month's data depending on whether the months immediately prior or subsequent to that month's displayed values of between 96% and 100%.

Maximum RH data exhibited another characteristic of RH observations unique to the Vaisalla instrument which is the principal RH recording device employed by South African AWSs, and from which the bulk of data was selected. It was observed that at times a sequence of values were repeated e.g. 95,94,93,95,94,93 etc. If a persistence in this sequence was observed, it was assumed that the recording instrument was at fault and subsequently the entire month's record was omitted. In the event of one or more days (but <10 days) of data missing in a given month, that particular day's value would be assigned the previous day's value. This would ensure a realistic range of vapour pressure data for missing days. The checking procedures described in the previous two paragraphs are the protocols employed by the ARC-ISCW for their countrywide weather station network.

Table 4.1 presents the data efficiency of the individual weather stations employed in the vapour pressure analyses. Where a long-term monthly average vapour pressure value depended on less than two months of data, the entire record for that station was omitted (e.g. Cape Columbine in Table 4.1). Figure 4.1 presents the distribution of weather stations presented in Table 4.1. Fewer weather stations are displayed in Figure 4.1 as those stations which had their entire record omitted were not included in this map.

Table 4.1. Data efficiency of weather stations employed in the vapour pressure sections of this dissertation

Location	Total number of months on record	Months of data omitted	Length of record
Alexander Bay	108	32	1993-2001
Alldays	120	25	1993-2001
Augrabies	37	1	1999-2001
Beaufort West	111	43	1994-2002
Bloemfontein	127	0	1992-2002
Bloemhof	118	0	1993-2002
Bisho	117	51	1993-2002
Brandvlei	48	6	1994-1998
Cape Columbine	119	119	1992-2002
Cape Point	84	10	1995-2002
Cape Town	123	2	1992-2002
Cedara	48	0	1997-2000
Ceres	38	7	1997-2000
Charter's Creek	104	75	1994-2002
Clanwilliam	24	24	2000-2002
Doornlaagte	44	3	1997-2002
Elliott	109	109	1993-2002
Ellisras	97	15	1993-2001
Fauresmith	25	25	2001-2002
Ficksburg	120	15	1993-2002
Geelbek	63	63	1997-2002
Giant's Castle	78	8	1994-2000
Graaf Reinett	108	39	1993-1999
Grahamstown	120	120	1992-2002
Graskop	113	39	1993-2002
Grenshoek	62	2	1997-2002
Greytown	84	6	1993-2002
Harrismith	47	47	1993-1997
Hoedspruit	72	72	1997-2002
Ixopo	62	13	1994-2000
Jamestown	96	1	1994-2001
Johannesburg	131	1	1992-2002
Joubertina	63	40	1997-2002
Kimberley	228	1	1978-1996
Klerksdorp	115	4	1993-2002
Knysna	68	0	1996-2002
Komatidraai	46	46	1993-1996
Komatipoort	38	0	1999-2001
Kroonstad	8	0	1993-2001

Table 4.1 continued

Kuruman	228	1	1978-1996
Lamberts Bay	96	96	1994-2002
Laingsburg	86	0	1995-2002
Langebaan	33	33	1994-1997
Lichtenburg	96	25	1995-2002
Lydenburg	120	120	1992-2002
Mafiking	96	49	1994-2002
Margate	72	40	1994-2002
Marken	76	2	1993-2000
Mbazwana	60	60	1997-2002
Middelburg	62	21	1993-1998
Mtunzini	72	11	1997-2002
Nelspruit	96	26	1993-2002
Newcastle	132	54	1990-2002
Nietvoorbij	36	0	1999-2001
Noupoort	108	18	1994-2002
Paarl	74	0	1996-2002
Paddock	60	19	1994-1998
Patensie	87	40	1993-2000
Phalaborwa	112	112	1993-2002
Piet Retief	108	27	1994-2002
Pietermaritzburg	113	113	1997-2002
Pietersburg	127	9	1992-2002
Plettenberg Bay	118	0	1993-2002
Pomfret	118	10	1993-2002
Pongola	117	117	1993-2002
Port Alfred	108	74	1992-2002
Port Edward	113	113	1993-2002
Port Elizabeth	125	0	1992-2002
Porterville	84	26	1996-2002
Postmasburg	96	43	1995-2002
Potchefstroom	68	16	1997-2002
Potgietersrus	94	5	1993-2000
Pretoria	120	15	1993-2002
Prieska	48	2	1999-2002
Prince Albert	86	86	1993-1999
Queenstown	84	44	1994-2000
Richard's Bay	109	109	1993-2002
Rietvallei	81	26	1993-1999
Robertson	72	4	1997-2002
Roodeplaat	38	3	1999-2001
Rustenburg	118	1	1993-2000

Table 4.1 continued

Sezela	37	2	1996-1999
Shaka's Rock	58	14	1993-1998
Springs	60	60	1994-1998
Struisbaai	117	96	1993-2002
Taung	96	20	1995-2002
Thabazimbi	111	111	1993-2002
Tshipiesie	51	0	1995-1999
Tsitsikama	72	10	1997-2002
Uitenhage	77	0	1993-1999
Ulundi	99	60	1994-2002
Upington	128	2	1992-2002
Van Reenen	93	2	1995-2002
Vanzylsrus	111	26	1993-2002
Ventersdorp	39	2	1997-2000
Venterstad	93	5	1993-2000
Virginia (KZN)	97	5	1994-2002
Vioolsdrif	108	53	1993-2002
Vrede	113	32	1993-2002
Welkom	113	28	1993-2002
Wepener	43	43	1999-2002
Witbank	84	49	1993-2000
Worcester	72	6	1997-2002

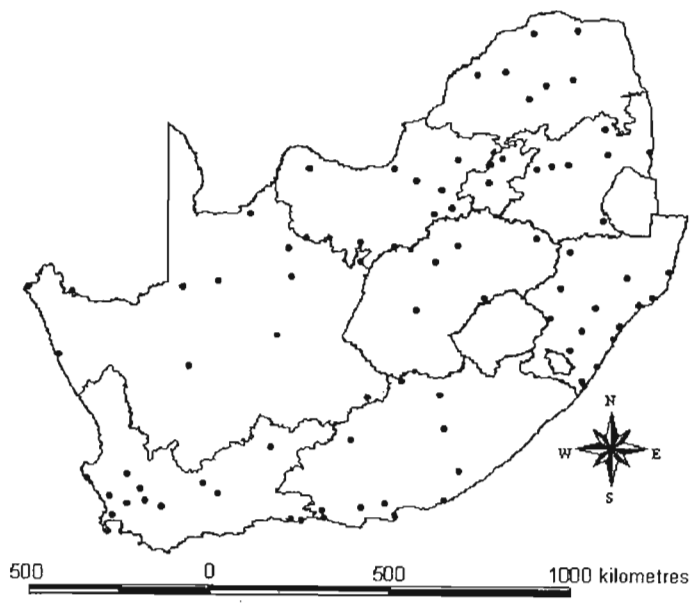

Figure 4.1 Distribution of weather stations used in the vapour pressure analyses

4.2 Solar Radiation

Like vapour pressure data, exclusive use was made of data from automatic weather stations. Unlike vapour pressure, solar radiation data employed in the following analyses depended on several different types instruments. Instruments employed usually depended on the operating authority and the level of technology at the time at which these data were collected. These factors shall be described in greater detail in Section 4.2.2.

4.2.1 Data Sources

The majority of solar radiation data records were obtained from the ARC-ISCW and SASEX, with exceptions being made at Cedara and Port Elizabeth (SAWS). The SAWS data coverage was not considered in this study as data from only 12 solar radiation measuring stations countrywide were readily available. Where other SAWS data were employed, they were to cover any gaps in the solar radiation data coverage, e.g. at Port Elizabeth. An executable Microsoft EXCEL file, constructed by the Agrometeorology section of the University of KwaZulu-Natal, was employed for the specific calculation of daily extraterrestrial solar radiation at each location. A list of all weather stations employed in the solar radiation sections of this dissertation, is given in Table 4.2. Figure 4.2 which accompanies Table 4.2 present the climate of the individual stations.

4.2.2 Methodologies and Models

Unlike vapour pressure, no further calculations had to be undertaken in order to achieve useable values of solar radiation. All solar radiation values were integrated values in units of $MJ/m^2/day$. Solar radiation data were obtained from two types of instruments, *viz.* thermoelectric and photovoltaic. The earlier records (1970s to 1980s) tended to come from thermoelectric sensors. The Cedara and Dundee (SAWS) data sets are examples of data from thermoelectric

sensors. The majority of subsequent data sets were obtained from photovoltaic instruments.

4.2.3 Data Integrity

Data supplied were checked for extreme values of solar radiation, e.g. values greater than 80% of extraterrestrial solar radiation on a given day. Less consideration was given to minimum values of solar radiation. Meteorologists consider values of between 16% and 25% of extraterrestrial solar radation to be the lower possible limit of incoming solar radiation (Savage, 2003; pers com). Individual days' data of less than 16% of extraterrestrial solar radiation were nevertheless included. If, however, several successive days (+/-5) with solar radiation values of under 16% of extraterrestrial solar radiation were observed, this was taken to imply that the instrument was faulty. In the majority of circumstances, when this occurred, the suspicious data were considerably below the "16% of extraterrestrial solar radiation" criterion. When these data were discarded, data immediately prior to, and subsequent to the omitted data, were further scrutinised.

Table 4.2 presents the data efficiency of the individual weather stations considered in the solar radiation analyses. Where solar radiation records were discarded entirely (e.g. Bethlehem, De Aar etc.), this resulted from the majority of the record being considered unreliable according to a second test. In this test a profile of the entire record was drawn of daily solar radiation, accompanied by its commensurate daily extraterrestrial solar radiation. The profile was then scrutinised for a constant difference between the extraterrestrial solar radiation and the maximum possible (clear sky radiation). In the event of this difference being uneven, either part of the record or the entire record was omitted. The difference between extraterrestrial solar radiation and clear sky radiation is dealt with in greater detail in Chapters 8 and 10.

Table 4.2 Data efficiency of weather stations considered in the solar radiation sections of this dissertation

Location	Months of data omitted	Total number of months on record	Period of record
Bergfontein	1	27	1995-1998
Bethlehem	112	112	1993-2002
Bleskop	1	51	1999-2003
Bloemfontein	1	31	2000-2003
Calvinia	117	117	1993-2002
Cape Point	64	64	1995-2000
Cedara	6	54	1983-2003
De Aar	112	112	1993-2002
De Tuin	11	69	1993-1999
De Vlei	16	67	1994-1999
Dundee	1	97	1975-1983
Durban	112	112	1993-2002
Elgin	2	46	1994-1997
Ermelo	117	117	1993-2002
Eston	0	78	1997-2003
Funeray	5	48	1999-2003
George	117	117	1993-2002
Hluhluwe	0	66	1998-2003
Irene	117	117	1993-1998
Joubertina	9	36	1995-1997
Kenhardt	26	72	1993-1998
Lilydale	1	54	1999-2003
Lydenburg	9	37	2001-2003
Mhlati	2	41	2000-2003
Mt. Edgecombe	0	78	1997-2002
Mtubatuba	0	42	2000-2003
Nelspruit	0	38	2000-2003
Pietersburg	96	96	1995-2002
Pondoland Sugar	24	54	1999-2003
Port Elizabeth	0	121	1992-2002
Richmond	3	78	1997-2003
Rietrivier	9	37	1996-1999
Rustenburg	7	78	1997-2003
St. Lucia	12	78	1997-2003
Springbok	127	127	1992-2002
Tenbosch	5	50	1999-2003
Tsolo	1	54	1999-2003
Vaalhartz	6	73	1997-2003
Wartburg	0	85	1997-2003

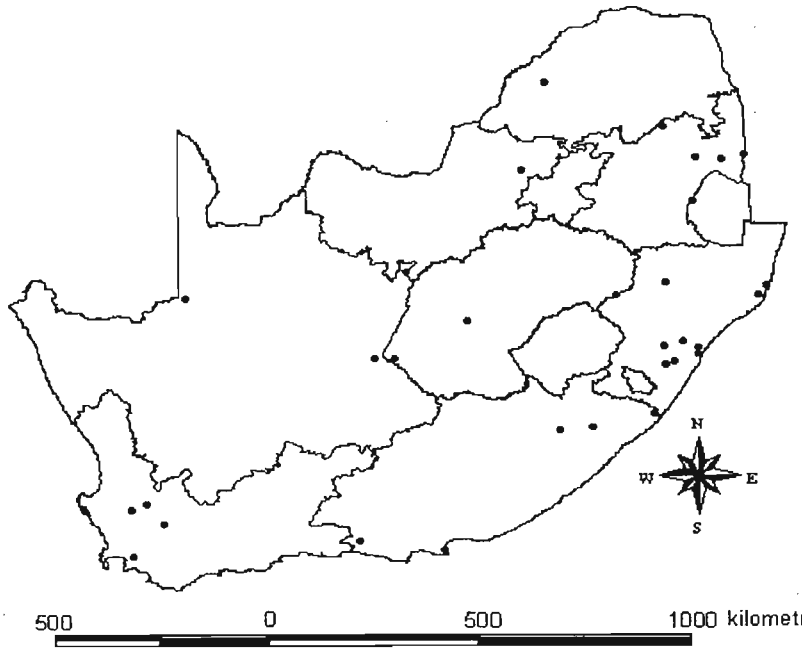

Figure 4.2 Distribution of weather stations used in the solar radiation analyses

4.3 General Data Integrity

The context of this dissertation is the estimation of daily vapour pressure and solar radiation using readily available surrogate data, *viz.* temperature and rainfall. Since the technology of recording temperature and rainfall is considerably older and simpler than that of vapour pressure and solar radiation, less scope exists for errors in these data.

Daily temperature data were scanned for extremely high and extremely low values and for any instances in which minimum temperature data were recorded to be of a higher value than maximum temperature on the same day. For rainfall data, the data records were scanned a month at a time in order to establish the longest period without rainfall being recorded. Depending on location, time of the year and scrutiny of records from nearby stations, a decision was then taken to either discard or include a given data set.

In this chapter a brief overview of basic methodologies employed for all the subsequent analyses has been described. In Chapters 5 to 8 that follows, temperature and rainfall together with invariate data (e.g latitude, altitude and distance from the sea) are used to estimate vapour pressure and solar radiation throughout South Africa (*cf.* "Roadmap" on following page).

Problem Statement: In order to estimate daily reference potential evaporation using the Penman-Monteith equation, values of daily vapour pressure and solar radiation are required

Objectives: To review current literature on current models for the estimation of daily vapour pressure and solar radiation, thereafter to employ and improve upon current method and models of estimating vapour pressure and solar radiation

Problem Statement

Broad Objectives	Literature Survey	Methods and Methodologies	Vapour Pressure Estimation	Solar Radiation Estimation	Conclusions and Recommendations
Specific Objectives	i) Introduction (Chapter 1) ii) Definitions relating to, and factors, affecting vapour pressure and solar radiation (Chapter 2) iii) Review of literature on current methods of estimating daily vapour pressure (Chapter 3) iii) Review literature on current methods of estimating daily solar radiation (Chapter 3)	i) Methods and methodologies employed in Chapters 5 to 9 (Chapter 4)	i) Characterisation of the vapour pressure regime in South Africa (Chapter 5) ii) Development of new models and methodologies of estimating vapour pressure (Chapter 6) iii) Verification of new methods of estimating vapour pressure (Chapter 6) iv) Mapping of vapour pressure, relative humidity and vapour pressure deficit over South Africa (Chapter 7)	i) Factors affecting solar radiation at ground level (Chapter 8) ii) Development of new models and methodologies of estimating solar radiation (Chapter 8) iii) Verification of new methods of estimating solar radiation (Chapter 8) iv) Mapping of solar radiation over South Africa (Chapter 9)	i) Conclusions and recommendations for future research (Chapter 10)

Chapter 5

VARIABLES AND INVARIATES ASSOCIATED WITH VAPOUR PRESSURE

5.1 Introduction

Easily measurable and readily available surrogates are sought from which to estimate actual vapour pressure at locations where it is not measured, and for the further estimation of vapour pressure deficit, which is a variable used in the Penman-Monteith equation for potential evaporation. As may be observed from the "Roadmap", Chapter 5, in which the analyses commence, is devoted to describing what effect commonly measured weather variables, *viz.* temperature and rainfall and geographical location, have on daily and monthly vapour pressure regime at a given location.

Those factors considered to affect daily and monthly vapour pressure regime are divided into two categories; "invariate" and "variate". The term "invariate" describes such factors as continentality, latitude and seasonality. Altitude would also fall into this category, however, since water vapour follows the gas laws, the effects of altitude are already well understood. Precise equations exist for describing the effects of altitude have on vapour pressure (decreasing with increasing altitude). It is for this reason that altitude is omitted from Chapter 5. The second category consists of variates, e.g. temperature, rainfall and the influence of air masses.

The locations of the weather stations employed for the analyses described in Chapter 5 are displayed in Figure 5.1. A brief summary of the long-term climate recorded at each station is given in Table 5.1.

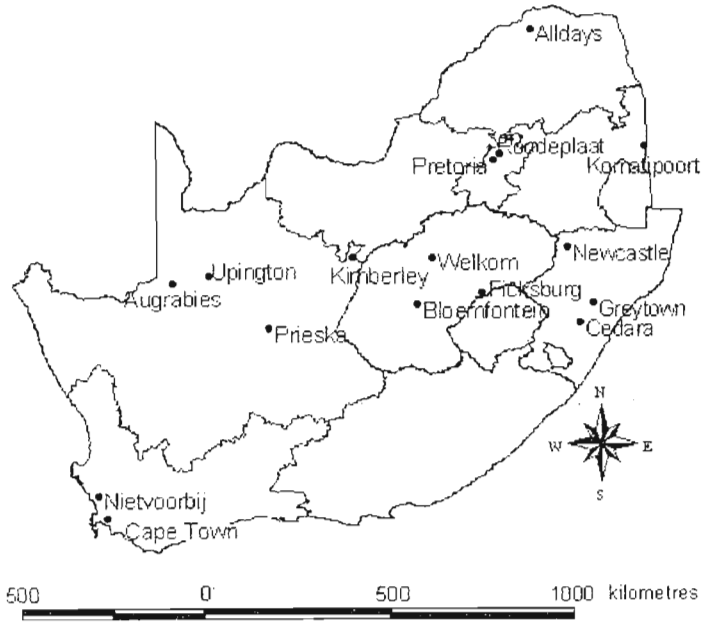

Figure 5.1 Locations of the weather stations used for the estimation of vapour pressure in Chapter 5

Table 5.1 Climate statistics for the weather stations used for the estimation of vapour pressure in Chapter 5

Location	Altitude (m)	January Mean of Daily Maximum Temperature (°C)	January Mean of Daily Minimum Temperature (°C)	July Mean of Daily Maximum Temperature (°C)	July Mean of Daily Minimum Temperature (°C)	Mean Annual Precipitation (mm)
Alldays	693	32.8	20.4	24.8	5.2	388
Augrabies	650	36.5	17.2	22.4	1.5	95
Bloemfontein	1359	30.5	15.6	17.4	-1.3	530
Cape Town	35	27.6	14.9	17.1	8.3	790
Cedara	1076	25.4	15.5	19.4	3.8	831
Greytown	1110	26.4	15.7	19.3	3.8	988
Ficksburg	1640	26.7	13.9	16.0	-0.3	720
Kimberley	1197	32.1	17.5	21.6	4.1	379
Komatipoort	189	31.4	21.4	24.5	8.6	784
Newcastle	1235	30.2	16.1	21.2	3.7	883
Nietvoorbij	146	28.1	15.5	17.3	8.0	767
Pretoria	1310	28.7	16.8	21.0	1.0	758
Prieska	947	35.9	18.6	19.2	0.5	251
Roodeplaat	1200	29.6	16.8	21.0	1.0	656
Upington	841	35.4	20.8	18.5	3.4	193
Welkom	1343	31.3	16.4	18.6	1.1	437

5.2 Vapour Pressure and Daily Minimum Temperature

Bristow (1992) and Kimball *et al.* (1996) used the relationship $T_d \equiv T_{mn}$ to estimate vapour pressure for the further estimation of potential evaporation. As has been noted in Chapter 2, both above authors assumed that T_d is usually attained at minimum air temperature and that little variation in the vapour pressure regime occurred throughout a given day. The authors also noted, that these assumptions failed to be upheld in the arid regions.

5.2.1 Testing the Assumptions of Bristow (1992)

Since Bristow and Kimball *et al.* (1997) both stated that Bristow's (1992) method failed in arid locations, it became necessary to demonstrate precisely how the Bristow (1992) method functioned in different locations, i.e. areas with differing degrees of aridity, and in which circumstances Bristow's (1992) method failed to be upheld.

5.2.2 Methods

Hourly vapour pressure data were obtained from Komatipoort, Roodeplaat and Augrabies to represent moist sub-tropical, semi-arid and arid climates respectively. Saturated vapour pressure (e_a, kPa) was calculated for the minimum temperature for each 24 hour period using the Tetens equation (*cf.* Chapter 4 on Methods and Methodologies). This value was then used to represent the actual vapour pressure value over the whole day.

5.2.3 Results and Discussion

As may be observed from Figures 5.2 to 5.4, the method produced reasonable estimates of daily vapour pressure in the moist and semi-arid areas. This method, however, clearly overestimated vapour pressure at Augrabies in an arid region.

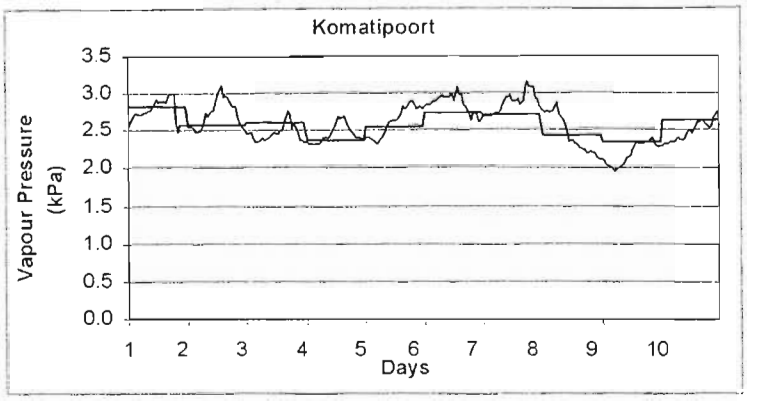

Figure 5.2 Estimated daily vapour pressure (—) versus observed hourly vapour pressure ( ), over ten consecutive days at Komatipoort, 1 January 2000 to 10 January 2000

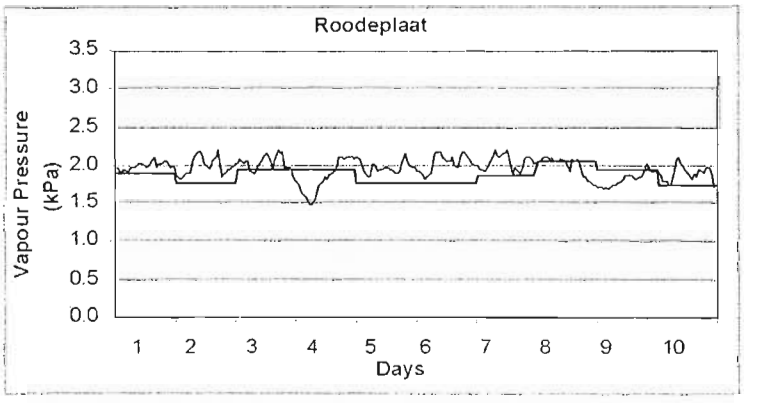

Figure 5.3 Estimated daily vapour pressure (—) versus observed hourly vapour pressure ( ), over ten consecutive days at Roodeplaat, 1 January 2000 to 10 January 2000

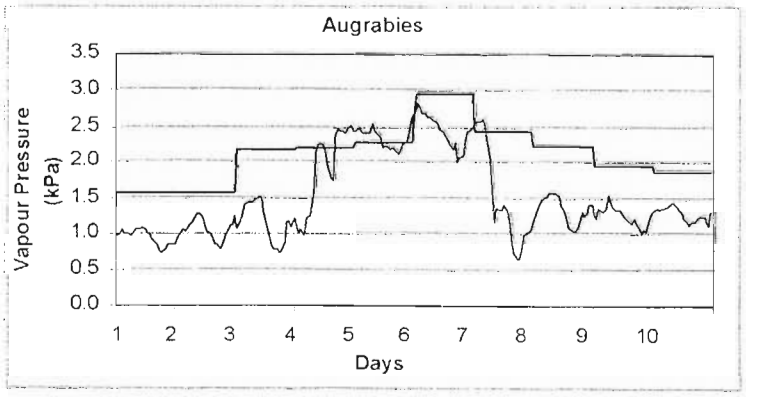

Figure 5.4 Estimated daily vapour pressure (—) versus observed daily vapour pressure ( ) from hourly data, over ten consecutive days at Augrabies, 1 January 2000 to 10 January 2000

A further test of the validity of the associated assumptions, *viz.* that there is relatively little intra-daily variation in vapour pressure on a given day, showed that this was not always the case. Figure 5.5 is a graph of hourly vapour pressure values between 7/1/2000 and 8/1/2000. As can be observed from Figure 5.5, a 400% variation in vapour pressure may be experienced on some days (7/1/2000) over a 24 hour period, while on other days it varies very little (8/1/2000).

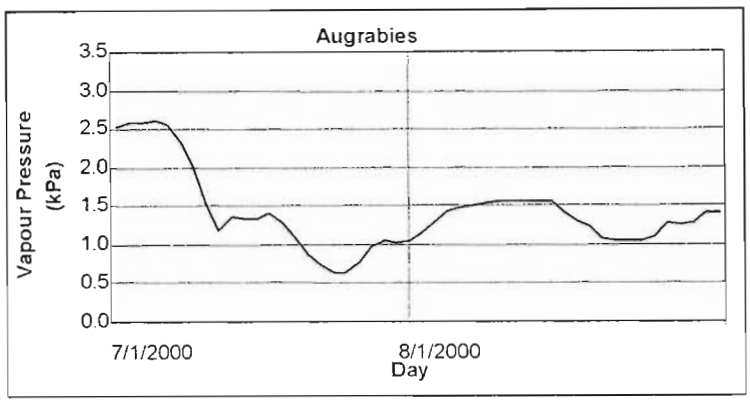

Figure 5.5 Hourly vapour pressure measured over two consecutive days at Augrabies, 7 January 2000 to 8 January 2000

5.2.4 Conclusions

From this and other similar results (not shown) it was concluded that calculating saturated vapour pressure from minimum air temperature, in order to estimate vapour pressure, did not yield accurate results in arid locations. Not only was dew point temperature frequently not attained by minimum air temperature (Figure 5.4) in arid locations, but sometimes there was considerable variation in vapour pressure throughout a given 24 hour period (Figure 5.5).

Vapour pressure *per se* is not an often sought-after variable. As has already been stated, the variable is utilised to calculate the more relevent elements of RH and VPD. The following section is devoted to demonstrating how Bristow's (1992) method is utilised for just one element, RH.

5.3 Estimation of Daily RH from Minimum Air Temperature

RH is a universally used variable to describe atmospheric moisture status. The numerator in the equation is actual vapour pressure (*cf.* Section 4.1.2). The following section is, therefore, devoted to describing the use of minimum air temperature to estimate actual vapour pressure in the RH equation in varying climatic regimes throughout the country. Despite the statistical inappropriateness of comparing two relative values, it was decided to regress RH calculated using the Bristow (1992) method against observed RH data from three increasingly arid locations. In order of increasing aridity, Komatipoort, Roodeplaat and Augrabies were selected as the locations.

5.3.1 Methods

Minimum temperature data from Komatipoort, Roodeplaat and Augrabies, where these stations represented moist subtropical, semi-arid and arid regions respectively, were used to estimate vapour pressure for the further estimation of RH. In the examples displayed (Figures 5.6 to 5.8), the exercises were conducted over one specific day (*viz.* 1 January 2000).

5.3.2 Results and Discussion

As may be observed from the Komatipoort plot (Figure 5.6), the RH values at this sub-tropical location tended to be concentrated in the moist end of the scale. In Figure 5.7, the Roodeplaat plot produced a greater spread of values and also the closest regression to the desired 1:1 slope and intercept of 0. In Figure 5.8, Augrabies, which is in the most arid of the three locations, produced the highest R^2. However, the RH is systematically overestimated. This overestimation is the most significant indication of the drawback of using minimum air temperature to estimate vapour pressure for RH in arid regions.

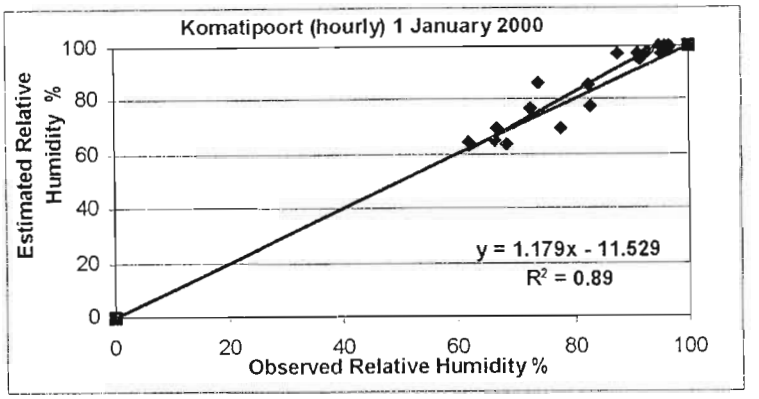

Figure 5.6 Hourly relative humidity at Komatipoort, estimated from the saturated vapour pressure at minimum temperature, versus observed relative humidity

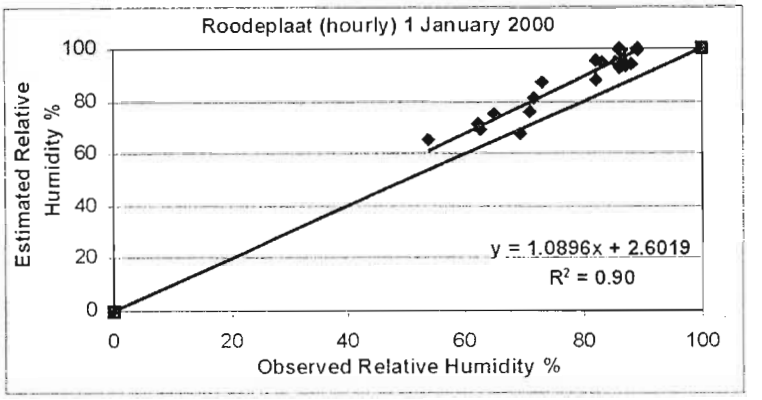

Figure 5.7 Hourly relative humidity at Roodeplaat, estimated from the saturated vapour pressure at minimum temperature, versus observed relative humidity

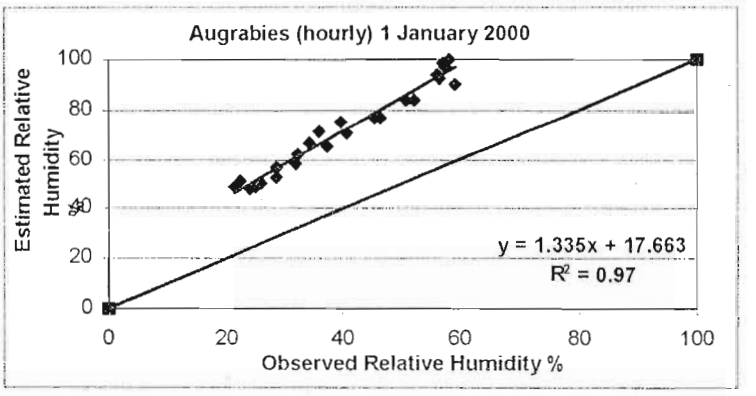

Figure 5.8 Hourly relative humidity at Augrabies, estimated from the saturated vapour pressure at minimum temperature, versus observed relative humidity

5.3.4 Conclusions

From the above examples in Sections 5.2, it was concluded that the two assumptions made, *viz.* $T_d \equiv T_{mn}$, and that there is little intra-daily variation, were upheld in the semi-arid, moist subtropical and temperate regions. However, in arid regions, the assumptions were not upheld. The reasons for this are that minimum dry bulb temperatures were generally well above dew point temperature in arid areas. It was also concluded that the method of using minimum air temperature to estimate vapour pressure for the further estimation of RH, works best outside of arid locations, but that one requires a reasonable range of temperature data in order to produce an acceptable estimate of RH.

5.4 Vapour Pressure and Daily Temperature Range

Other means of presenting temperature are sought in the form of temperature range and maximum temperature. Scientists have long known that the properties of water allow it to act as a "heat sink". It was hypothesized, therefore, that higher vapour pressures experienced at a given locations act as an attenuator of temperature range.

5.4.1 Methods

By way of example, daily temperature and vapour pressure data were obtained from the SAWS weather station at Ficksburg in the eastern Free State, for the year 1999. Ficksburg was selected since its climate could be considered neither sub-tropical nor arid in character. Its location allows it to experience a considerable range in daily and monthly temperatures. Vapour pressure and temperature range values were then plotted against each other. The results can be observed in Figure 5.9.

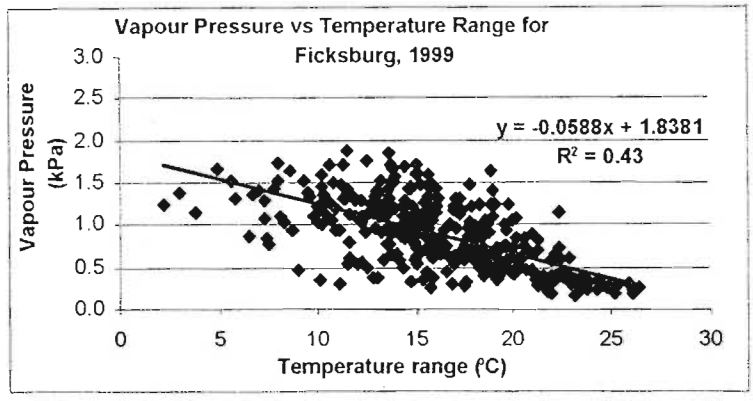

Figure 5.9 A plot of daily vapour pressure versus daily temperature range at Ficksburg, eastern Free State, for the year 1999

5.4.2 Results and Discussion

A negative correlation was found to exist between vapour pressure and daily temperature range and as may be observed in Figure 5.9. Further scrutiny of the relationship revealed that low vapour pressure values associated with high daily temperature ranges were concentrated almost exclusively in the late winter and early spring period, from July to September. Conversely, the high vapour pressure values and low daily temperature ranges were associated with the peak summer months and usually on days on which rainfall occurred. The latter relationship, was not, however exclusive to the summer season.

5.4.3 Conclusions

It was concluded that an inverse relationship does exist between daily temperature range and vapour pressure. This relationship, however, could also be explained by rainfall seasonality.

5.5 Vapour Pressure and Rainfall

In light of the findings of Section 5.3, it was decided to further investigate the relationship between monthly rainfall and vapour pressure. Logically, the advent of rainfall should increase ambient vapour pressure. Rainfall may, however, be characterised by location with respect to prevailing rainfall type. For example,

the winter rainfall region in South Africa tends to experience longer duration, low intensity rainfall events, whereas the summer rainfall regions tend to experience higher intensity, short duration, local events.

5.5.1 Methods

Daily rainfall data for the years 1996 to 1998 were obtained from Nietvoorbij, near Stellenbosch, to represent the winter rainfall areas and from Cedara, in KwaZulu-Natal, to represent the summer rainfall areas. Raindays per month were then compared with average vapour pressure during those given months. The results may be seen in Figures 5.10 and 5.11.

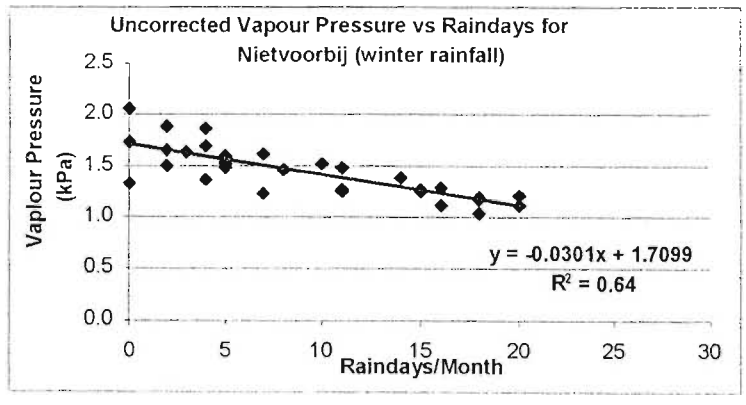

Figure 5.10 A comparison of averaged monthly vapour pressure versus raindays per month, from 1996 to 1998, at Nietvoorbij which experiences winter rainfall

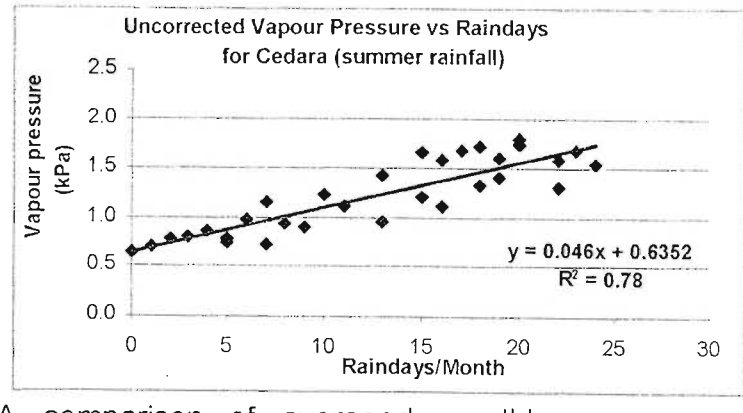

Figure 5.11 A comparison of averaged monthly vapour pressure versus raindays per month, from 1996 to 1998, at Cedara which experiences summer rainfall.

5.5.2 Results and Discussion

As may be observed, strong (albeit different) relationships exist between raindays per month and averaged monthly vapour pressure at both locations. One should consider the fact that that the lowest monthly vapour pressure is still experienced at Nietvoorbij during the winter months, despite those being the wet months. It is for this reason that that the relationship between vapour pressure and rainfall is considered associative rather than causative.

5.5.3 Conclusions

It was concluded that the relationship between raindays per month versus averaged monthly vapour pressure, would be unlikely to succeed in a vapour pressure model, as each location would produce a unique slope and intercept in the relationship.

5.6 Vapour Pressure and Air Masses

Air masses exert a considerable influence on the variability of any given weather element. The degree of influence will itself be influenced by such factors as geographical location and the origin of the air mass. For example, rainfall in South Africa during the winter months is influenced predominantly by air masses originating over the South Atlantic, with the winter rainfall regions being located the southern parts of South Africa. During the summer months, rainfall, in particular convectional storms, are associated with air masses originating from equatorial regions. The summer rainfall areas are located predominantly in the northern and eastern parts of the country.

5.6.1 Methods

In the first analysis, daily vapour pressure for Upington, Prieska and Kimberley was plotted for the same month, January 2000. These three stations, were chosen for their location in the more arid regions of South Africa, despite being separated by several hundred kilometres from one another.

5.6.2 Results and Discussion

As may be observed in Figure 5.1.2, daily averaged uncorrected vapour pressure for January 2000 at all three locations produced a similar profile, thereby indicating that all three locations were being affected by the same body of air.

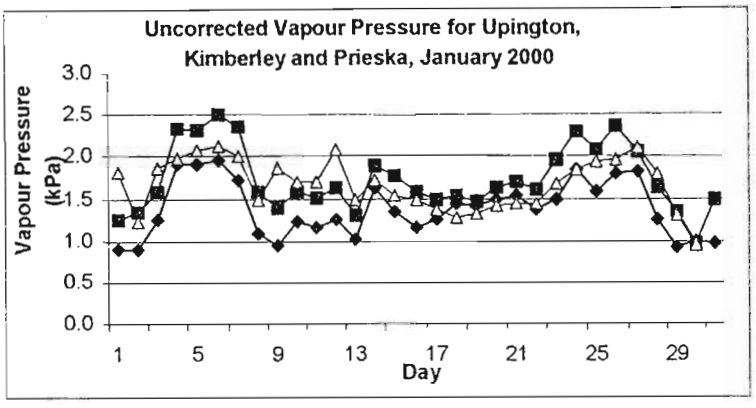

Figure 5.12 Comparison of daily average uncorrected vapour pressure for three locations, Upington (-◆-), Kimberley (-☆-) and Prieska (-■-) in the Northern Cape

5.6.3 Conclusions

It was concluded that daily vapour pressure at different locations could be influenced by the same body of air. This characteristic has important implications in modelling of daily vapour pressure as it enables interpolation of vapour pressure between nearby locations.

5.7 Daily Vapour Pressure and the Origin of the Air Mass

In light of the findings of Section 5.5.3, it was further hypothesised that the geographical origin of air masses and the fetch (i.e. the distance travelled by the air mass over land) play a role in the vapour pressure at a given point.

5.7.1 Methods

Six months of daily vapour pressure values for 1994 were compared with the South African Weather Service's daily synoptic chart for the same period for two

stations, *viz.* Greytown in KwaZulu-Natal, to represent a sub-humid location and Upington in the Northern Cape, to represent an arid location. The intention of the analysis was to track the origin of the air mass and, thereby, to observe the influence of the given air mass on daily vapour pressure.

5.7.2 Results and Discussion

For Upington, it was found that only those air masses originating in the equatorial and tropical regions produced a positive influence (increased) vapour pressure. Air masses that originated off the eastern seaboard, the Western Cape coast or even the closer Atlantic coast, reduced the daily vapour pressure.

Figures 5.13 to 5.16 present a sequential display of synoptic events leading up the rapid rise in vapour pressure observed between days 4 and 5 in Figure 5.17. For ease of understanding, the general direction of air movement on a given day's synoptic chart is represented by black arrows. The location of Upington is represented by a black diamond.

For the Greytown analysis it was observed, that, in addition to air masses originating from equatorial regions, air masses originating off the KwaZulu-Natal coast also drove the daily vapour pressure up. As in the case of Upington, south westerlies and westerlies, brought a decline in daily vapour pressure.

5.7.3 Conclusions

It was concluded that air masses play a very important role in determining vapour pressure over a given period. If the influence of air masses were linked to any other weather variable, it would be wind direction. Wind direction, however, cannot be considered in the same frame of reference as rainfall and temperature, as its data are at least as rare as vapour pressure data in contemporary South African climate databanks. For this reason, the influence of air masses, despite their considerable significance on the daily vapour pressure regime at a given location, had to be omitted from the models described in subsequent chapters.

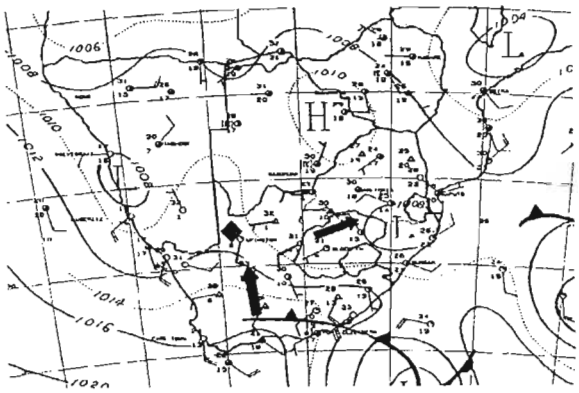

Figure 5.13 Upington, 3 January 1994: direction of air movement is north, ahead of an approaching cold front

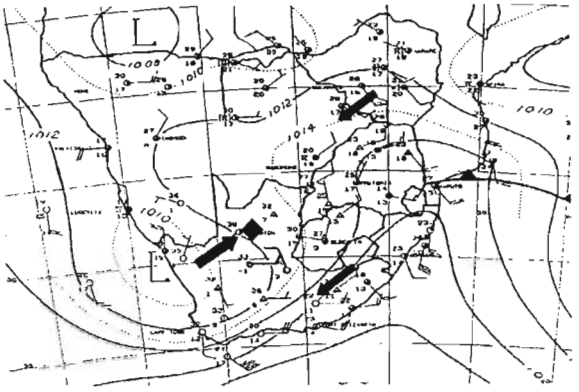

Figure 5.14 Upington, 4 January 1994: direction of air movement still north, the cold front has passed through

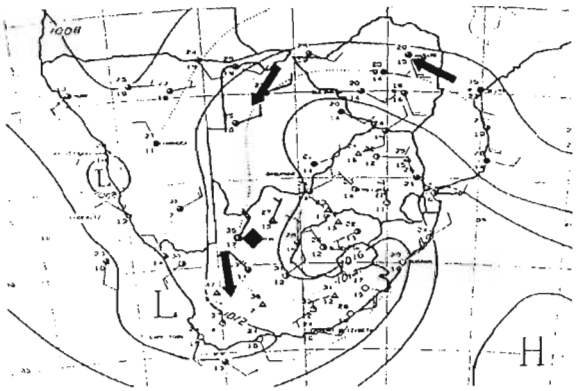

Figure 5.15 Upington, 5 January 1994: direction of air movement still south

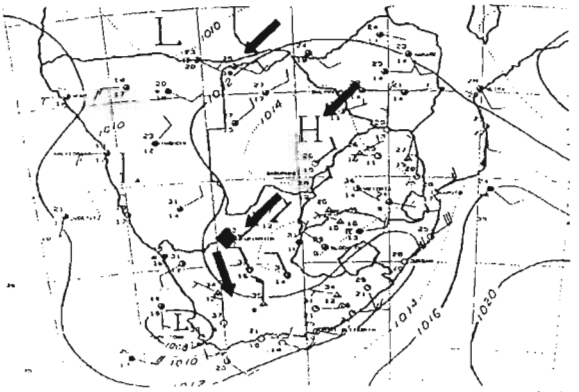

Figure 5.16 Upington, 6 January 1994: direction of air movement now south-west

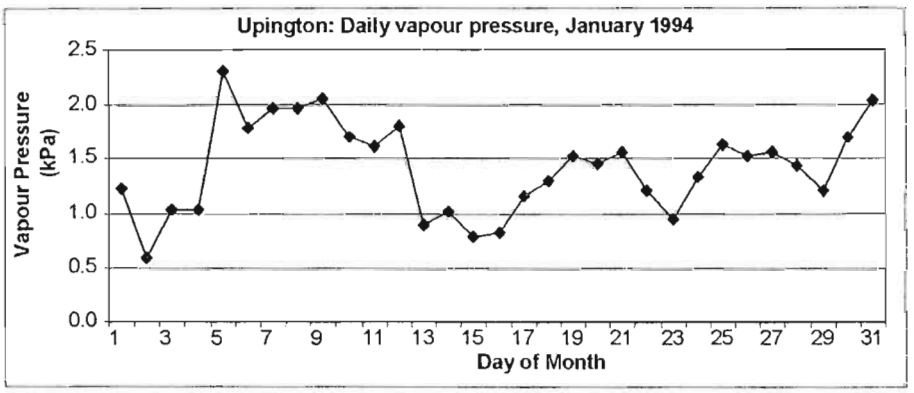

Figure 5.17 A plot of daily vapour pressure at Upington during January 1994

5.8 Vapour Pressure and Continentality

The term "continentality" can be described as a change experienced by a given weather variable with increasing distance from the ocean. If one were to move from east to west across South Africa from the Indian Ocean, towards the interior along the same line of latitude, increasing aridity is experienced until one begins to feel the effects of the proximity of the Atlantic coast. It is noteworthy that the cool Benguella ocean current that washes the Atlantic coast causes the aridity that is experienced by the west coast interior where an equivalent distance from the Indian Ocean would be experiencing sub-humid conditions. Common sense dictates, therefore, that there would be a general decrease in average monthly vapour pressure the further one moves into the interior. The following analyses were undertaken to demonstrate the effects of increased distance from the coast on average monthly vapour pressure.

5.8.1 Methods

In the following analysis on vapour pressure and continentality, three weather stations' monthly average of daily vapour pressure values, calculated from 10 years of daily data, were compared with one another. The stations were Newcastle (114 km from the Indian Ocean), Welkom (472 km from the Indian Ocean) and Upington (434 km and 635 km from the Atlantic and Indian Oceans respectively). All three stations lie within the latitudes of 27° to 29° South. Despite the inclusion of Upington, which is considered to be affected by both the Atlantic and the Indian Oceans, particular attention was paid to the effects of continentality from the warmer Indian Ocean, as the West coast and it's adjacent interior is recognised to be much more arid in character.

5.8.2 Results and Discussion

As may be observed from Figure 5.18, the further one moves into the interior, the lower the monthly mean of daily vapour pressure becomes, particularly in the summer months. It is, however, noteworthy that all three locations under

observation experience similar uncorrected vapour pressure during the cooler and drier winter months.

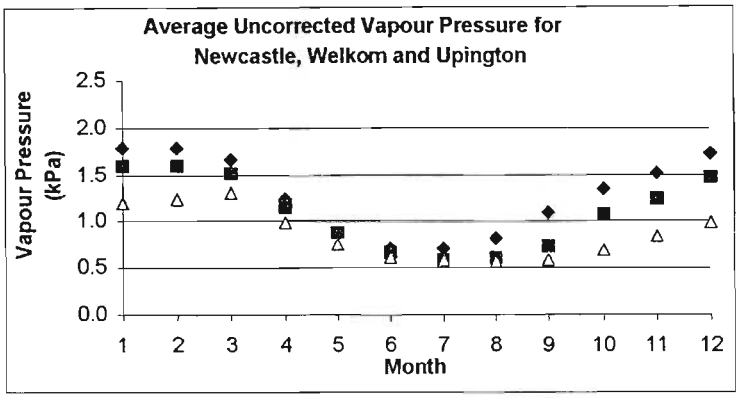

Figure 5.18 Average monthly vapour pressure versus months, for Newcastle (◆), Welkom (■) and Upington (△), displaying decreasing vapour pressure with increasing distance from the sea

5.8.3 Conclusions

It was concluded that increasing continentality, expressed as distance from the oceans produces a decrease in average monthly vapour pressure. Continentality could, therefore, readily be included in a vapour pressure model.

5.9 Vapour Pressure and Latitude

Southern Africa spans a range of latitudes from 22° to 34°S. This range in latitudes allows for many different climates regimes to be experienced. For example, the Western Cape is strongly affected by frontal systems emanating from the South Atlantic, particularly during the winter months, whereas the summer rainfall regions are affected by moist air originating from the tropical and equatorial regions. It is hypothesised, therefore, that in the summer rainfall areas a progressive decline in average daily vapour pressure should be experienced as one moves from North to South.

5.9.1 Methods

An analysis was conducted to investigate the effects of increasing latitude on average monthly vapour pressure. In order to avoid the effects of rainfall seasonality, the following analysis excluded the winter rainfall regions. Average monthly uncorrected vapour pressure was plotted for Alldays (22.41° S, 29.06° E), Pretoria (25.46° S, 28.12° E) and Bloemfontein (29.07° S, 26.11° E). All three stations lie between 400 and 500 km from the Indian Ocean and all lie within the summer rainfall region. The results are shown in Figure 5.20.

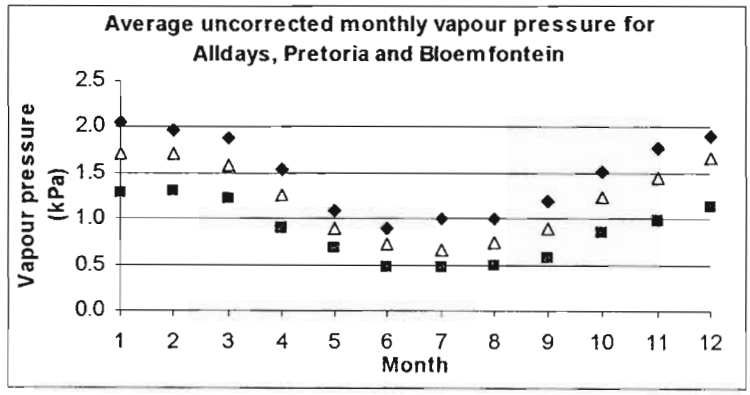

Figure 5.19 Averaged monthly uncorrected vapour pressure for Alldays (◆) Pretoria (△) and Bloemfontein (■), displaying a vapour pressure decrease with increasing latitude

5.9.2 Results and Discussion

As can be observed in Figure 5.19, as one moves south a clear decline in averaged monthly vapour pressure is observed. These observed trends are therefore, hypothesised to be linked, in part, to latitude. Increasing latitude brings with it increased daily temperature ranges (*cf.* Section 5.2) and an increased distance from the source of the humid air masses, *viz.* the Inter Tropical Convergence Zone.

5.9.3 Conclusions

Continentality and distance from the source of air masses combine to decrease the average monthly vapour pressure with increasing latitude in the summer

rainfall regions. Any model for estimating vapour pressure should, therefore, include latitude as a factor.

5.10 Vapour Pressure and Seasonality

As with all climate elements, any given location's vapour pressure regime is likely to be strongly affected by seasonality. It was originally hypothesised, that in the winter rainfall regions, vapour pressure would increase in winter. It was subsequently noted, that vapour pressure values attained their minimum values during winter in these regions, (*cf.* Section 5.3 on vapour pressure and rainfall).

5.10.1 Methods

An analysis was conducted on ten years of daily vapour pressure values obtained from records for Newcastle in KwaZulu-Natal, to represent the summer rainfall region, and Cape Town in the Western Cape, to represent the winter rainfall areas. Records from these two stations were chosen because of their similar lengths. The results are presented in Figure 5.18.

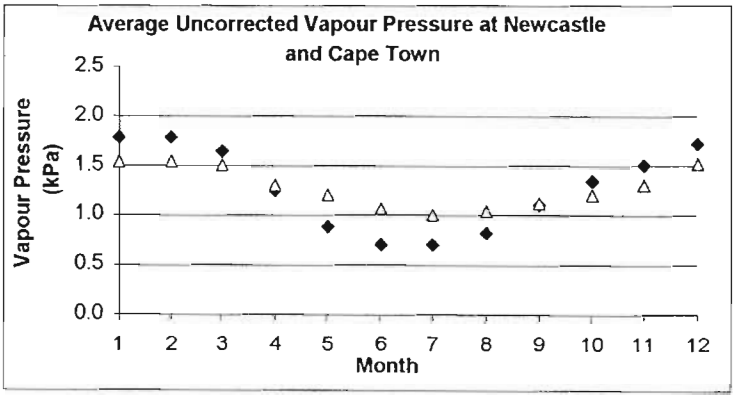

Figure 5.20 Average daily vapour pressure per month, for Newcastle (◆) in KwaZulu-Natal (summer rainfall region) and Cape Town (△) in the Western Cape (winter rainfall region), with averages calculated over a 10 year period for each station.

5.10.2 Results and Discussion

As may be observed in Figure 5.20, summer and winter rainfall climates both exhibit maximum and minimum vapour pressure values in their warm and cool seasons respectively. The amplitude of the curve does, however, reflect rainfall seasonality. For example, Cape Town's winter values are higher than Newcastle's. The converse is true for the summer months (rainy season Newcastle, dry season in Cape Town).

5.10.3 Conclusions

In was concluded from this analysis and from the results of the analysis described in section 5.3 that seasonality plays a significant role in the annual vapour pressure regime, as it does with every other weather variable. Unlike the conclusions of section 5.3, on the influence of rainfall seasonality, it was nevertheless concluded that vapour pressure seasonality could be taken into account in any subsequent model.

5.11 Location and Variability of Daily Vapour Pressure.

As was noted in Section 5.2 and in Figure 5.5, one could experience considerable variability in day-to-day vapour pressure at any given location. Since the context of the aforementioned analysis was aridity, i.e. more arid locations appeared to experience a greater degree of variability, it was decided to further investigate the daily vapour pressure variability and locations link. A better definition for this analysis would perhaps be daily vapour pressure variability and continentality.

5.11.1 Methods

An analysis was conducted to ascertain the degree of variability in daily vapour pressure experienced at a given location, over a given time. Upington was chosen to represent the arid regions and Newcastle was chosen to represent a more humid location. Daily vapour pressure for 10 years, 1990 to 2000, was

plotted for Newcastle and compared with a similar plot of Upington (1993) to 2000. The results may be observed in Figures 5.21 and 5.22.

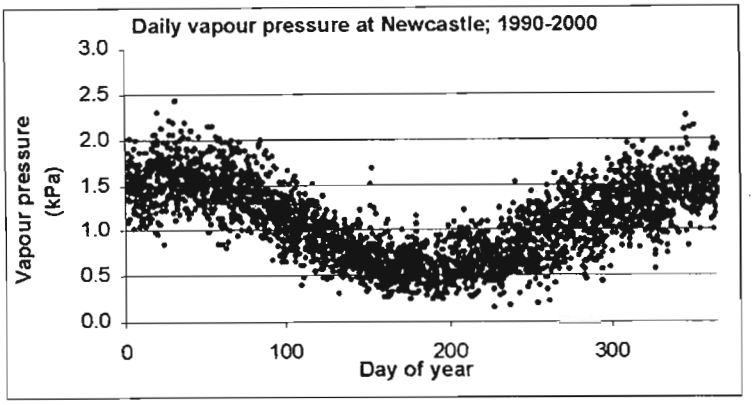

Figure 5.21 The variability of average daily vapour pressure throughout the year at Newcastle in KwaZulu-Natal, in a sub-humid climate

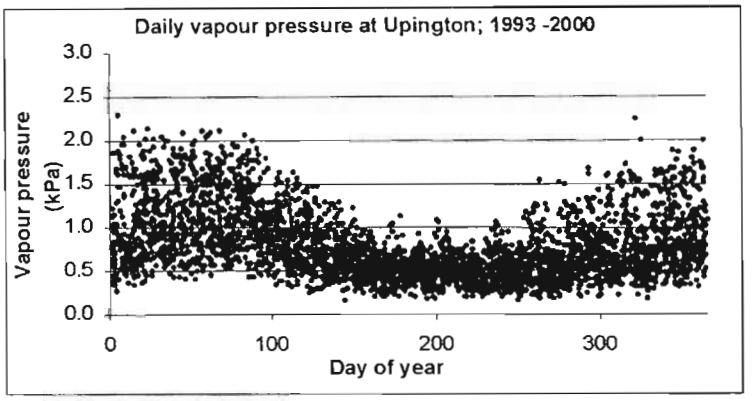

Figure 5.22 The variability of average daily vapour pressure throughout the year at Upington in the Northern Cape, in an arid region

5.11.2 Results and Discussion

As may be observed in a comparison of Figures 5.21 and 5.22, Upington experiences considerably greater variability in day-to-day vapour pressure than Newcastle. It was concluded that the more arid a given location, the greater the degree of variability at that location.

5.11.3 Conclusions

Little can be done to include daily vapour pressure variation in a vapour pressure

model, as any model would then have to include wind direction and windspeed (*cf.* Figures 5.13 to 5.16). Any user of a model to estimate daily or monthly vapour pressure must, however, consider the day-to-day variability (*cf.* Figures 5.4 and 5.5) and the intra-day variability (*cf.* Figure 5.4).

5.12 Overall Conclusions

Two resolutions of vapour pressure, monthly and daily are studied in this chapter. For average monthly vapour pressure it was concluded that a combination of invariate information, latitude, continentality and seasonality, and variable data in the form of temperature and temperature range data play a dominant role in determining vapour pressure at a given location.

For average daily vapour pressure, it was concluded that air masses were the dominant influence on vapour pressure at any given location. The influence of air masses depended largely on it origin and location of interest. In the study example (Upington) in Section 5.4, it was noted that air masses originating in equatorial regions always drove vapour pressure up whereas air masses originating over coastal regions drove daily vapour pressure down. There is nevertheless evidence that ocean temperature plays a considerable role in determining the ambient vapour pressure of a given air mass. In an identical study of Greytown, air masses originating off the warmer Indian Ocean, increased the vapour pressure in addition to equatorial/tropical air, which had a much longer fetch.

The ultimate objective of Chapter 5 is the identification of variable and invariate data for the modelling of vapour pressure at a given location in South Africa. It was decided that all the invariates; latitude, continentality (expressed as distance from the sea) and seasonality could be employed in a monthly vapour pressure model. The employment of variables, which would obviously be used to model vapour pressure at higher resolution (daily) posed a unique set of problems. Temperature and rainfall data, are easily obtainable data, however wind direction and wind speed data which would be required for modelling the movement of air

masses are not readily available on contemporary databanks. It was decided therefore that air masses could not be included in any model with the limited resources available for this dissertation.

In light of the findings of Chapter 5, in Chapter 6, is devoted to modelling vapour pressure on monthly basis, thereafter attempting to estimate RH and VPD by holding the vapour pressure constant for both equations.

Chapter 6

ESTIMATION OF VAPOUR PRESSURE OVER SOUTH AFRICA

In Chapter 5 various factors, which influence daily vapour pressure over South Africa were identified. These factors were divided into two categories, *viz.* the invariate factors such as seasonality, continentality and latitude and the variate factors such as daily temperature range, the occurrence of rainfall and characteristics of air masses. In this chapter, average monthly vapour pressure is to be modelled throughout South Africa using derivatives of all the aforementioned invariates/variables. Thereafter the models developed are to be verified against observed data at several locations throughout the country with widely different climatic characteristics.

6.1 Selection of Variables

All the invariate factors described in Chapter 5 were chosen, although not necessarily in their commonly used form. Continentality, for example, was simply expressed as distance from the sea. Latitude required no further alteration. In order to account for changes in seasonality, individual regressions were run for each month of the year, thereby isolating effects not only of temperature, but also of precipitation regimes.

The variables described in Chapter 5, *viz.* seasonality, continentality, latitude and temperature range, require further discussion. As was concluded in Chapter 5, the relationship between rainfall and uncorrected vapour pressure appears associative rather than causative. It is also known that rainfall from individual events can be highly variable over a short distance, particularly when it is of a convective nature or falls over mountainous areas. For these reasons it was decided that rainfall/raindays should not be considered as a variable.

It was concluded in Chapter 5 that air masses play the single most important role in day-to-day variability of vapour pressure within a given month. It was also

concluded that the origin of the air mass determined whether vapour pressure would be increased or decreased at that given location. Since it is not possible to determine the latter fact without complex models, air masses were not given further consideration.

A considerable volume of observed data, as well as estimated values, exist for average daily temperature range. This element was, therefore, also included as a variable in the multiple regression analysis.

In addition to the aforementioned variables, two others, which were not previously considered in any detail, were also included. These variables are longitude and altitude. Longitude was selected because of its association with a general west to east (increasing) gradient of influence on vapour pressure fluxes over South Africa (McGee, 1971), a feature which is also evident in Figure 6.1. Altitude was selected as a result of an earlier attempt during this research at mapping uncorrected vapour pressure over South Africa using spatial interpolation, as displayed in Figure 6.1. As may be observed, a rapid decrease in uncorrected vapour pressure occurs when moving inland to higher altitudes, from the coastal regions. The intensity of the vapour pressure gradients declines as one moves beyond the escarpment regions.

The regressions on uncorrected vapour pressure were performed by iteratively increasing the number of independent variables (note that the "invariate factors" also fall into this category).

6.2 Results of the Multiple Regression Analyses

Table 6.1 illustrates how the independent variables were transformed for use in the multiple regression equations, in order to ensure that they displayed similar ranges (~0 to 4). Tables 6.2 to 6.4 present the adjusted R^2 values of the multiple regression analyses, accompanied by the P-values of the independent variables, where P-values are defined as the probability of wrongfully excluding the given

independent variable. Results from the months of January (midsummer) and July (midwinter) are presented in each case, for progressively more complex iterations.

Table 6.1 The transformation of variables used in the multiple regression model

Invariate/Variable	**Transformation**
Distance from sea	Log[Distance from Sea (km)]
Latitude	[Latitude(degrees, decimal) -20]/6
Longitude	[Longitude(degrees, decimal) -10]/6
Altitude	[Altitude(m)]/1000
Temperature range	[Temperature Range(°C)]/10

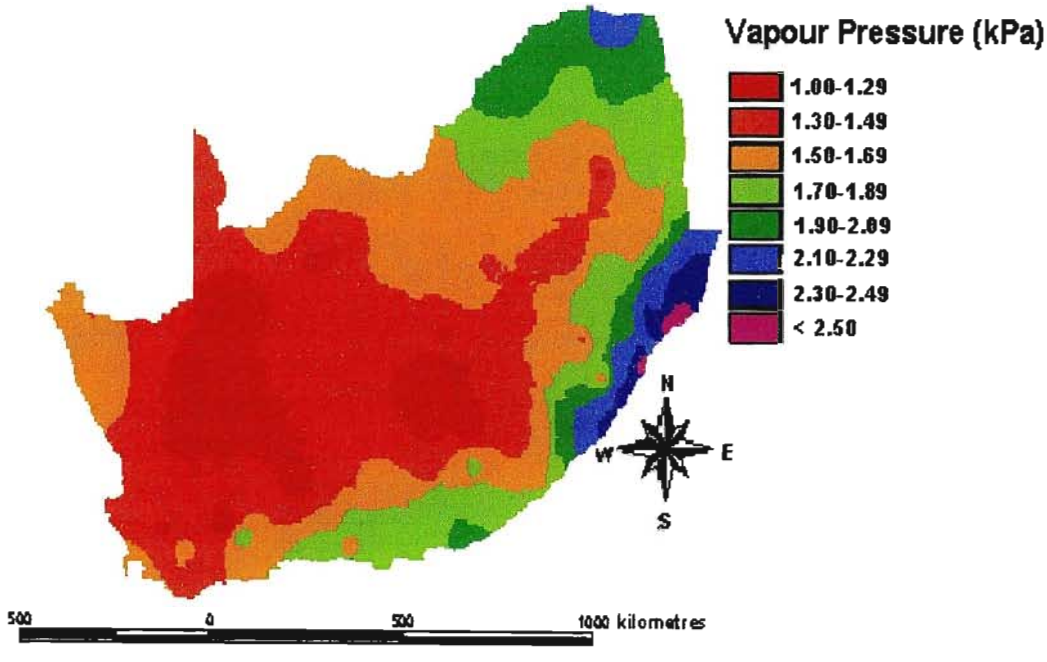

Figure 6.1 Average uncorrected vapour pressure over South Africa for the month of January, mapped using spatial intepolation

Table 6.2 Estimation of uncorrected monthly vapour pressure using geographical information only (n= 62)

Variate/Invariate	**January** R^2 = 0.71 P-value	**July** R^2 = 0.73 P-value
Intercept	1.05E-13	7.02E-14
Distance from sea	8.62E-13	4.92E-16
Latitude	1.28E-05	0.00102
Longitude	2.97E-05	0.45560

Table 6.3 Estimation of uncorrected monthly vapour pressure using geographical information and temperature range (n= 62)

Variate/Invariate	**January** R^2 = 0.71 P-value	**July** R^2 = 0.76 P-value
Intercept	1.16E -12	2.57E-14
Distance from sea	2.77E-07	5.08E-06
Latitude	3.3E-05	5.42E-05
Longitude	9.31E-05	0.92334
Temperature range	0.538693	0.00368

Table 6.4 Estimation of uncorrected monthly vapour pressure using geographical information, temperature range and altitude (n=62)

Variate/Invariate	**January** R^2 = 0.81 P-value	**July** R^2 = 0.89 P-value
Intercept	1.65E -13	7.06E-16
Distance from sea	0.02502	0.004460
Latitude	1.82E-05	1.81E-06
Longitude	1.95E-08	0.01115
Temperature range	0.756154	0.00531
Altitude	4.32E-07	7.37E-11

In a final exercise, South Africa (hitherto treated as a single geographical unit for the purposes of the regression equations) was split into two regions,

distinguishing between a region deemed to be affected by the warm Indian Ocean current and that region affected by the cooler Altantic Ocean in the west. The hypothesis to split South Africa was developed as a result of mapping vapour pressure by inverse distance weighting (*cf.* Figure 6.1), where a definite difference in the characteristics of uncorrected vapour pressure can be observed between the western quarter of the country and the remaining eastern and southern parts of South Africa.

Figure 6.2 illustrates how the country was partitioned. Note that owing to the low P-values associated with the longitude factor, this element was omitted from the regression. The results are presented in Tables 6.5 (Indian Ocean region) and 6.6 (Atlantic Ocean region) respectively.

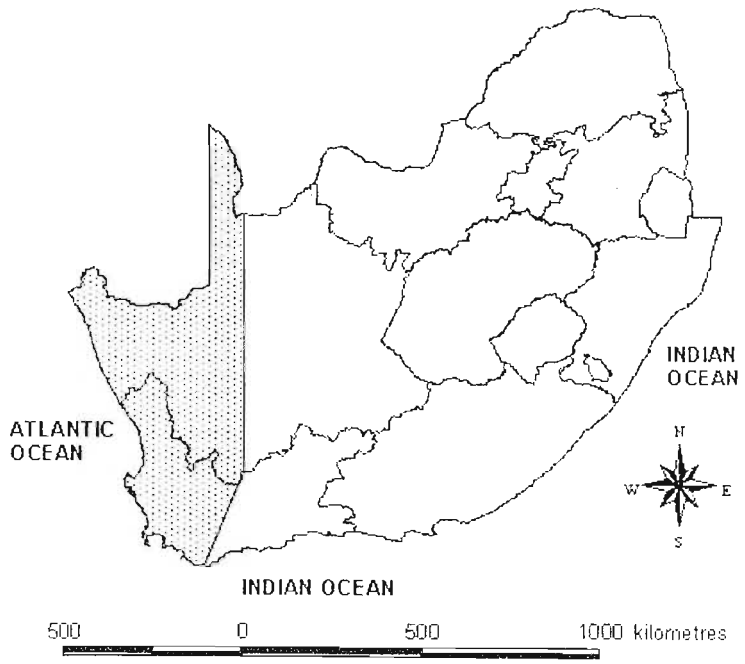

Figure 6.2 Partitioning of South Africa according to those regions deemed to be affected by the Indian and Atlantic Oceans respectively

Table 6.5 Estimation of uncorrected vapour pressure in that region of South Africa deemed to be affected by the Indian Ocean, using geographical information, temperature range and altitude (n = 50)

Variate/Invariate	**January** R^2 = 0.81 P-value	**July** R^2 = 0.93 P-value
Intercept	2.01E -26	6.59E-21
Distance from sea	0.02865	3.71E-08
Latitude	2.79E-05	3.07E-13
Altitude	0.01010	8.9E-09
Temperature range	0.01594	0.18992

Table 6.6 Estimation of uncorrected vapour pressure in that region South Africa deemed to be affected by the Atlantic Ocean, using geographical information, temperature range and altitude (n = 11)

Variate/Invariate	**January** R^2 = 0.69 P-value	**July** R^2 = 0.89 P-value
Intercept	0.06823	0.80330
Distance from sea	0.13806	0.06933
Latitude	0.57440	0.04035
Altitude	0.01964	0.00141
Temperature range	0.21283	0.09170

6.3 Discussion and Conclusions: Multiple Regression Analyses

The lowest P-values (*i.e.* most significant elements) were recorded by the intercept in the majority of cases (7 times out of 10). The intercept, therefore, was concluded to be the single most important factor used to estimate vapour pressure at a given location. Only in the final analysis (Table 6.6), where the western part of the country was analysed by itself, was this trend broken. In the final analysis of the variables used, altitude plays the most significant role in vapour pressure estimation, both during January (summer) and July (winter). The influence of altitude is discussed in subsequent paragraphs. It should also be noted that the penultimate analysis (Table 6.5) produced the most significant

values of all the analyses. Again, these values are associated with the intercept. This fact alone justifies partitioning the country when estimating vapour pressure.

The effects of adding altitude to the multiple regression model increased the variance by, on average, 10%. Multi-collinearity between distance from the sea and altitude partially explains the significant impact the latter invariate has on the multiple regression, but does not explain the phenomenon in full. It is hypothesised, therefore, that altitude is not a completely independent variable (Savage, 2003; personal communication).

Having introduced altitude into the model, latitude becomes the next most significant variable. It must be stated, however, that this factor remained highly significant throughout the multiple regression analysis.

Longitude appears to play a more significant role during the summer months, but becomes inconsequential during the winter months. It is hypothesised that during the winter months, when vapour pressure throughout the country is low, much smaller vapour pressure gradients are recorded longitudinally.

Finally, temperature range, which was the only non-geographical variable to be included in the multiple regression analysis, was also the least significant of the variables throughout the analyses. Temperature range becomes more significant in the winter months than the summer months. It is suggested that this is a result of the greater temperature ranges frequently experienced during these months.

It is clear that several methods are available to the researcher for estimating average monthly vapour pressure. It would be incorrect to conclude that geographical location determines a given location's vapour pressure regime to the exclusion of weather variables. It has already been explained that air masses had to be excluded on the grounds of complexity in estimating this variable. It was concluded that the method of delineating the country into a region affected by the Atlantic and one affected by the Indian Oceans produced

the highest amount of variance. In the verification section which follows, the last-named method, *viz.* that described in Tables 6.5 and 6.6, is therefore employed.

6.4 Verification: Vapour Pressure, Relative Humidity and Vapour Pressure Deficit

In Chapter 5 it was established that air masses play the most significant role in determining vapour pressure at a given location over a short time-span, e.g. daily. It was determined that in order to estimate daily vapour pressure, further surrogate data were required, principally in the form of windspeed and wind direction. Neither off these variables could be deemed "simple surrogates" in that both are relatively difficult data to obtain. This paucity is the result of there being fewer weather stations recording both these elements. Since vapour pressure values are being sought also for the further estimation of RH and vapour pressure deficit (hereafter VPD), it was decided to hold vapour pressure constant for a given month and allow daily RH and VPD fluctuations to be determined by the saturation vapour pressure part of the respective equations. In the following verification exercises estimates of monthly vapour pressure, and thereafter of daily RH and daily VPD are evaluated against observed values at several locations around South Africa, which display wide ranging climatic functions.

Ten verification stations were chosen throughout South Africa. Weather stations selected were: Alldays (tropical-humid), Beaufort West (arid), Bisho (coastal interior), Ceres (winter rainfall), Johannesburg Botanical Gardens (semi-arid), Joubertina (winter rainfall, coastal interior), Kimberley (arid), Piet Retief (highveld, moist) Postmasburg (arid) and Prieska (arid). The locations of these weather stations and their corresponding climate indices are displayed in Figure 6.3 and Table 6.7 respectively. Note that the eleventh station in Table 6.7, Upington, is not a verification station *per se*, but is nevertheless involved in the final verification exercise.

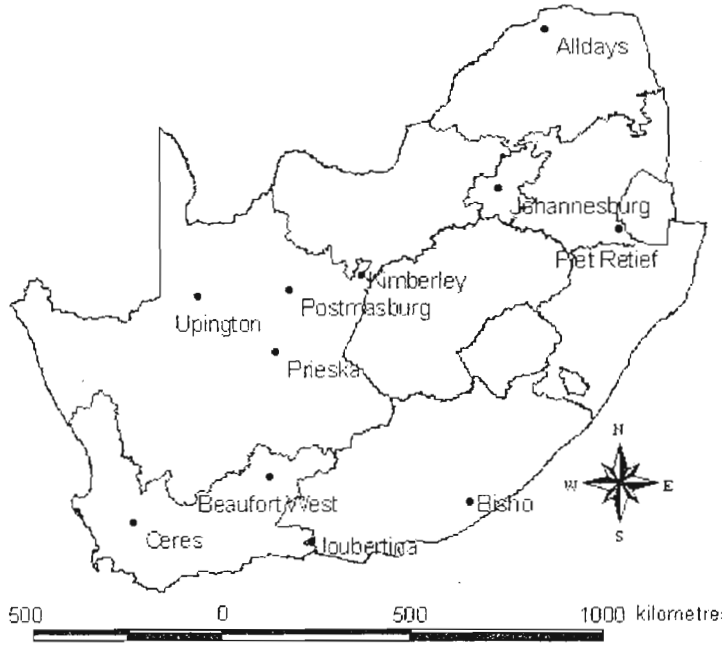

Figure 6.3 Locations of weather stations employed in the vapour pressure verification analyses

Table 6.7 Climate statistics from the weather stations employed in the vapour pressure verification analyses

Location	Altitude (m)	January Mean of Daily Maximum Temperature (^{0}C)	January Mean of Daily Minimum Temperature (^{0}C)	July Mean of Daily Maximum Temperature (^{0}C)	July Mean of Daily Minimum Temperature (^{0}C)	Mean Annual Precipitation (mm)
Alldays	693	32.8	20.4	24.8	5.2	388
Beaufort West	899	31.0	16.0	24.8	-3.6	369
Bisho	596	28.8	18.3	22.8	9.7	465
Ceres	1079	30.2	16.2	16.2	2.5	573
Johannesburg	1652	24.2	13.4	17.1	2.0	804
Joubertina	722	27.2	13.2	19.5	3.3	501
Kimberley	1197	32.1	17.5	21.6	4.1	379
Piet Retief	1232	25.4	16.1	20.9	3.5	929
Postmasburg	1323	29.7	16.4	19.4	1.2	264
Prieska	947	35.9	18.6	19.2	0.5	251
Upington	779	33.1	17.6	21.5	3.5	129

6.5 Verification of the Monthly Vapour Pressure Models

All the required geographical and temperature range data were obtained for the aforementioned stations, transformed (*cf.* Table 6.1) and then keyed into the multiple regression model. Model results are shown for two months, *viz.* January (midsummer) and July (midwinter). The results, which are displayed for the 10 verification stations in Figures 6.4 and 6.5, are a comparison with observed averaged data for January and July.

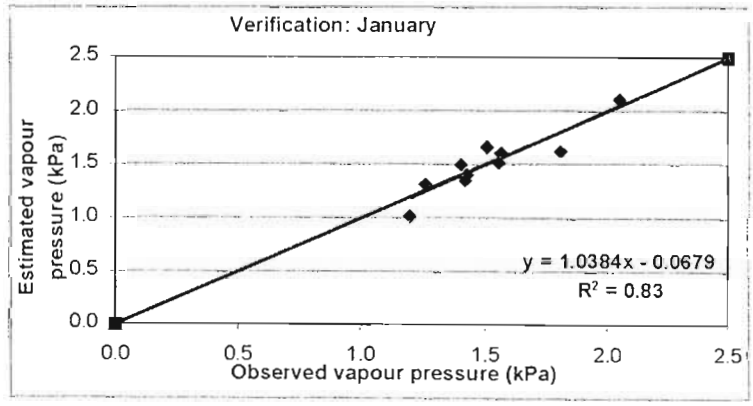

Figure 6.4 A comparison of estimated averaged monthly vapour pressure versus observed averaged monthly vapour pressure for 10 verification stations for the month of January

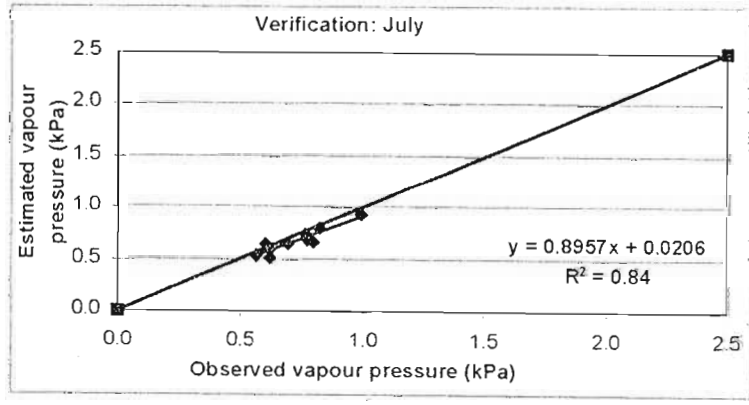

Figure 6.5 A comparison of estimated averaged monthly vapour pressure versus observed averaged monthly vapour pressure for 10 verification stations for the month of July

As may be observed, averaged monthly vapour pressure can be accurately estimated using the multiple regression models developed in Sections 6.1 and 6.2. For summer and winter, the intercepts were under 1 kPa and the R^2 were 0.83 and 0.84 for January and July respectively. The errors associated with the above models were considered to be very small, thereby allowing for the aforementioned models application to be tested for use in the estimation of more directly applicable climate elements associated with vapour pressure, *viz.* RH and VPD.

6.6 Application of the Monthly Vapour Pressure Models to Estimate Monthly Relative Humidity

Vapour pressure values *per se* are not a sought-after element. The requirements for vapour pressure information, for the purposes of this dissertation, is for obtaining the numerator in the relative humidity equation and as a factor in the vapour pressure deficit equation. The objectives of Sections 6.6 and 6.7, therefore, are to use the vapour pressure models to estimate daily RH and VPD by employing the vapour pressure models for two given months, January (midsummer) and July (midwinter).

Data from four stations were selected for this verification exercise. Bisho, Piet Retief, Postmasburg and Ceres were selected to represent coastal interior, moist highveld, arid and winter rainfall climates respectively. Postmasburg was used in place of Prieska for reasons of data integrity. The year 1997 was chosen as it had the most complete record for the four stations. July 1994 data were used in place of 1997 data for Piet Retief because of unreliable records at that station in July 1997.

The relative humidity equation is described as follows:

$$\text{Relative humidity} = \frac{\text{Actual Vapour Pressure}}{\text{Saturated Vapour Pressure}} \times 100, \quad \text{i.e. } \mathbf{RH} = \frac{e_d}{e_a} \times 100$$

Maximum and minimum RH were estimated according to the following methodology. Actual vapour pressure was held constant for a given month at the given locations, i.e. the vapour pressure was estimated using the vapour pressure models from Tables 6.5 and 6.6. The saturated vapour pressures at maximum and minimum temperatures were calculated using the Teten's equation. The method recommended by Bristow (1992) of estimating actual vapour pressure by calculating saturated vapour pressure at minimum air temperature, was also included in the verification exercise of minimum RH. Bristow's (1992) method was not used in the verification of maximum RH exercise, as this method always assumes maximum relative humidity to be 100%.

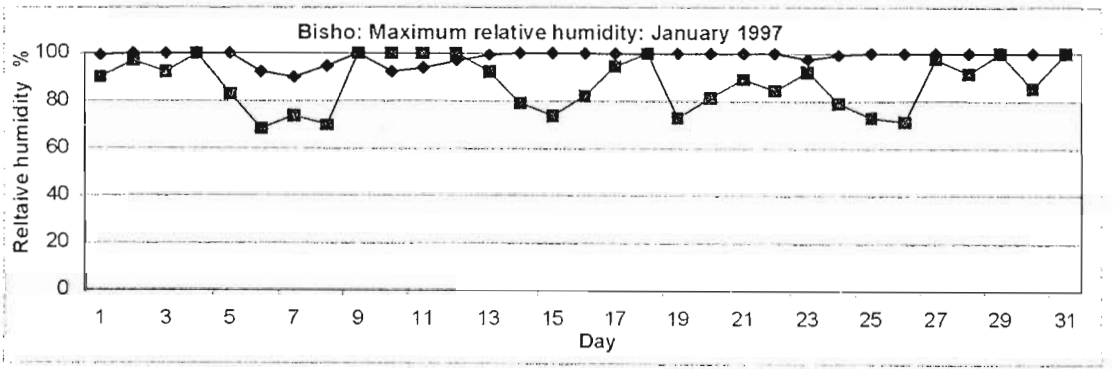

Figure 6.6 Comparison between January observed daily maximum RH (—♦—) and daily maximum RH estimated using the vapour pressure model (—■—) at Bisho in the Eastern Cape

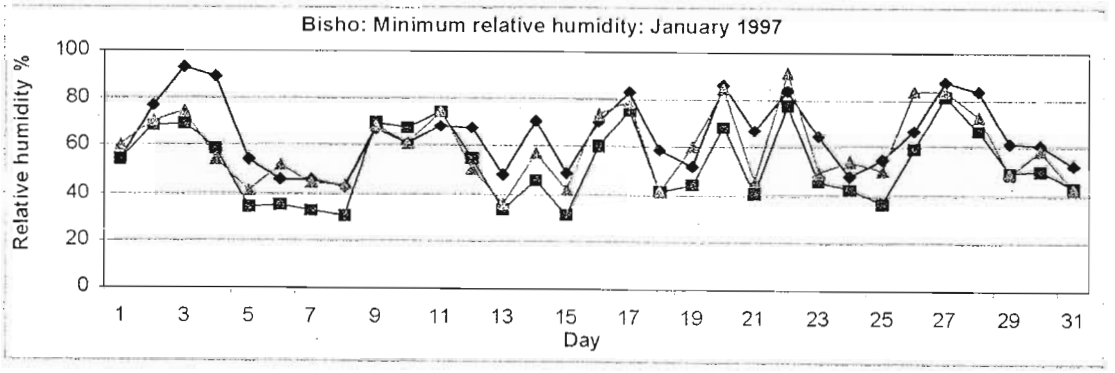

Figure 6.7 Comparison between January observed daily minimum RH (—♦—) and daily minimum RH estimated using the vapour pressure model (—■—) and Bristow's (1992) model (···✱···) at Bisho in the Eastern Cape

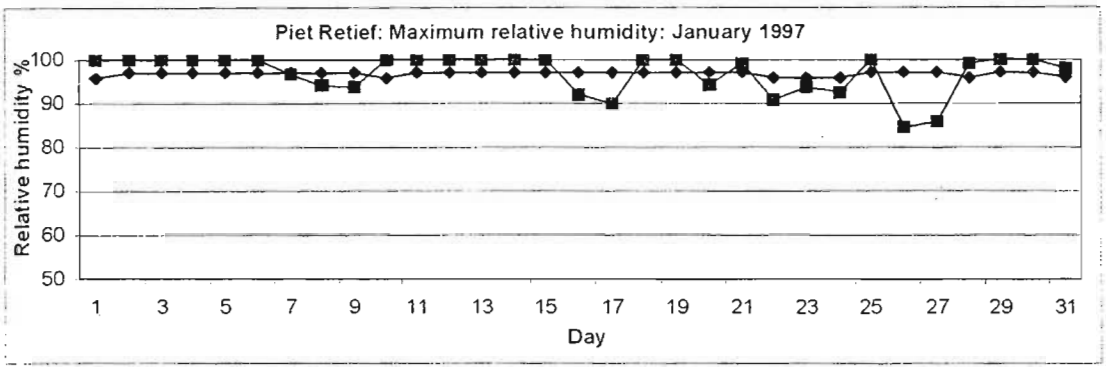

Figure 6.8 Comparison between January observed daily maximum RH (—♦—) and daily maximum RH estimated using the vapour pressure model (—■—) at Piet Retief in Mpumalanga

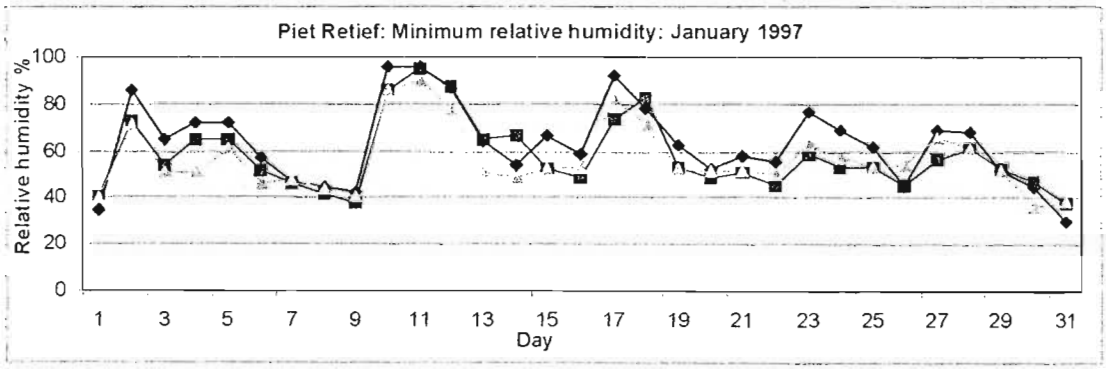

Figure 6.9 Comparison between January observed daily minimum RH (—♦—) and daily minimum RH estimated using the vapour pressure model (—■—) and Bristow's (1992) model (—▲—) at Piet Retief in Mpumalanga

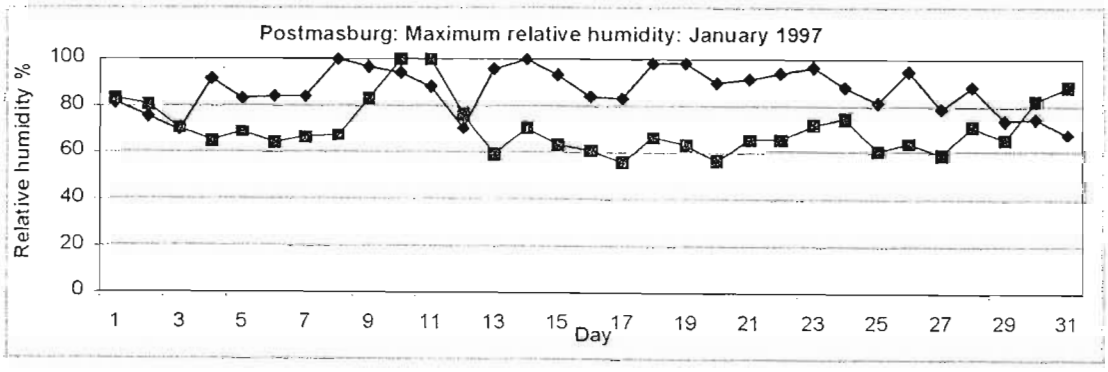

Figure 6.10 Comparison between January observed daily maximum RH (—♦—) and daily maximum RH estimated using the vapour pressure model (—■—) at Postmasburg in the Northern Cape

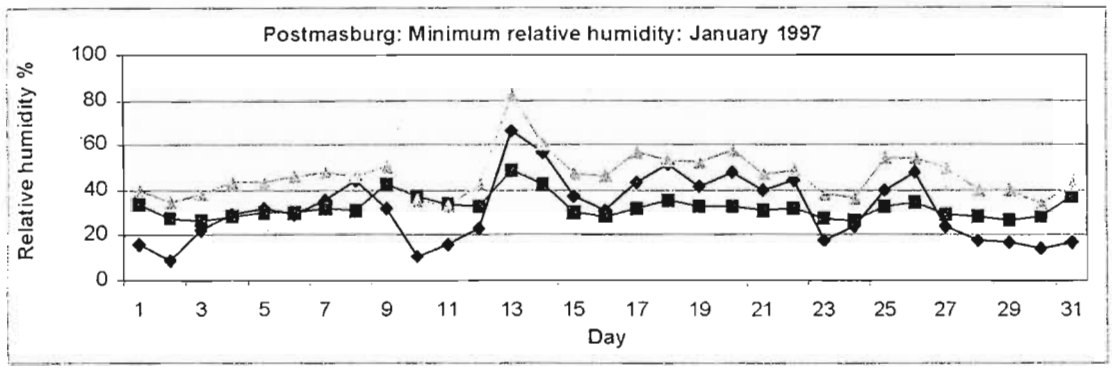

Figure 6.11 Comparison between January observed daily minimum RH (—♦—) and daily minimum RH estimated using the vapour pressure model (—■—) and Bristow's (1992) model (—▲—) at Postmasburg in the Northern Cape

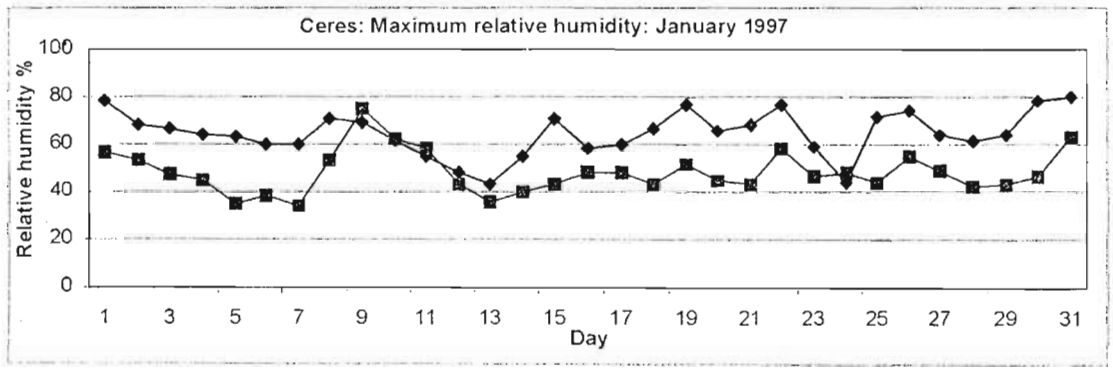

Figure 6.12 Comparison between January observed daily maximum RH (—♦—) and daily maximum RH estimated using the vapour pressure model (—■—) at Ceres in the Western Cape

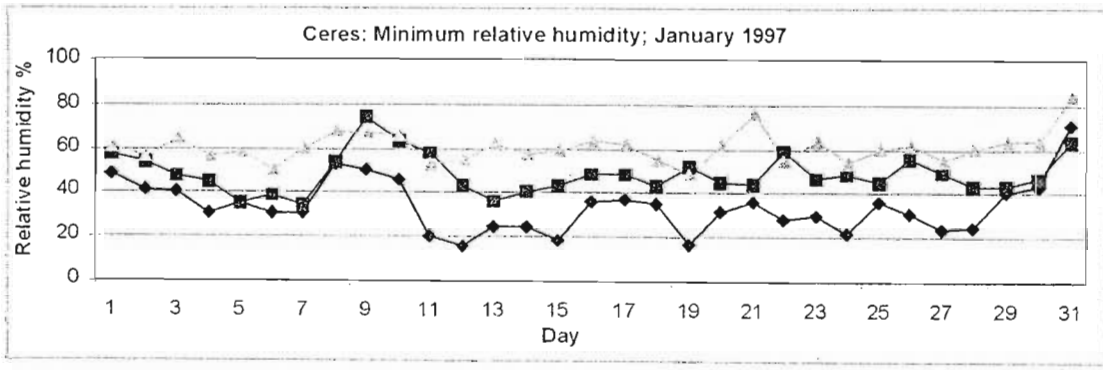

Figure 6.13 Comparison between January observed daily minimum RH (—♦—) and daily minimum RH estimated using the vapour pressure model (—■—) and Bristow's (1992) model (—▲—) at Ceres in the Western Cape

For Postmasburg (Figures 6.10 and 6.11) and Ceres (Figures 6.12 and 6.13), using the vapour pressure model improved on the estimation of maximum and minimum relative humidity over using Bristow's (1992) method. In both cases, the profile drawn by using the vapour pressure model tended to attenuate the peaks and troughs of the relative humidity regime, and in the case of Postmasburg there was a systematic overestimation. The overestimation was not, however, as extreme as that by Bristow's (1992) method. The fact that both successes occurred in relatively arid locations (Ceres' hot and dry summers could be classified as arid) implied that estimating daily relative humidity from the monthly vapour pressure model worked better in arid locations. In the following analysis, this exercise is repeated for the month of July for the four locations.

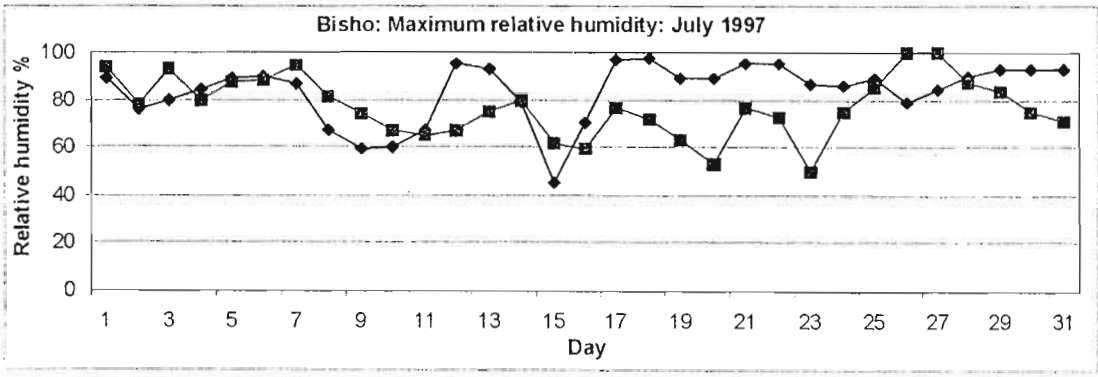

Figure 6.14 Comparison between July observed daily maximum RH (—♦—) and daily maximum RH estimated using the vapour pressure model (—■—) at Bisho in the Eastern Cape

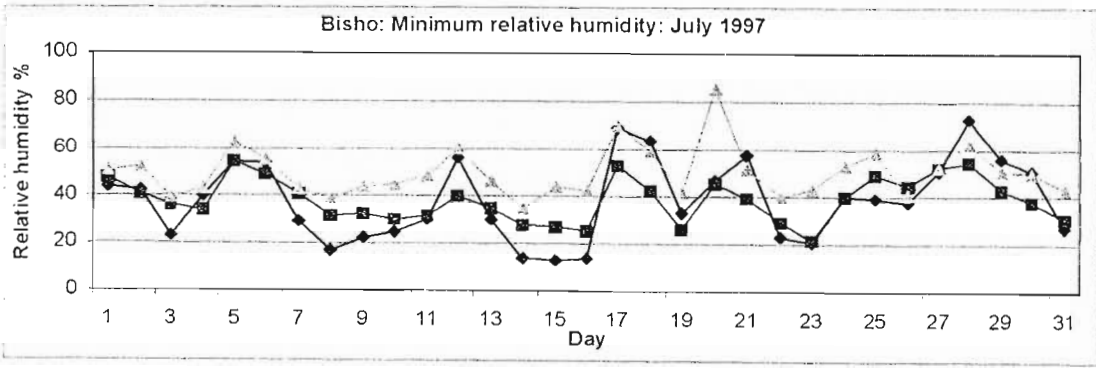

Figure 6.15 Comparison between July observed daily minimum RH (—♦—) and daily minimum RH estimated using the vapour pressure model (—■—) and Bristow's (1992) model (—✱—) at Bisho in the Eastern Cape

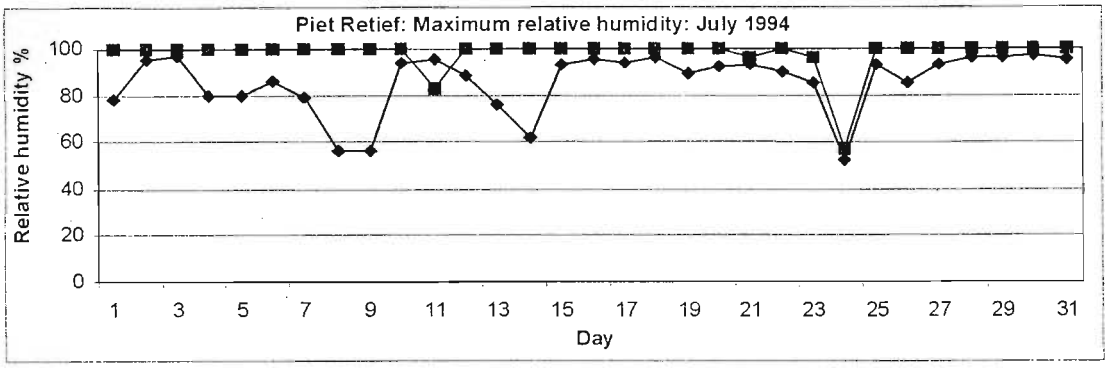

Figure 6.16 Comparison between July observed daily maximum RH (—♦—) and daily maximum RH estimated using the vapour pressure model (—■—) at Piet Retief in Mpumalanga

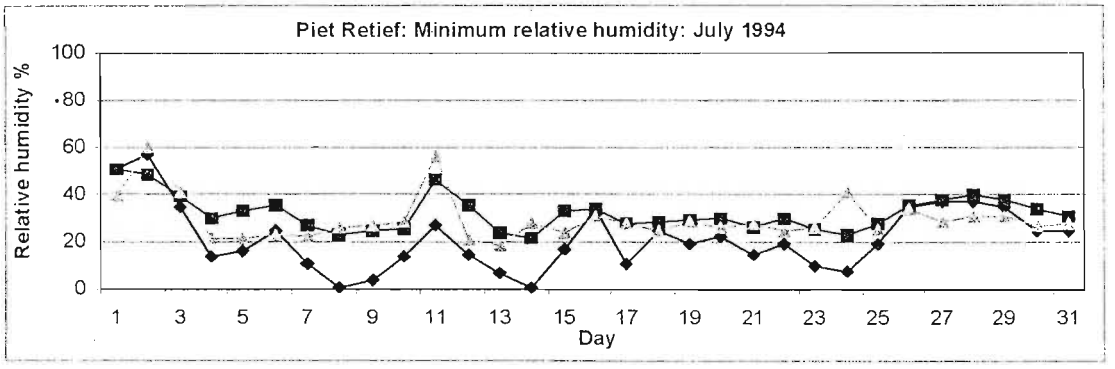

Figure 6.17 Comparison between July observed daily minimum RH (—♦—) and daily minimum RH estimated using the vapour pressure model (—■—) and Bristow's (1992) model (—▲—) at Piet Retief in Mpumalanga

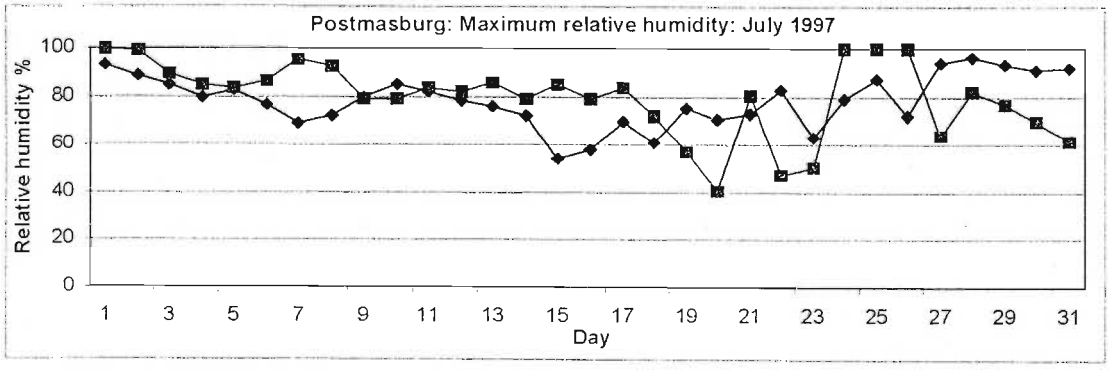

Figure 6.18 Comparison between July observed daily maximum RH (—♦—) and daily maximum RH estimated using the vapour pressure model (—■—) at Postmasburg in the Northern Cape

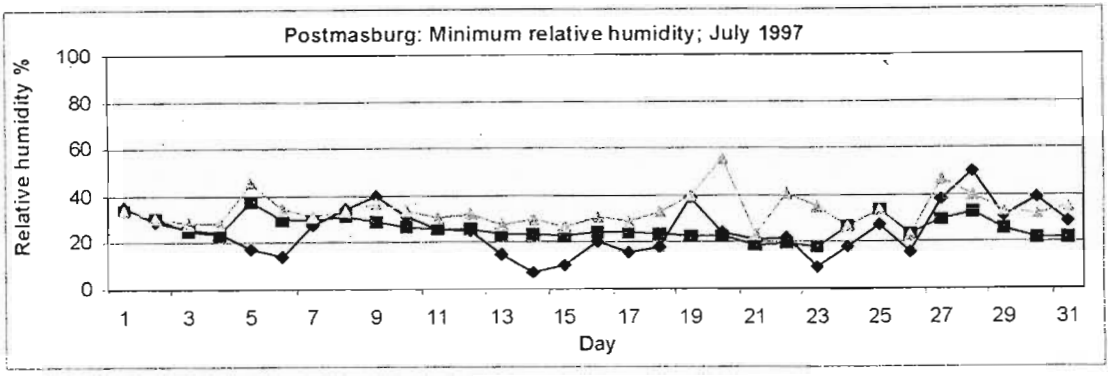

Figure 6.19 Comparison between July observed daily minimum RH (—◆—) and daily minimum RH estimated using the vapour pressure model (—■—) and Bristow's (1992) model (—▲—) at Postmasburg in the Northern Cape

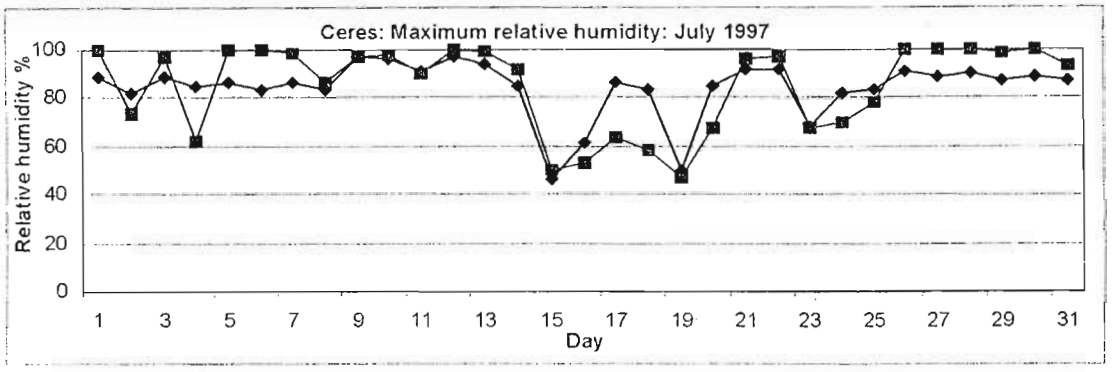

Figure 6.20 Comparison between July observed daily maximum RH (—◆—) and daily maximum RH estimated using the vapour pressure model (—■—) at Ceres in the Western Cape

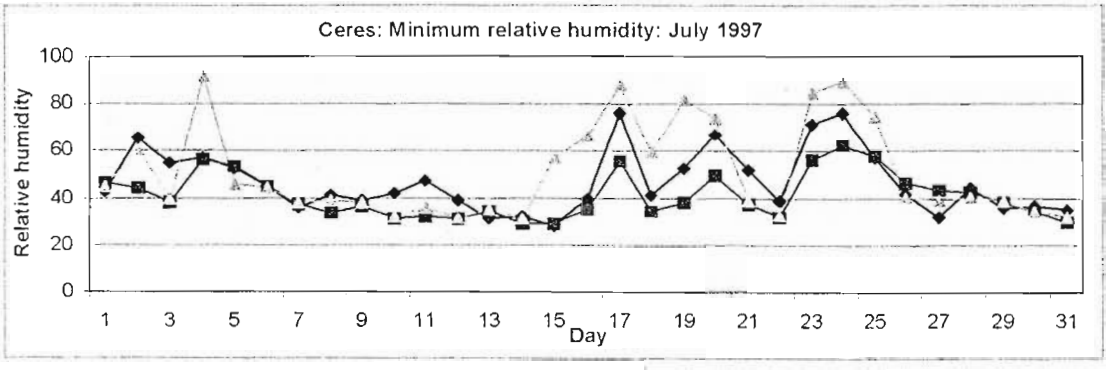

Figure 6.21 Comparison between July observed daily minimum RH (—◆—) and daily minimum RH estimated using the vapour pressure model (—■—) and Bristow's (1992) model (—▲—) at Ceres in the Western Cape

In all cases, with the exception of Piet Retief (*cf.* Figure 6.17), holding vapour pressure constant for the entire month when using the vapour pressure model, improved on the estimation of maximum and minimum relative humidity for the month of July.

It may be concluded that the method of holding vapour pressure constant for an entire month produces a reasonable estimate of daily maximum and minimum relative humidity in that month, particularly during the winter months. It must be stated, however, that if one is estimating daily relative humidity in a moist or humid location, it is advisable to use Bristow's (1992) method, which assumes that actual vapour pressure equals saturation vapour pressure at minimum air temperature.

6.7 Application of the Monthly Vapour Pressure Model to Estimate Daily Vapour Pressure Deficit

In the following analyses, data from four weather stations *viz.* Bisho (coastal interior), Piet Retief (moist, highveld), Postmasburg (arid) and Ceres (winter rainfall) were selected to compare observed with estimated vapour pressure deficit for two months of the year, *viz.* January (midsummer) and July (midwinter). In a manner similar to the relative humidity verification study above, Bristow's (1992) method of estimating actual vapour pressure by calculating vapour pressure deficit at minimum temperature is also employed, in order to establish which method is better suited to estimating vapour pressure deficit.

Vapour pressure deficit is estimated by using the vapour pressure models to calculate actual vapour pressure. Saturated vapour pressure is calculated by first calculating saturated vapour pressure at maximum temperature, then at minimum temperature and finally, averaging the two values. In effect, an average saturated vapour pressure is examined. The format of the following analysis is a repetition of that used in the relative humidity study in Section 6.6, in that January and July values of vapour pressure deficit are presented separately.

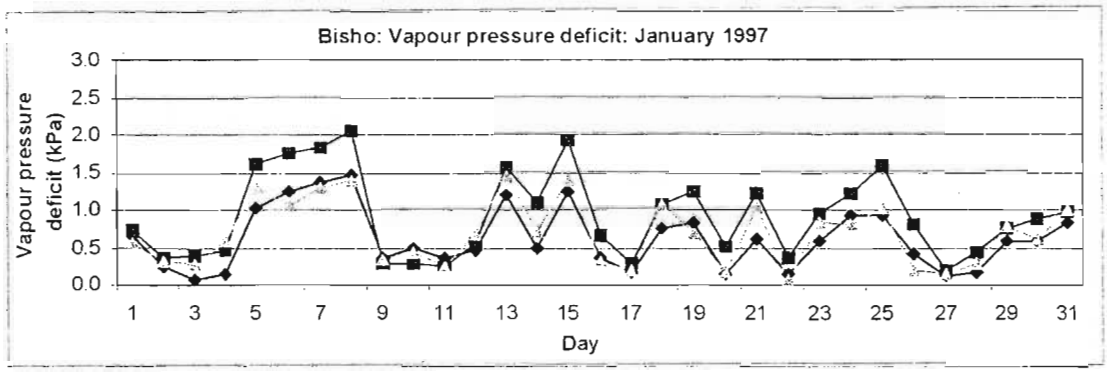

Figure 6.22 Comparison between January observed daily VPD (—♦—) with daily VPD estimated using the monthly vapour pressure models (—■—) and Bristow's (1992) model (···★···) at Bisho in the Eastern Cape

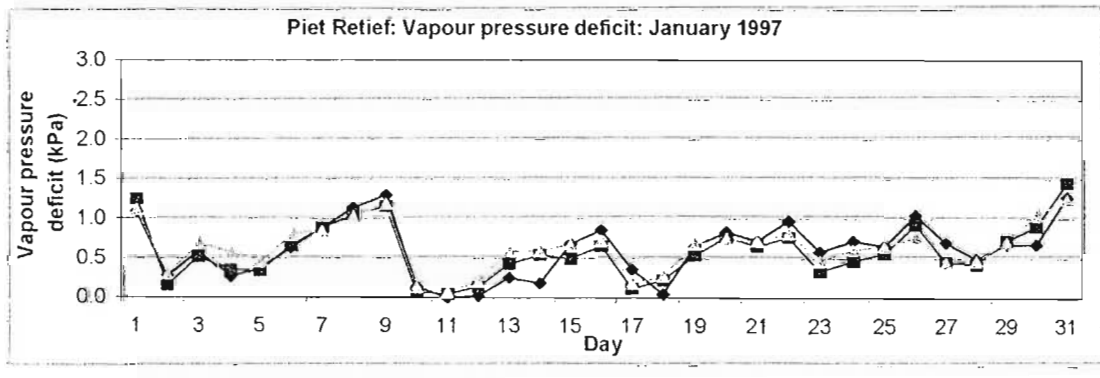

Figure 6.23 Comparison between January observed daily VPD (—♦—) with daily VPD estimated using the monthly vapour pressure models (—■—) and Bristow's (1992) model (···★···) at Piet Retief in Mpumalanga

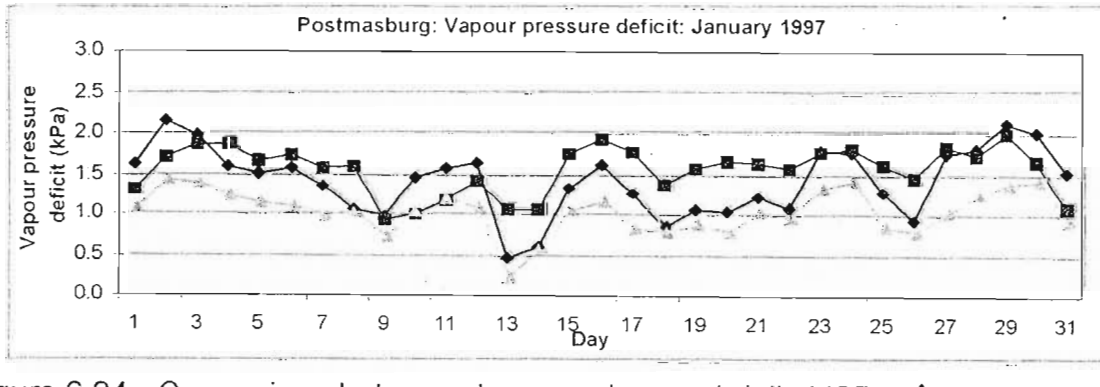

Figure 6.24 Comparison between January observed daily VPD (—♦—) with daily VPD estimated using the monthly vapour pressure models (—■—) and Bristow's (1992) model (···★···) at Postmasburg in the Northern Cape

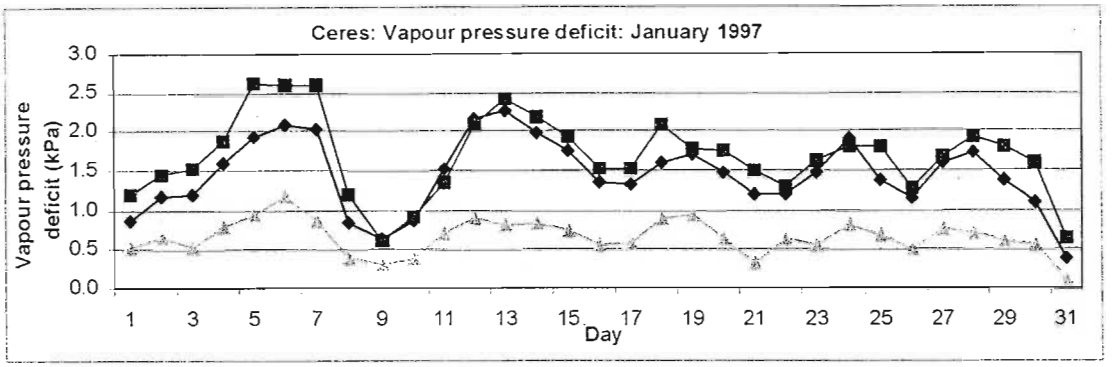

Figure 6.25 Comparison between January observed daily VPD (—♦—) with daily VPD estimated using the monthly vapour pressure models (—■—) and Bristow's (1992) model (···▲···) at Ceres in the Western Cape

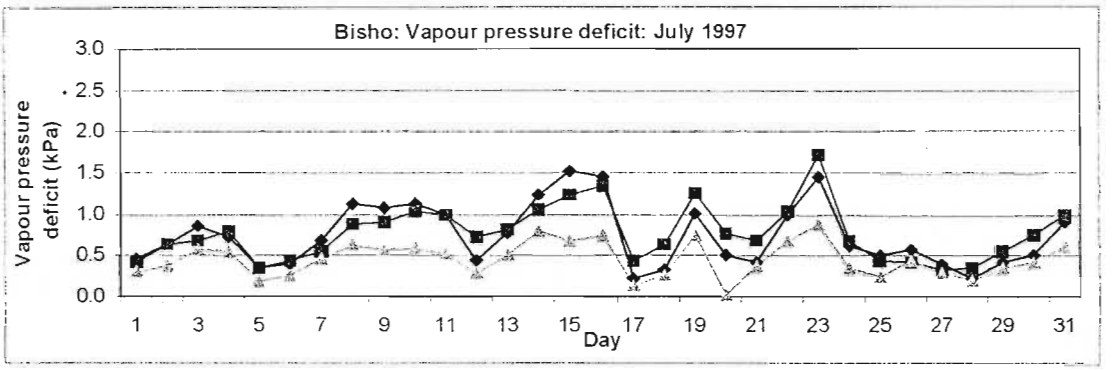

Figure 6.26 Comparison between July observed daily VPD (—♦—) with daily VPD estimated using the monthly vapour pressure models (—■—) and Bristow's (1992) model (···▲···) at Bisho in the Eastern Cape

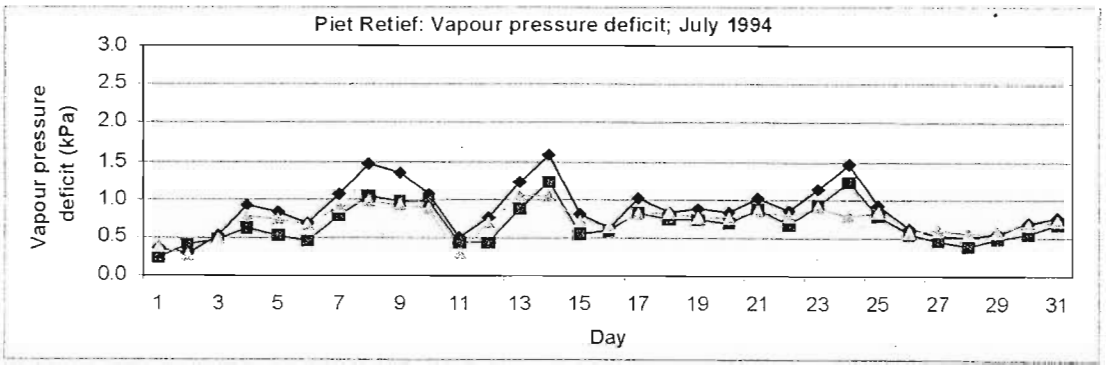

Figure 6.27 Comparison between July observed daily VPD (—♦—) with daily VPD estimated using the monthly vapour pressure models (—■—) and Bristow's (1992) model (···▲···) at Piet Retief in Mpumalanga

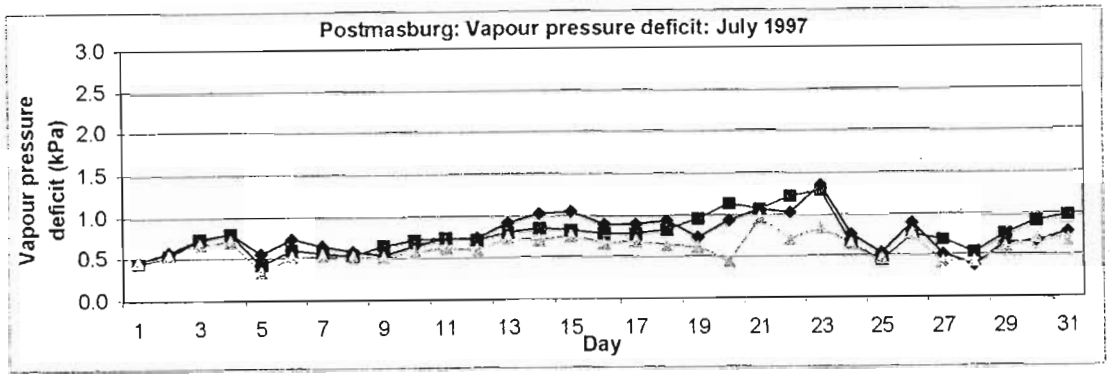

Figure 6.28 Comparison between July observed daily VPD (—♦—) with daily VPD estimated using the monthly vapour pressure models (—■—) and Bristow's (1992) model (—▲—) at Postmasburg in the Northern Cape

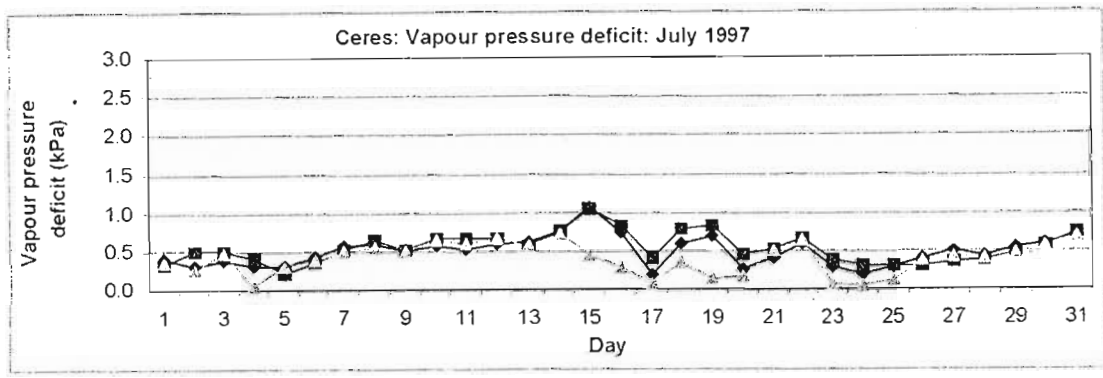

Figure 6.29 Comparison between July observed daily VPD (—♦—) with daily VPD estimated using the monthly vapour pressure models (—■—) and Bristow's (1992) model (—▲—) at Postmasburg in the Northern Cape

Two broad trends are evident from Figures 6.22 to 6.29. First, the method of using the monthly vapour pressure model to calculate average monthly vapour pressure deficit by holding vapour pressure constant for a given month, tended to overestimate daily vapour pressure deficits, compared to an underestimation of daily vapour pressure deficit produced when using Bristow's (1992) method. This was more evident in the summer months than in the winter months. The second broad trend reflected similarities to the relative humidity results, *viz.* that the method worked better in the arid locations and in the drier months. Ceres (Figure 6.25), which is located in a winter rainfall climate, produced the best results in the hot and dry month of January. However, even Ceres produced acceptable results for the month of July (middle of the Western Cape rainy

season). Similarly, Bisho (Figure 6.26) and Postmasburg (Figure 6.28), both in summer rainfall climates, produced their best results in winter (July). For Piet Retief (Figure 6.27), both methods of estimation underestimated the vapour pressure deficit in July.

It was concluded that the method of holding vapour pressure constant for a given month of the year, yielded better results than the Bristow (1992) method. Bristow's (1992) method proved to be better in the winter months (of summer rainfall areas) than in summer months and it produced better results in arid locations throughout the year.

6.8 Temporal Analysis of the Vapour Pressure Models for Estimating Daily Vapour Pressure Deficit

In light of the previous conclusions and of the conclusions of Sections 6.1 to 6.2, where it was indicated that arid locations experience considerably greater variability in daily vapour pressure than more humid locations (*cf.* Figure 6.30, which is a copy of Figure 5.22 from Chapter 5), for Upington in the Northern Cape province), it was decided to repeat the exercise at one location, *viz.* Postmasburg, for its entire length of good record, in this case five years. January was chosen over July as Figure 6.30 indicates that the summer months experience considerably greater variability in average daily vapour pressure than the winter months. Figures 6.31 to 6.35 present the results of this analysis.

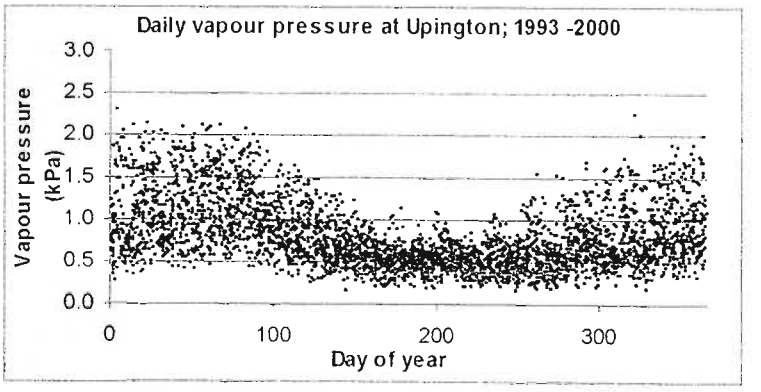

Figure 6.30 The variability of average daily vapour pressure throughout the year for Upington in the Northern Cape

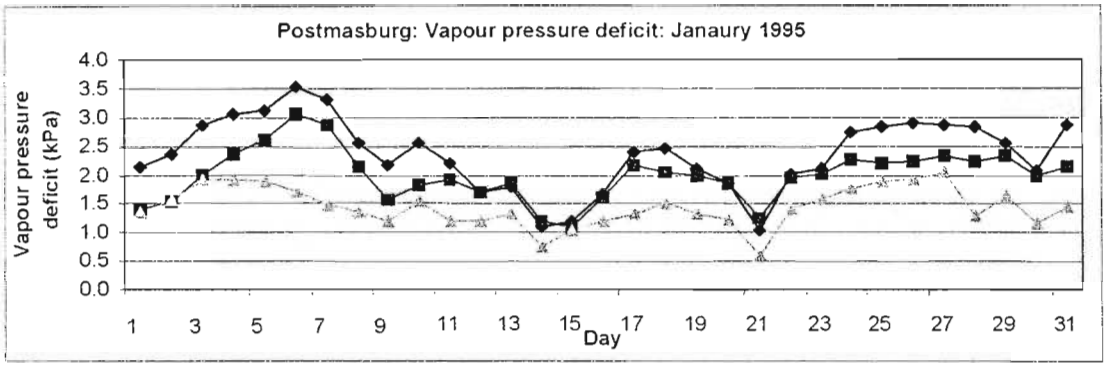

Figure 6.31 Comparison between January 1995 observed daily VPD (—♦—) with daily VPD estimated from the monthly vapour pressure models (—■—) and Bristow's (1992) model (···▲···) at Postmasburg, Northern Cape

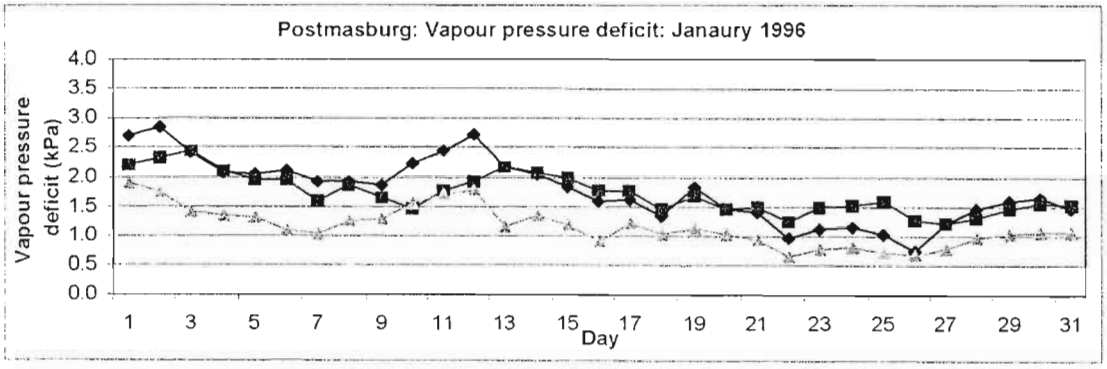

Figure 6.32 Comparison between January 1996 observed daily VPD (—♦—) with daily VPD estimated from the monthly vapour pressure models (—■—) and Bristow's (1992) model (···▲···) at Postmasburg, Northern Cape

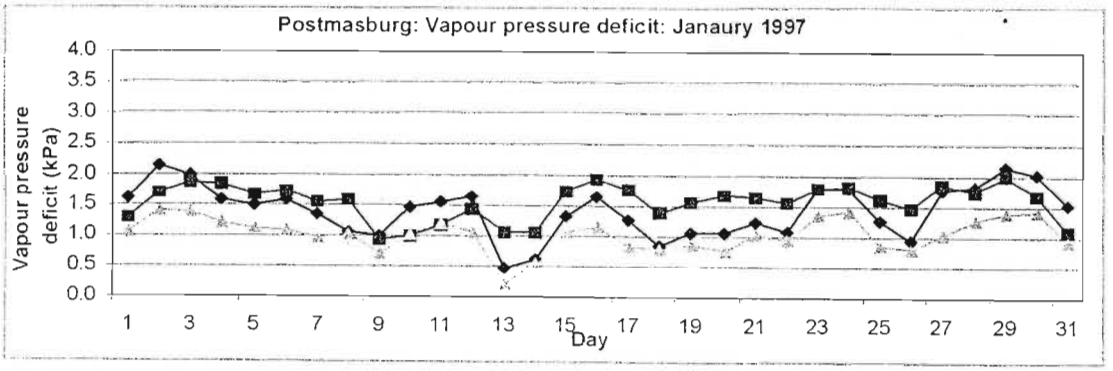

Figure 6.33 Comparison between January 1997 observed daily VPD (—♦—) with daily VPD estimated from the monthly vapour pressure models (—■—) and Bristow's (1992) model (···▲···) at Postmasburg, Northern Cape

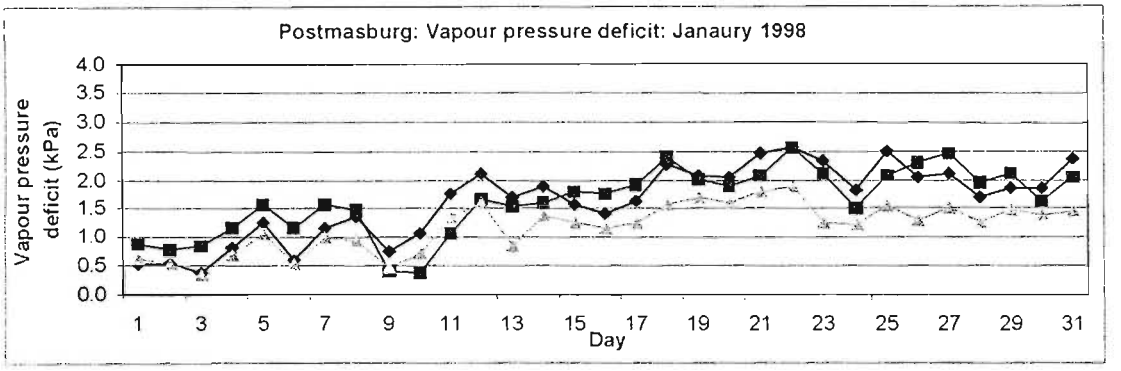

Figure 6.34 Comparison between January 1998 observed daily VPD (—♦—) with daily VPD estimated from the monthly vapour pressure models (—■—) and Bristow's (1992) model (—▲—) at Postmasburg, Northern Cape

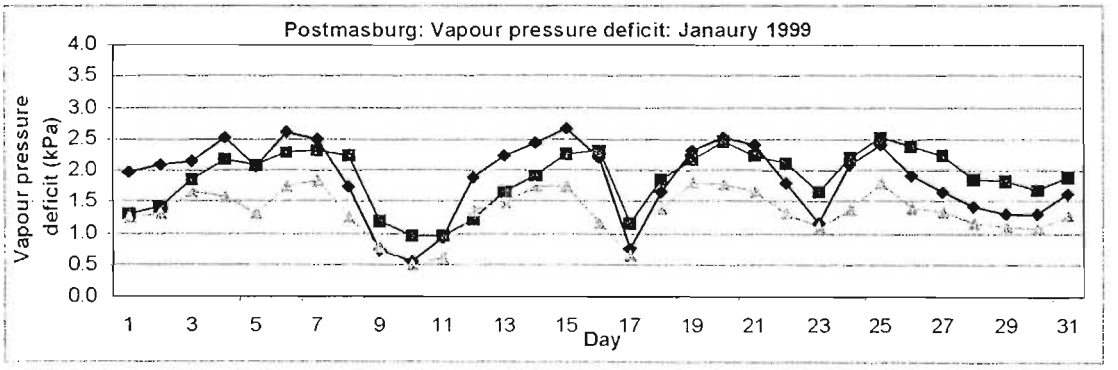

Figure 6.35 Comparison between January 1999 observed daily VPD (—♦—) with daily VPD estimated from the monthly vapour pressure models (—■—) and Bristow's (1992) model (—▲—) at Postmasburg, Northern Cape

The trends commented on in the previous section repeated themselves, *viz.* that using one value of actual vapour pressure for an entire month (estimated using the vapour pressure model) tended to overestimate vapour pressure deficit when compared to using Bristow's (1992) method, which itself, tended to underestimate vapour pressure deficit in arid locations. The extreme variability in daily vapour pressure noted in Section 5.8, failed to sufficiently influence the estimation of daily vapour pressure deficit. The results were, therefore, considered acceptable.

To summarise the findings of all the exercises in Section 6.1 to 6.7, it was concluded that using monthly vapour pressure models to estimate relative humidity and vapour pressure deficit produced acceptable results. The improvements on Bristow's (1992) method occurred in more arid locations and in the dry winter months of the summer rainfall locations.

In the following chapter the monthly vapour pressure models are employed to produce monthly vapour pressure maps for South Africa, whereafter the same values are employed to produce relative humidity and vapour pressure deficit maps.

CHAPTER 7

MAPPING OF VAPOUR PRESSURE, RELATIVE HUMIDITY AND VAPOUR PRESSURE DEFICIT

In Chapter 6 several different models were presented for the estimation of averaged monthly vapour pressure. It was concluded that two different methods were the "best" available for the estimation of monthly vapour pressure over the whole country. The first such method involved employing five variables: Distance from the sea, latitude, longitude, temperature range and altitude. The second method omitted longitude, but the longitudinal effects were implicitly incorporated by splitting the country into two regions according to which area is deemed to be affected by the warm Indian Ocean (three quarters of the surface area of South Africa) those deemed to be affected by the cooler Atlantic Ocean (*cf.* Figure 6.2). Chapter 7 is devoted to employing these variables for the construction of vapour pressure, relative humidity and vapour pressure deficit maps.

7.1 Mapping of Daily Mean Actual Vapour Pressure

For convenience, one model for each month of the year was employed for each vapour pressure map, for the entire country. For this reason it was decided to employ the coefficients displayed in Table 7.1, which is a repetition of the contents of Table 6.3 (altitude omitted) in the preceding chapter. Early attempts at modelling uncorrected vapour pressure produced markedly low values of average uncorrected daily vapour pressure in the Drakensberg escarpment. It is for this reason that the coefficients in Table 6.3 and not those in Table 6.4 were employed.

Throughout the mapping exercise in this chapter, wherever values of monthly means of daily maximum and minimum temperatures were employed, these values were taken from digital information at 1'X1' latitude by longitude from the South African Atlas of Agrohydrology and -Climatology (Schulze, 1997).

In Figures 7.1 and 7.2 the average monthly vapour pressure for South Africa is mapped for the months of January and July respectively.

7.2 Mapping of Daily Mean Maximum and Minimum Relative Humidity

In order to produce maps of RH, the values for the numerator and denominator of the RH equation, given below, had to be determined.

$$RH = \frac{\text{Actual vapour pressure X 100}}{\text{Saturated vapour pressure}}$$

The monthly vapour pressure models described in Section 7.1 were employed to determine the numerator in the RH equation. The denominator was calculated using the saturated vapour pressure (Teten's) equation. The only variable in the denominator is temperature. Therefore, for the construction of maximum RH maps, monthly means of daily minimum temperatures were employed, and for the minimum RH maps, the monthly means of daily maximum temperatures were employed since maximum temperature occurs with minimum RH and *vice versa*. For temperature values, the 1' X 1' gridded values from the South African Atlas of Agrohydrology and –Climatology (Schluze, 1997) were used.

Figures 7.3 and 7.4 show distributions of means of monthly minimum RH for the months of January (midsummer) and July (midwinter) while Figures 7.5 and 7.6 show distributions of maximum RH, again for the months of January and July.

7.3 Mapping of Daily Mean Vapour Pressure Deficit

Vapour pressure deficit (VPD), a key element in the Penman-Monteith equation for reference potential evaporation, is defined as:

VPD = (Saturated Vapour Pressure) -(Actual Vapour Pressure)

$= e_a - e_d$ (kPa)

Monthly means of vapour pressure deficit were estimated using the monthly vapour pressure models to calculate e_d, while Teten's equation was employed to calculate e_a. Monthly means of daily maximum temperatures were employed in order to calculate e_a. Monthly means of daily maximum temperatures were employed in order to calculate saturated vapour pressure. Figures 7.7 and 7.8 illustrate the spatial variation over South Africa of estimated monthly means of vapour pressure deficit for the months of January (midsummer) and July (midwinter) respectively.

Table 7.1 Variables employed in the vapour pressure models

Variate/Invariate	January	July
Intercept	1.16E -12	2.57E-14
Distance from sea	2.77E-07	5.08E-06
Latitude	3.3E-05	5.42E-05
Longitude	9.31E-05	0.92334
Temperature range	0.538693	0.00368

7.4 Interpretation and Discussion

All six maps were cursorily verified by transposing observed values of vapour pressure, maximum and minimum relative humidity and vapour pressure deficit, obtained from several randomly selected weather stations onto their respective surfaces. It was found that, in the mountainous regions of the country. the actual vapour pressure surfaces tended to overestimate actual vapour pressure for both January and July. This was evident in the Drakensberg escarpments of both the KwaZulu-Natal/Lesotho border regions and Mpumalanga province. This overestimation of actual vapour pressure led to an underestimation of vapour pressure deficit in the same locations. For the remainder of the country, the surfaces were, however, considered to be accurate.

Text continued on page 92

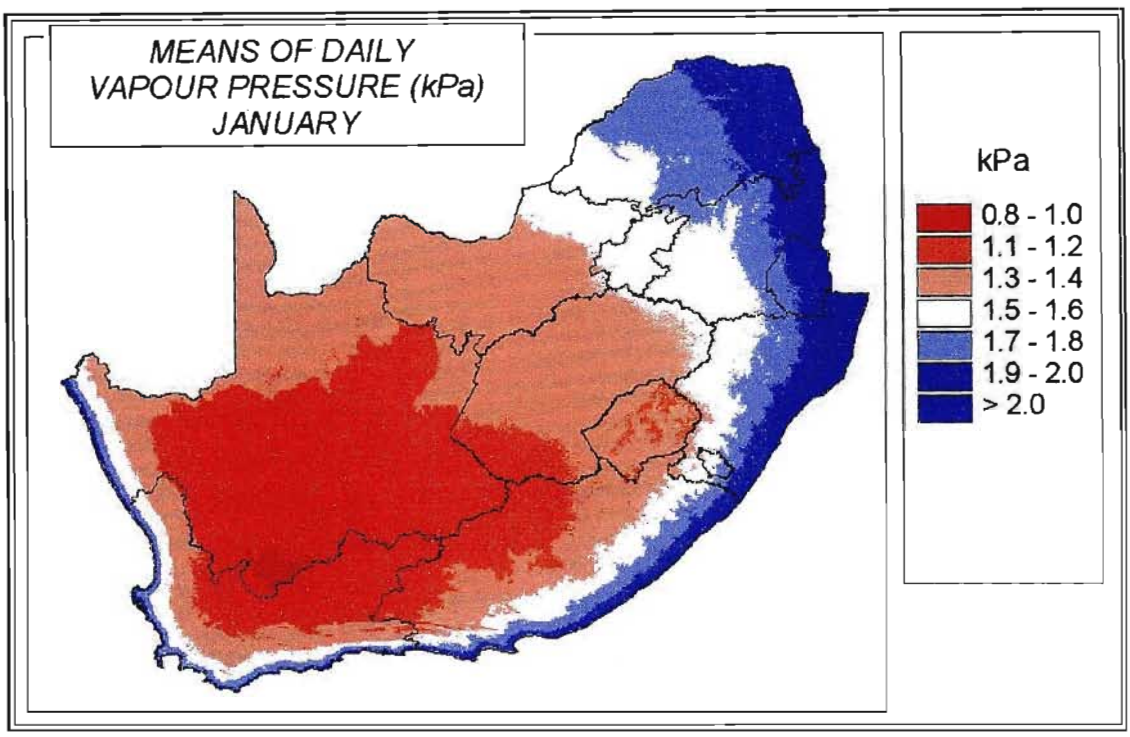

Figure 7.1 Monthly means of daily vapour pressure over South Africa for January

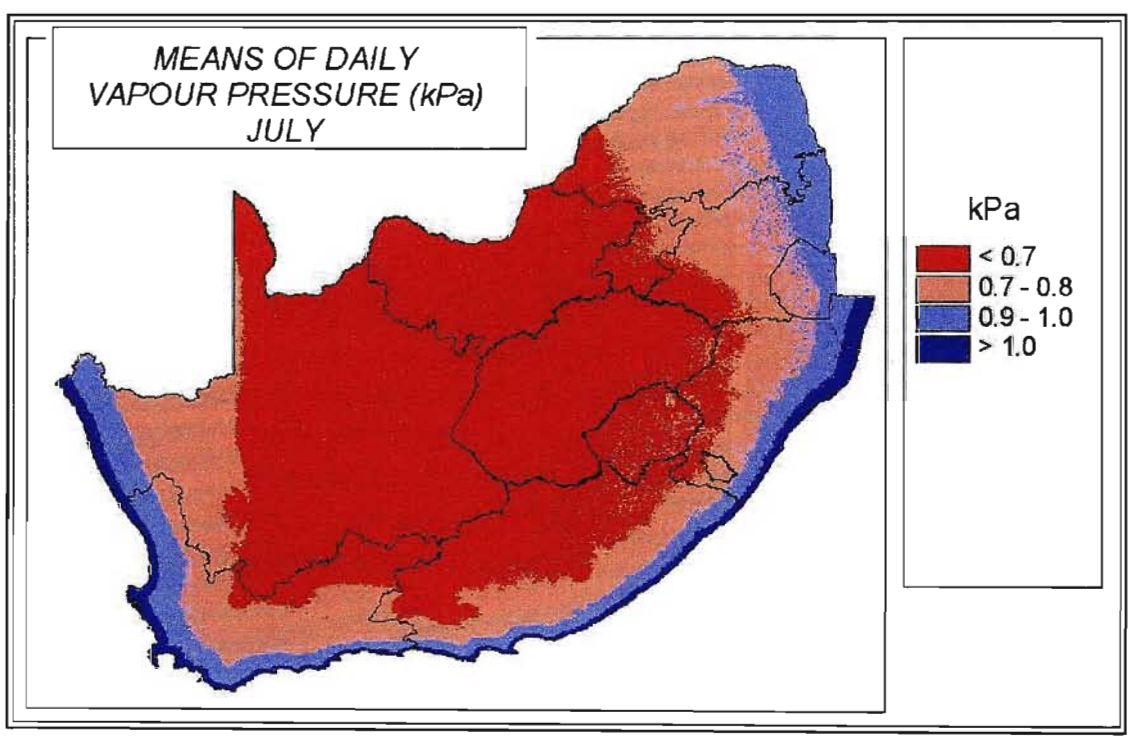

Figure 7.2 Monthly means of daily vapour pressure over South Africa for July

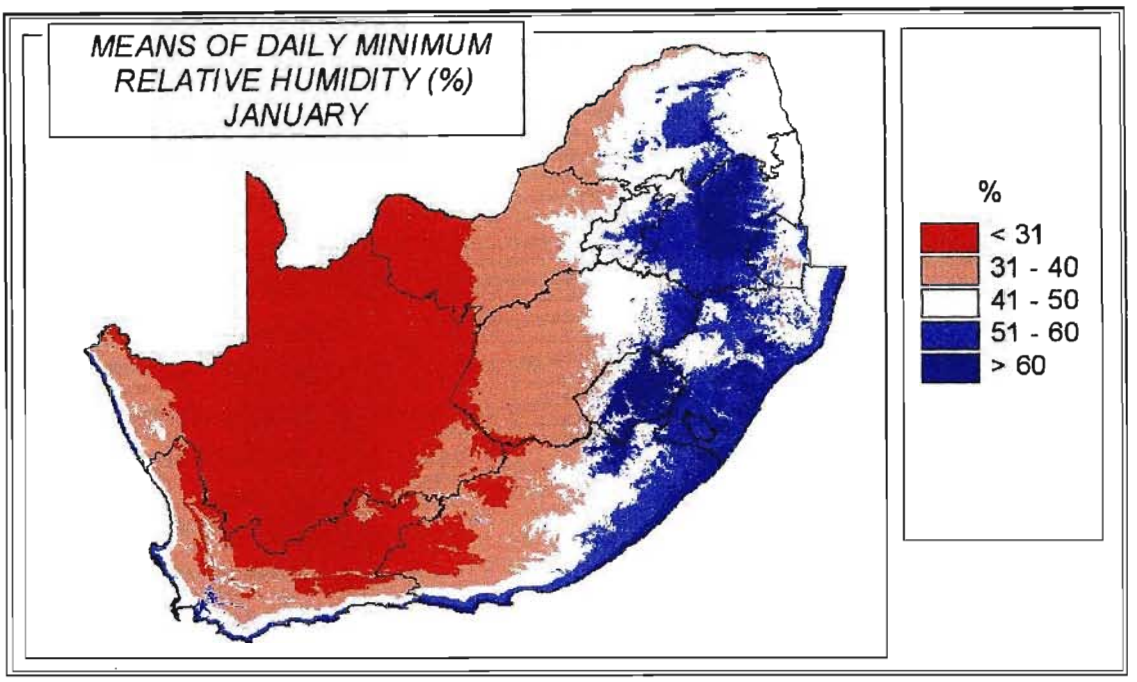

Figure 7.3 Monthly means of daily minimum relative humidity over South Africa for Janaury

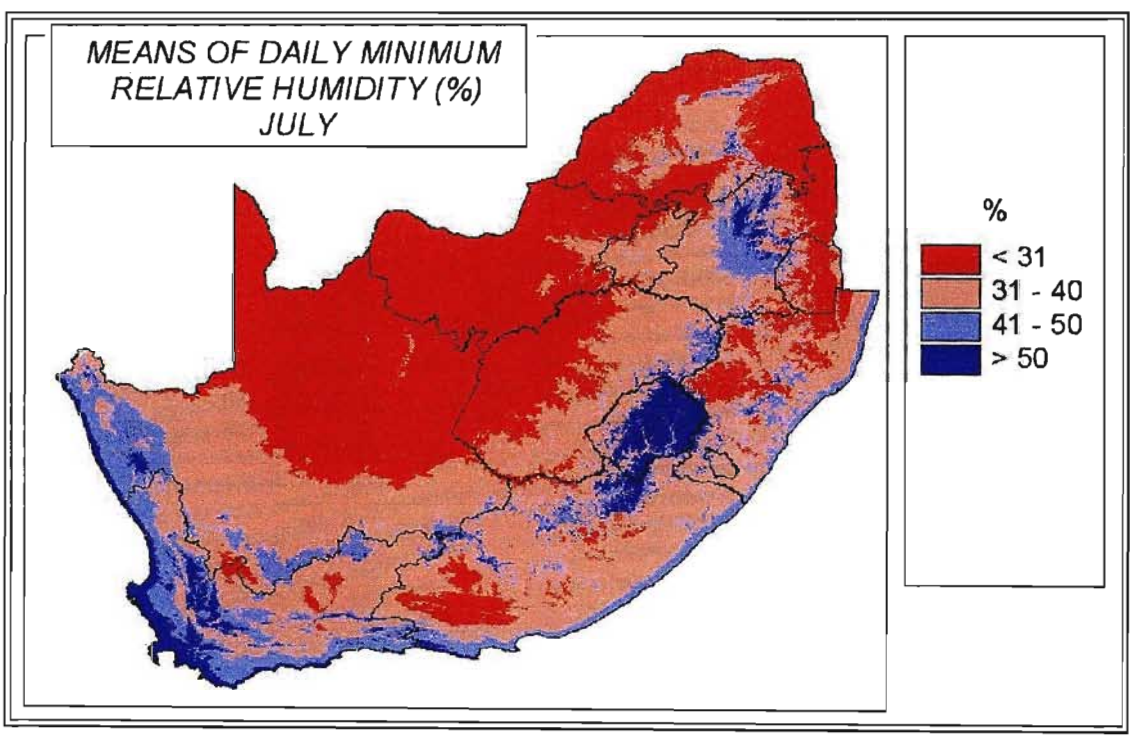

Figure 7.4 Monthly means of daily minimum relative humidity over South Africa for July

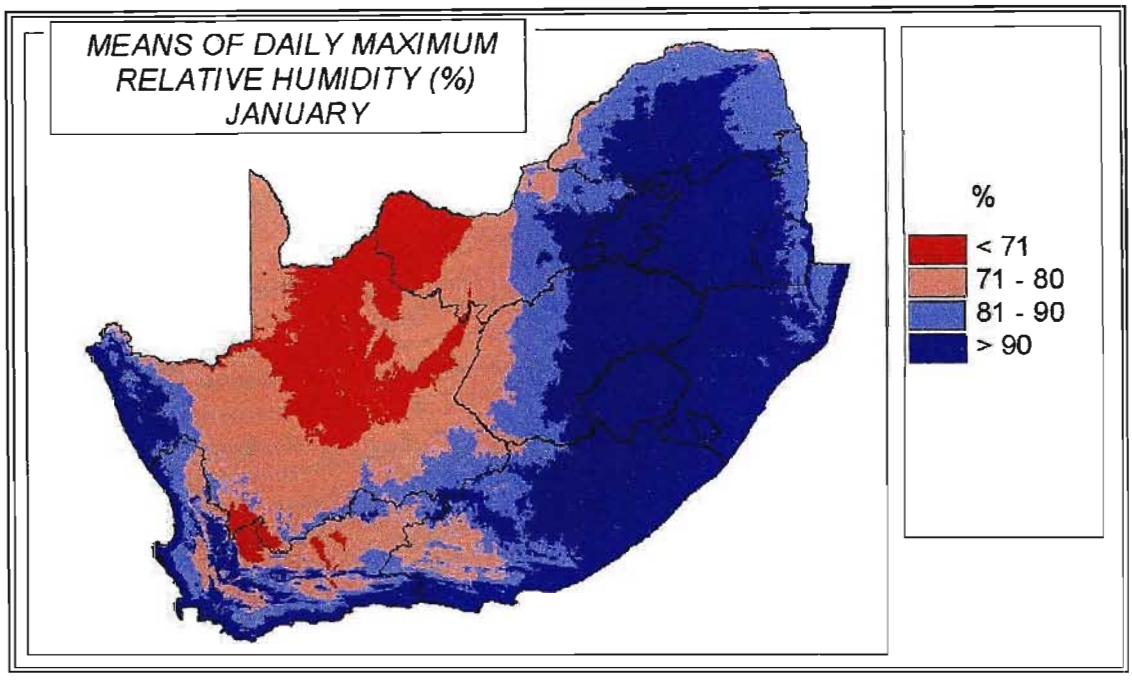

Figure 7.5 Monthly means of daily maximum relative humidity over South Africa for January

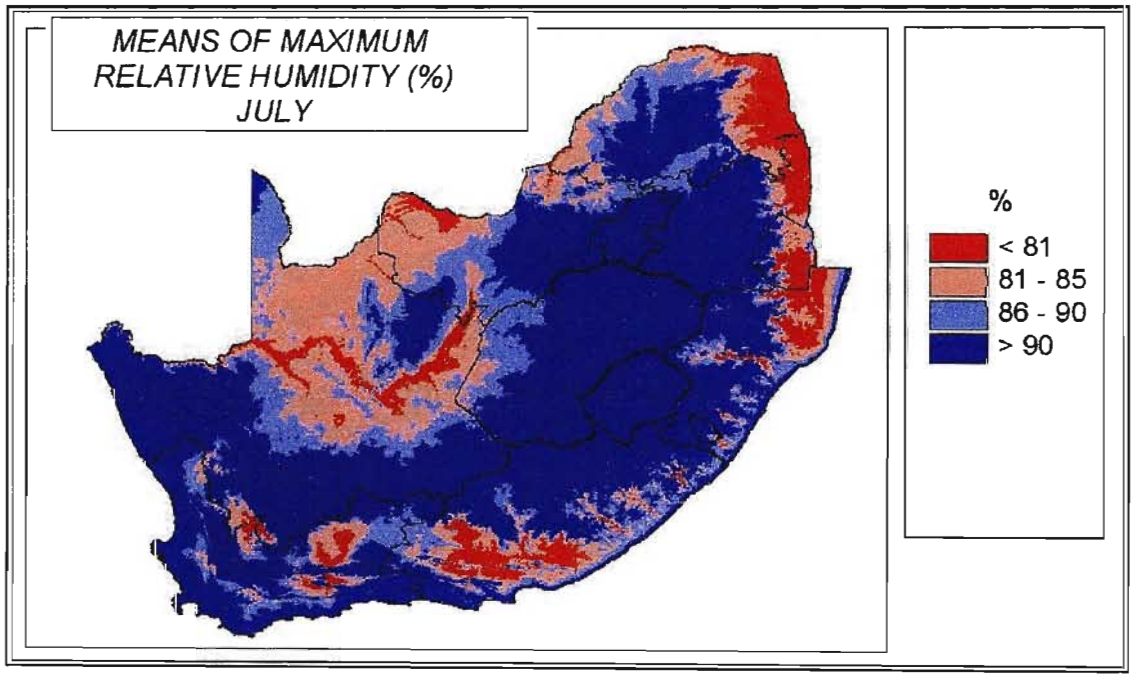

Figure 7.6 Monthly means of daily maximum relative humidity over South Africa for July

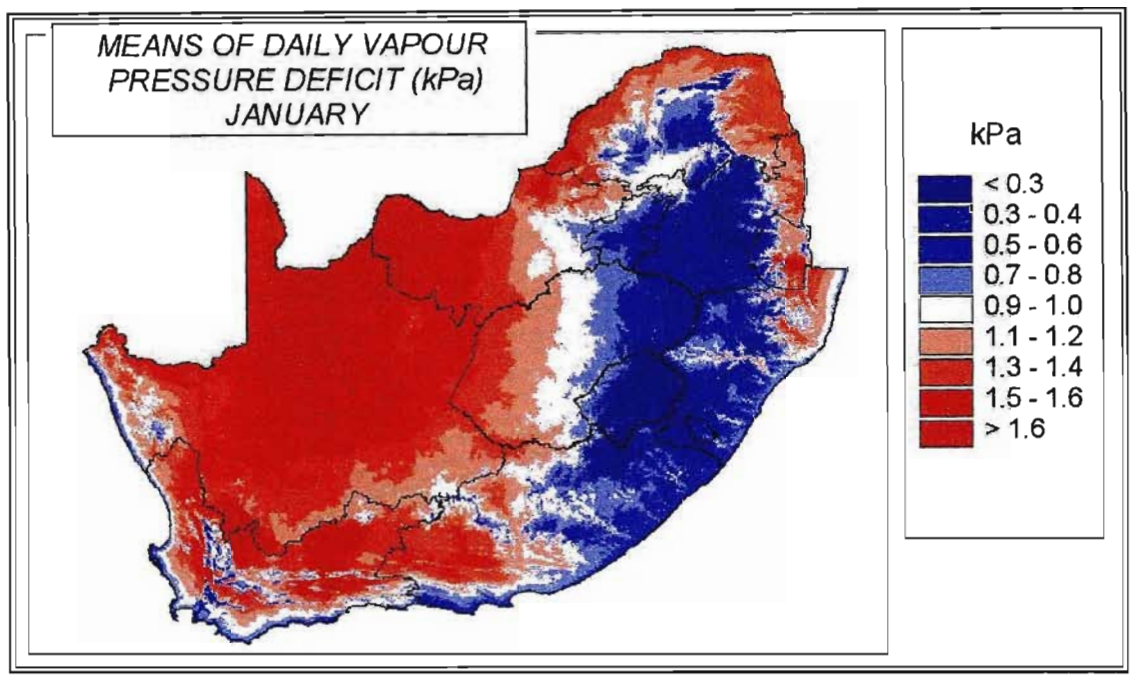

Figure 7.7 Monthly means of daily vapour pressure deficit for South Africa for January

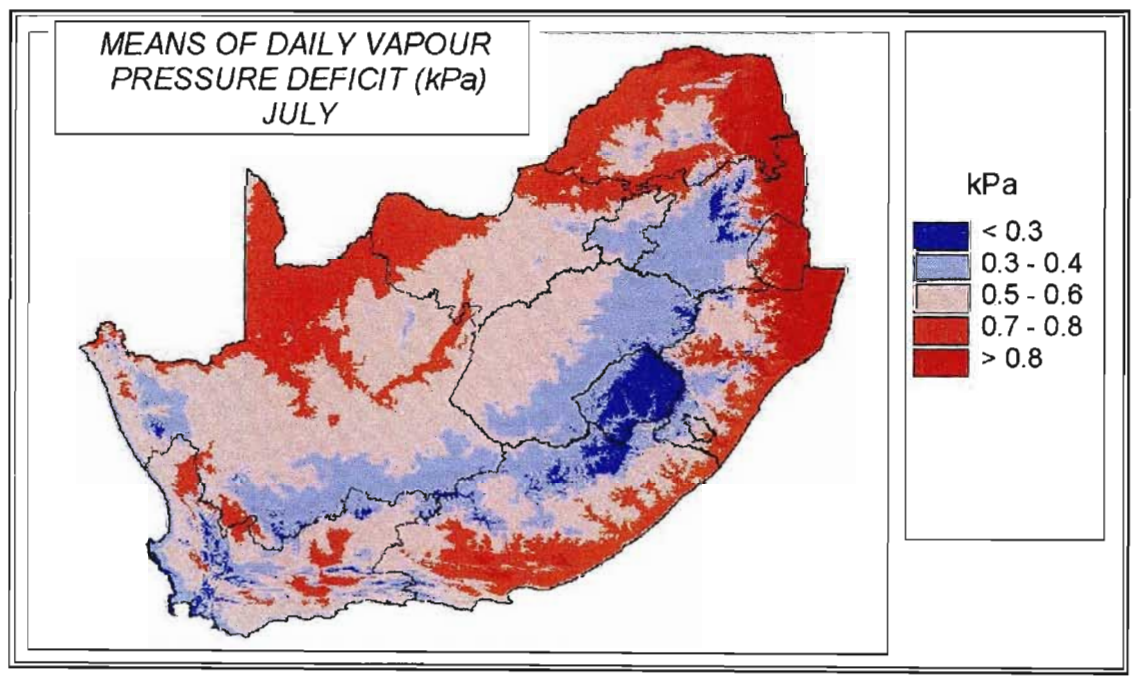

Figure 7.8 Monthly means of daily vapour pressure deficit for South Africa for July

Of the eight maps on display, only minimum RH had previously been mapped in the South African Atlas of Agrohydrology and –Climatology (Schulze, 1997). The method employed in the creation of the "Atlas" maps was that of Bristow's (1992) *viz.* of calculating saturated vapour pressure at minimum air temperature. Bristow (1992) and Kimball *et al.* (1997) noted that this method tended to overestimate vapour pressure in arid regions. This fact becomes evident when viewing Schulze's (1997) maps of minimum RH, as may be observed, particularly in January in the summer rainfall regions. Maximum RH for January and July (not displayed in the South African Atlas of Agrohydrology and –Climatology (Schulze, 1997), was considered to be accurately represented in Figures 7.5 and 7.6.

The following two chapters of this dissertation are devoted to the estimation of solar radiation over South Africa (*cf.* "Roadmap" on the following page). As is evident from Chapter 3, a considerably greater volume of published material exists on this subject than for atmospheric moisture estimation. Owing to the needs solar radiation information not only in the Penman-Monteith equation for potential evaporation, but also in such diverse fields as architecture, civil engineering and irrigation scheduling, the research philosophy on estimating solar radiation at ground level is considerably older than it is for atmospheric moisture. Atmospheric moisture in its varying forms such as relative humidity, vapour pressure deficit, or simply vapour pressure, is however, the single most important impediment to incoming solar radiation at ground level. As shall be observed in the chapters which follow, considerable attention is focused on involving atmospheric moisture in a solar radiation model.

Problem Statement: In order to estimate daily reference potential evaporation using the Penman-Monteith equation, values of daily vapour pressure and solar radiation are required

Objectives: To review current literature on current models for the estimation of daily vapour pressure and solar radiation, thereafter to employ and improve upon current method and models of estimating vapour pressure and solar radiation

Problem Statement

Broad Objectives	Literature Survey	Methods and Methodologies	Vapour Pressure Estimation	Solar Radiation Estimation	Conclusions and Recommendations
Specific Objectives	i) Introduction (Chapter 1) ii) Definitions relating to, and factors affecting vapour pressure and solar radiation (Chapter 2) iii) Review of literature on current methods of estimating daily vapour pressure (Chapter 3) iv) Review of literature on current methods of estimating daily solar radiation Chapter 3	i) Methods and methodologies employed in Chapters 5 to 9 (Chapter 4)	i) Characterisation of the vapour pressure regime in South Africa (Chapter 5) ii) Development of new models and methodologies of estimating vapour pressure (Chapter 6) iii) Verification of new methods of estimating vapour pressure (Chapter 7) iv) Mapping of vapour pressure, relative humidity and vapour pressure deficit (Chapter 7)	i) Factors affecting solar radiation at ground level (Chapter 8) ii) Development of new models and methodologies of estimating solar radiation (Chapter 8) iv) Verification of new methods of estimating solar radiation (Chapter 8) iv) Mapping of solar radiation over South Africa (Chapter 9)	i) Conclusions and recommendations for future research (Chapter 10)

Chapter 8

ESTIMATION OF SOLAR RADIATION OVER SOUTH AFRICA

In this chapter, as indicated on the "Roadmap", (*cf.* previous page) a brief overview is presented of those factors affecting daily solar radiation at ground level. Thereafter those models which were selected from the literature survey (*cf.* Chapter 3, Table 3.1), are compared with observed solar radiation data from weather stations throughout South Africa in order to establish which model is the "best" available. Subsequent sections of the solar radiation analyses are devoted to attempts at improving the estimation of solar radiation by including an RH term. Finally, having selected a single model, that model's integrity is to be verified over a range of climatic conditions throughout South Africa.

Of the two elements studied in this dissertation, solar radiation is unique in that it is the one element that depends on an extraterrestrial driver, *viz.* extraterrestrial solar radiation. The single most important factor attenuating solar radiation, when measured at ground level, is atmospheric moisture, principally in the form of clouds and it is, *inter alia*, for this reason that vapour pressure was the subject of the first part of this dissertation.

8.1 Atmospheric Elements Affecting Solar Radiation

Section 2.4 (Factors Affecting Solar Radiation) in the literature review, presents a detailed description of the major factors which attenuate solar radiation when it is measured at ground level. Section 8.1 presents the more relevant factors in a colloquial context. These sections furthermore describe how the factors are to be incorporated into the relevant solar radiation models.

Atmospheric water vapour: This element is described in the literature as either actual water vapour or precipitable water vapour. Revfiem (1997) states "another indicator of low transmission or cloud thickness is vapour pressure, which

commonly has a seasonal march in parallel with mean daily sunshine". It is partially for this reason that the estimation of water vapour was conducted in the first part of this dissertation.

Dust concentration: This is not a weather element *per se*. However, it could still be classified as an atmospheric variable affecting solar radiation. Schulze (1974), working in the Drakensberg mountains of KwaZulu–Natal, noted the then lack of available data on dust concentrations anywhere in the world. Working from research by Kimball (1927), conducted at mountainous locations in the USA, Schulze (1974) proceeded to estimate seasonal variations in dust concentrations in the Drakensberg where, for the rainy season months of December to February, dust concentrations were estimated at 0.3 particles/cm^3, 0.4 particles/cm^3 for November and March to July and 0.5 particles/cm^3 for August to October, when atmospheric conditions tended to be more stable. Schulze (1974) further showed that depletion of solar radiation due to dust concentration was only of the order of about 4 %. Since few data on dust concentrations are currently available, and this factor is relatively insensitive to the depletion of solar radiation, the dust concentration factor is not considered further in subsequent sections

Clouds: With the exception of dust concentration, all of the stated variables and invariates (see factors which follow) which affect measured solar radiation relate to one single factor, *viz.* clouds. Clouds are the single most important cause of depletion of incoming solar radiation. Cloud type, cloud fraction and cloud thickness are functions of invariate factors such as seasonality, topography and geographical location. For example, the Drakensberg escarpment experiences considerably greater cloud cover throughout the year due to the forced rising of advected onshore air (personal observation). Cumulonimbus clouds have the greatest vertical extent of all the cloud formations and are, therefore, the most impenetrable to incoming radiation on account of their depth. Their occurrence is almost exclusive to the hot summer months in the summer rainfall regions of

South Africa. In addition to being affected by seasonality, cloud cover is, therefore, also a function of rainfall regime.

Satturland and Means (1978) reported an R^2 of 0.99 when comparing their model output against observed data when they included cloud fraction in their equation. In subsequent analyses in this dissertation, little consideration is given to Satturland and Means' (1978) equation, as it only estimated solar radiation at the exact location where cloud fraction was originally measured. In South Africa, the only records of cloud types and cloud fraction that exist are personal observations made by observers at first order weather stations operated by the South African Weather Service. Since these values are becoming increasingly difficult to obtain with the change from manually read instruments to automatically recording weather stations, cloud fraction values were not considered.

Continentality: All weather variables are affected by continentality. Higher summer temperatures, higher temperature ranges, lower humidity, fewer raindays as well as lower rainfall totals are but a few of the consequences of increasing continentality on weather variables. It stands to reason, therefore, that solar radiation *per se* is affected by all of the aforementioned variables, which themselves are affected by continentality. As shall be noted in subsequent sections of this dissertation (Section 8.6), care is taken to verify solar radiation models in different parts of the country with different continentality indices.

Altitude: Optical density is inversely proportional to altitude, with higher altitudes experiencing higher values of solar radiation, all else being equal. Iziomon and Mayer (2002), working in the Bavarian Alps in Germany, calculated the clear sky radiation to be 76% at 1500 m as against 68% at 220 m altitude. The influence of altitude and atmospheric transmissivity is covered in greater detail in the sections on atmospheric transmissivity.

Latitude: Cape Town, at 33 °55' S and Beit Bridge at 22 °00 S experience similar

extraterrestrial solar radiation values of 42.6 MJ/m^2/day and 44.3 MJ/m^2/day, respectively, at the summer solstice (December 21). These values change to 16.4 MJ/m^2/day for Cape Town and a higher 22.8 MJ/m^2/day for Beit Bridge for their respective winter solstice (June 21) extraterrestrial solar radiation. Solar radiation measured at ground level is, therefore, directly dependent on extraterrestrial solar radiation, and is thus a function of latitude as well as time of year, i.e. seasonality. Few of the solar radiation models displayed in Table 3.1 include any of these invariate factors since all factors can be explained either by extraterrestrial solar radiation (seasonality or latitude) or by the surrogate data involved, e.g. temperature range, rainfall or raindays (continentality and altitude).

8.2 Solar Radiation Data Collation

Figure 8.1 displays the locations of all the weather stations from which data were used in the analyses presented in this Chapter. Climate statistics associated with stations in Figure 8.1 are listed in Table 8.1.

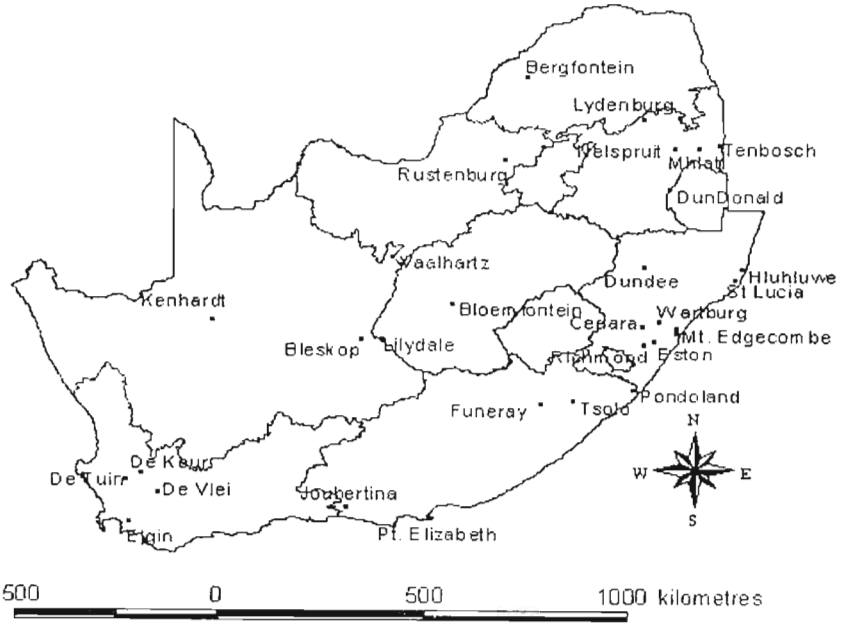

Figure 8.1 Locations of weather stations used in the estimation of solar radiation analyses

Table 8.1 Climate statistics of all weather stations used for the estimation of solar radiation in Chapter 8

Location	Altitude (m)	January Means of Daily Maximum Relative Humidity and Temperature (^{0}C) RH (%)	T	January Means of Daily Minimum Relative Humidity and Temperature (^{0}C) RH (%)	T	July Means of Daily Maximum Relative Humidity and Temperature (^{0}C) RH (%)	T	July Means of Daily Minimum Relative Humidity and Temperature (^{0}C) RH (%)	T	Mean Annual Precipitation (mm)
Bergfontein	940	N/A*	32.3	N/A*	21.5	93.8	24.0	77.9	6.7	1151
Bleskop	1189	83.6	32.7	27.1	15.6	87.5	19.2	28.6	1.5	332
Bloemfontein	1359	76.1	30.5	17.2	15.6	89.0	17.4	33.3	-1.3	530
Cedara	1076	95.3	25.4	53.1	15.5	84.7	19.4	33.0	3.8	831
De Keur	823	84.1	27.8	44.0	11.9	94.1	16.1	65.6	3.9	631
De Tuin	80	81.3	32.9	48.3	17.2	93.9	17.8	64.4	5.2	526
De Vlei	490	90.7	31.1	49.2	14.1	85.7	17.5	47.0	3.9	153
Dundee	1219	94.6	26.5	43.5	15.1	88.1	19.5	30.9	1.8	816
DunDonald	1606	93.9	25.3	47.1	15.1	82.1	18.2	32.3	4.0	1038
Elgin	305	93.6	26.8	62.7	14.8	94.0	16.4	65.6	4.4	938
Eston	785	87.3	25.5	72.8	16.1	70.5	19.3	40.8	8.1	834
Funeray	1550	98.7	25.5	51.2	13.5	78.6	17.6	28.5	4.4	597
Hluhluwe	35	84.3	30.0	69.4	20.5	87.3	24.1	51.5	10.6	758
Joubertina	640	90.7	27.3	42.9	13.6	89.2	18.8	35.4	3.9	477
Kenhardt	442	71.0	38.3	35.5	22.0	76.4	22.3	28.1	7.1	112
Komatipoort	189	78.7	31.4	50.2	21.4	84.7	24.5	35.7	8.6	784
Lilydale	1143	77.5	32.9	21.9	16.7	88.2	19.3	27.6	0.3	292
Lydenburg	954	99.3	31.0	72.5	18.4	91.7	22.9	47.6	4.2	522
Mhlati	301	98.8	31.6	46.3	19.7	97.2	25.9	35.5	9.1	576
Mt.Edgecombe	96	79.0	20.0	70.0	27.7	73.3	22.9	54.0	11.0	1060
Nelspruit	650	97.1	28.9	47.4	18.2	91.8	22.6	31.9	6.4	824
Pondoland	385	97.6	28.8	66.6	17.9	93.1	22.4	37.7	8.7	999
Pt. Elizabeth	85	86.1	25.8	39.5	18.0	86.0	20.1	49.2	8.8	499
Richmond	800	86.5	25.5	71.5	15.6	66.9	20.7	37.4	8.2	809
Rustenburg	1157	89.1	29.1	36.4	16.4	88.1	20.8	29.9	3.4	598
St. Lucia	48	85.0	30.7	73.0	21.1	88.2	24.4	64.4	11.2	1196
Tsolo	925	96.6	26.2	54.4	15.4	89.7	21.9	26.5	4.5	628
Vaalhartz	888	75.5	33.4	40.0	17.0	81.1	18.5	28.1	3.5	423
Wartburg	990	81.2	26.7	66.9	16.3	71.7	52.6	20.3	7.7	1013

* N/A = no data available

8.3 Selection and Testing of Solar Radiation Models

The objectives of this chapter are to select several models from Table 3.1 and to test the output from the selected models against observed data from stations throughout the country. In this chapter particular attention is focused on the models developed by Liu and Scott (2001) and Hunt *et al.* (1998), who conducted almost identical research in their respective countries (Australia and Canada) by comparing many of the models displayed in Table 3.1 with observed solar radiation data.

8.3.1 Selection of Benchmark Solar Radiation Models

Hargreaves *et al.* (1985), De Jong and Stewart (1993), Meinke *et al.* (1994), Hunt *et al.* (1998), Liu and Scott (2001), Winslow *et al.* (2001) and Bezuidenhout (2002) all refer to the Bristow and Campbell (1984) model in their research. It is for this reason that the Bristow and Campbell (1984) model was chosen as a benchmark against which to compare any new solar radiation model. Clemence's (1992) model was chosen as a second benchmark, since his model had been developed using South African data and was employed in the South African Atlas of Agrohydrology and -Climatology (Schulze, 1997). Finally, it was decided to also include the Hargreaves *et al.* (1985) model with this group, as Liu and Scott (2001) and Hunt *et al.* (1998) use this model as a benchmark model along with that of Bristow and Campbell (1984).

Richardson's (1985) solar radiation model (*cf.* Table 3.1) was eliminated because of its close similarity with the Hargreaves *et al.* (1985) model. In the same context, Ratkowsky's (1990) model and that of De Jong and Stewart (1993) were also eliminated because of the similarities to that of Hunt *et al.* (1998). It should be noted that De Jong and Stewart (1993) refer to a second model by Hunt *et al.* (1998), which is not displayed in Table 3.1. This model depends solely on air temperature. Hunt *et al.* (1998) declined to recommend this latter model, claiming "instability". The Hunt *et al.* (1998) model displayed in Table 3.1 was

chosen as they, like Liu and Scott (2001), had compared their own model output with many of with other current models displayed in Table 3.1 and concluded that their model produced the "best results". For this reason, both aforementioned models were employed as benchmarks. Donatelli and Campbell (1998) merely reformulated Bristow and Campbell's (1984) model. They did not, however, indicate that they had compared output from their model to that of any other current models, with the exception of Bristow and Campbell's (1984) model. Thus, the Donatelli and Campbell (1998) model was also included as a benchmark model.

8.3.2 Testing the Robustness of Solar Radiation Models

Solar radiation records from four weather stations with widely varying climatic conditions were selected against which to test the selected solar radiation benchmark models. The records employed were from De Vlei (record length: 1994 to 1997), to represent a winter rainfall climate, Mount Edgecombe (record length: 1997 to 2003), to represent a humid coastal climate, Vaalhartz (record length: 1997 to 2003) to represent a semi-arid climate and Kenhardt (record length: 1993 to 1999) to represent an arid environment.

8.3.3 Methods

Output from the six chosen benchmark models, *viz.* the Bristow and Campbell (1984), Hargreaves *et al.* (1985), Clemence (1992), Donatelli and Campbell (1998), Hunt *et al.* (1998) and the Liu and Scott (2001) models were compared against observed data. Microsoft Excel 2000 and SPSS were employed for the analyses of data.

8.3.4 Results and Discussion

Figures 8.2 to 8.7 and Tables 8.2 to 8.5 are graphical and tabular representations respectively, of the performances of the six models at one location, *viz.* De Vlei in the Western Cape.

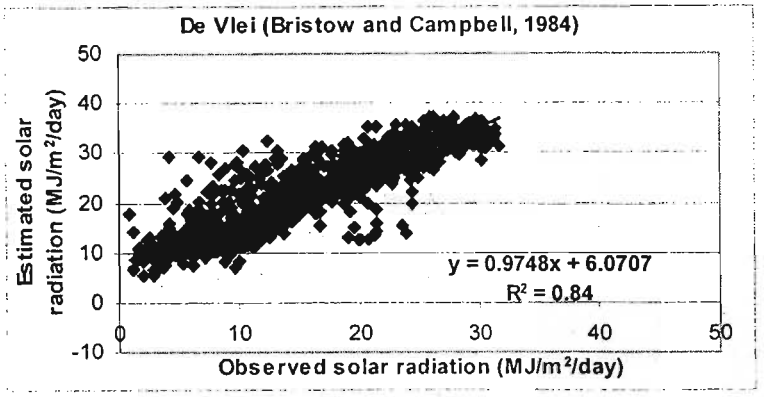

Figure 8.2 Bristow and Campbell's (1984) solar radiation model performance at De Vlei in the Western Cape

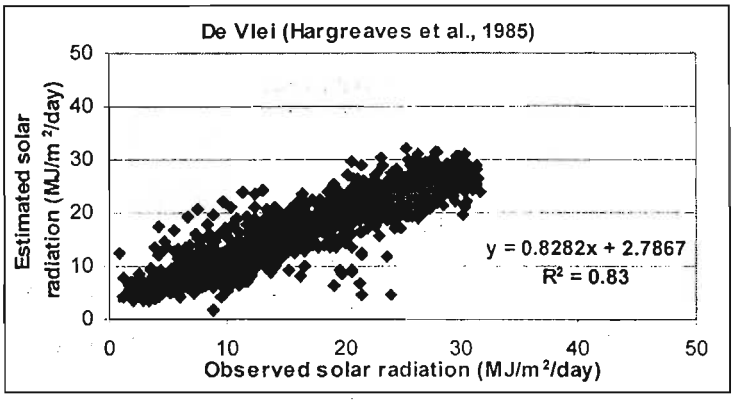

Figure 8.3 The Hargreaves *et al.* (1985) solar radiation model performance at De Vlei in the Western Cape

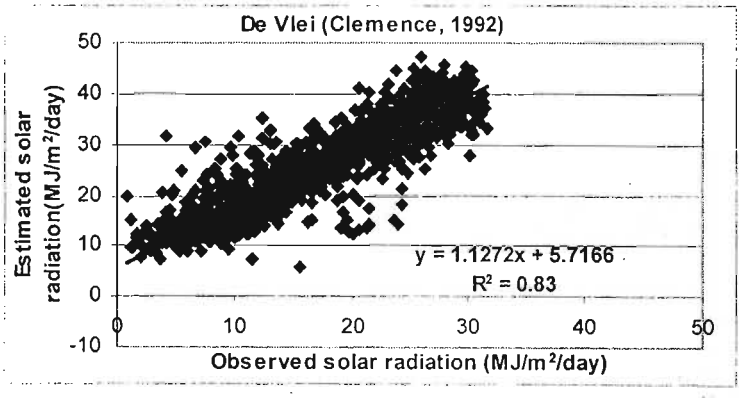

Figure 8.4 Clemence's (1992) solar radiation model performance at De Vlei in the Western Cape

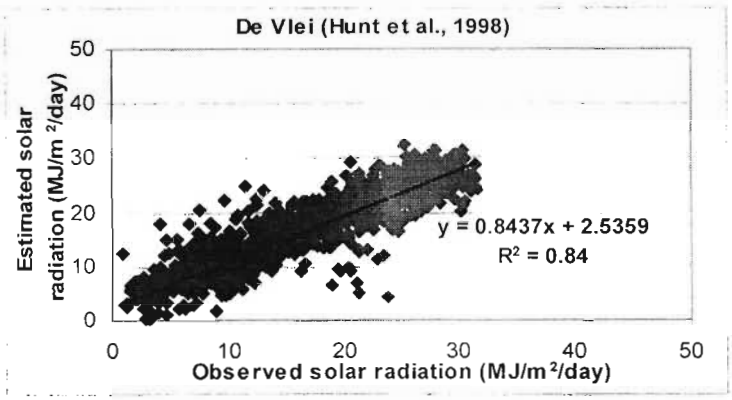

Figure 8.5 The Hunt *et al.* (1998) solar radiation model performance at De Vlei in the Western Cape

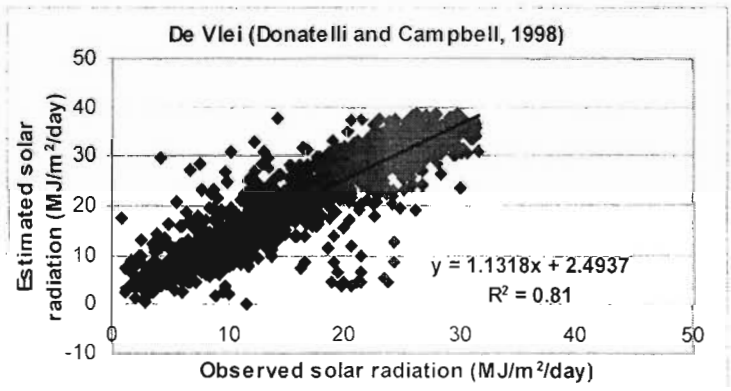

Figure 8.6 Donatelli and Campbell's (1998) solar radiation model performance at De Vlei in the Western Cape

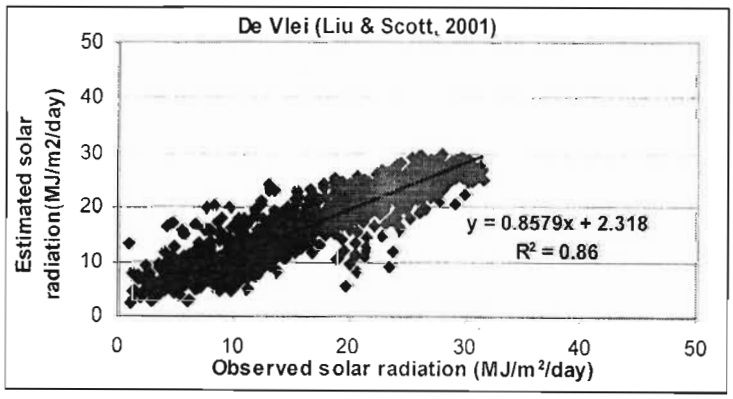

Figure 8.7 The Liu and Scott (2001) solar radiation model performance at De Vlei in the Western Cape

Table 8.2 A comparison of solar radiation model performance, i.e. estimated values versus observed data, at De Vlei in the Western Cape

Model	Slope	Intercept	R^2	RMSE
Bristow and Campbell (1984)	0.97	6.40	0.84	2.39
Hargreaves *et al.* (1985)	0.83	2.79	0.83	2.24
Clemence (1992)	1.13	5.72	0.83	2.80
Hunt *et al.* (1998)	0.83	2.54	0.84	2.14
Donatelli and Campbell (1998)	1.13	2.49	0.83	2.72
Liu and Scott (2001)	0.86	2.31	0.86	2.03

Table 8.3 A comparison of solar radiation model performance, i.e. estimated values versus observed data, at Mt. Edgecombe in KwaZulu-Natal

Model	Slope	Intercept	R^2	RMSE
Bristow and Campbell (1984)	0.62	6.20	0.61	3.15
Hargreaves *et al.* (1985)	0.55	7.33	0.55	3.77
Clemence (1992)	0.47	11.5	0.55	4.26
Hunt *et al.* (1998)	0.58	6.75	0.58	3.64
Donatelli and Campbell (1998)	1.01	9.26	0.60	3.75
Liu and Scott (2001)	0.65	5.92	0.67	2.87

Table 8.4 A comparison of solar radiation model performance, i.e. estimated values versus observed data, at Vaalhartz in the North-West province

Model	Slope	Intercept	R^2	RMSE
Bristow and Campbell (1984)	0.87	6.29	0.81	2.21
Hargreaves *et al.*, (1985)	0.78	4.50	0.78	5.08
Clemence (1992)	0.96	7.14	0.77	5.40
Hunt *et al.* (1998)	0.80	4.98	0.80	2.65
Donatelli and Campbell (1998)	0.96	5.00	0.80	2.66
Liu and Scott (2001)	0.84	3.29	0.84	2.07

Table 8.5 A comparison of solar radiation model performance, i.e. estimated values versus observed data, at Kenhardt in the Northern Cape

Model	Slope	Intercept	R^2	RMSE
Bristow and Campbell (1984)	0.78	4.1	0.80	2.51
Hargreaves *et al.* (1985)	0.76	4.60	0.77	5.92
Clemence (1992)	1.01	6.30	0.70	3.45
Hunt *et al.* (1998)	0.80	4.98	0.80	2.65
Donatelli and Campbell (1998)	1.11	3.00	0.80	2.69
Liu and Scott (2001)	0.82	3.63	0.82	2.21

In the Western Cape, all six models produced similar output with the Liu and Scott (2001) model producing the most favourable output. This pattern is largely repeated in the remaining three locations. However, the differences in model performance becomes more apparent in summer rainfall locations.

Predictably, all six models employed at the most humid of the stations *viz.* Mt. Edgecombe produced the lowest R^2 of all the four stations tested. While the RMSE's of all six models were generally higher at Mt. Edgecombe, they were considerably higher for Hargreaves (1985) and Clemence (1992) at Vaalhartz and Kenhardt. At Mt. Edgecombe the Liu and Scott (2001) model again produced the best results as it did at Vaalhartz (semi arid) and Kenhardt (arid).

8.3.5 Conclusions

From the above evaluation it was concluded that there was little to separate the models tested in the winter rainfall areas of the South Africa. Nevertheless, in humid locations, the Liu and Scott (2001) did appear to account for a significantly higher proportion of variance and had a significantly lower RMSE. The Liu and Scott (2001) model was therefore deemed to be best of the models tested.

The influence of higher atmospheric moisture content, particularly in the form of higher relative humidity, as a factor which decreases the variance accounted for by a given model when used with observed data, was a recurring finding throughout the study. For example, Elgin (results not displayed), which is situated only 18 km from the Western Cape coast, and is therefore considered to experience relatively high average humidity, recorded an R^2 of 0.74 compared to 0.86 at De Vlei, which is located 111 km from the same coast.

Despite the problems of estimating solar radiation when using the Liu and Scott (2001) model in humid locations, it was concluded that their model was still the best of all models displayed in Table 3.1. The influence of humidity on solar radiation has been a recurring theme throughout this study and in the literature surveyed. In the following section, depletion of solar radiation under clear sky conditions is investigated and, as shall be observed, relative humidity again plays a primary role in attenuating solar radiation.

8.4 Estimation of Maximum Clear Sky Transmissivity

One of the ultimate goals in estimating solar radiation is to account for the highest amount of variance in daily solar radiation. The climatic element of solar radiation is unique in that one has a clear indicator what the maximum possible value of solar radiation can be for any time of the year and at any given location in the world through the computation of daily extraterrestrial radiation. Most literature surveyed indicates a value of 0.72 to 0.80 as the maximum clear sky transmissivity (Satturland and Means, 1978; Bristow and Campbell 1984; Bristow *et al.*, 1986; Meek, 1997). What happens between the solar radiation striking the top of the atmosphere and reaching ground level is the subject of study in this section.

8.4.1 Methods

In the following analysis, the daily solar radiation records from 28 automatic weather stations located throughout South Africa were broken up into ten-day intervals. The maximum transmissivity values were then obtained for each ten-day interval. If a specific maximum was found to be significantly below the average value recorded at the same time for each year, that value was then excluded from the analysis. The most likely explanation for this would have been an extensive period of cloudiness. Similarly, if the recorded values of solar radiation were significantly different to the average for any extended period of time, this was interpreted as being the result of a faulty instrument and these values were therefore also omitted. In this manner, a profile was obtained for the maximum transmissivity throughout the year for each region in the country.

8.4.2 Results and Discussion

The results are summarised in Figures 8.8 to 8.13. It should be noted that 28 curves were obtained, one at each station analysed. Six transmissivity curves are displayed in the text that follows, the remainder being displayed, according to location, in Appendix 1. The six curves displayed were chosen according to their being considered representative of a given region/climate.

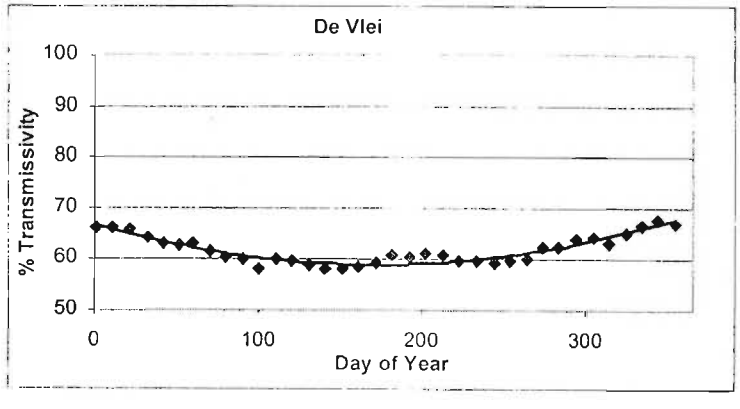

Figure 8.8 A typical maximum transmittance curve at De Vlei in the Western Cape, 1994-1999

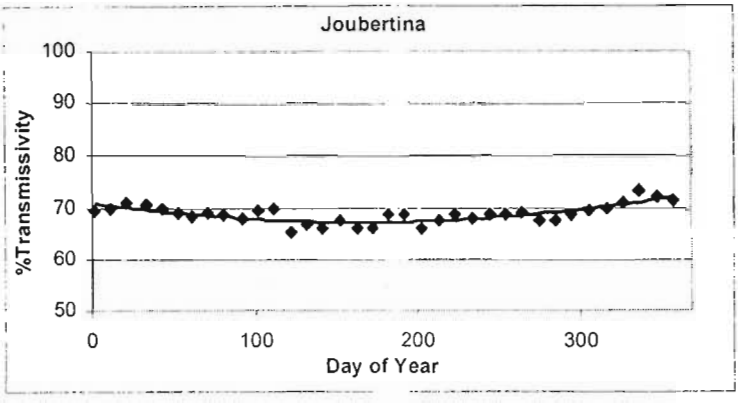

Figure 8.9 A typical maximum transmittance curve at Joubertina in the Eastern Cape, 1994-1997

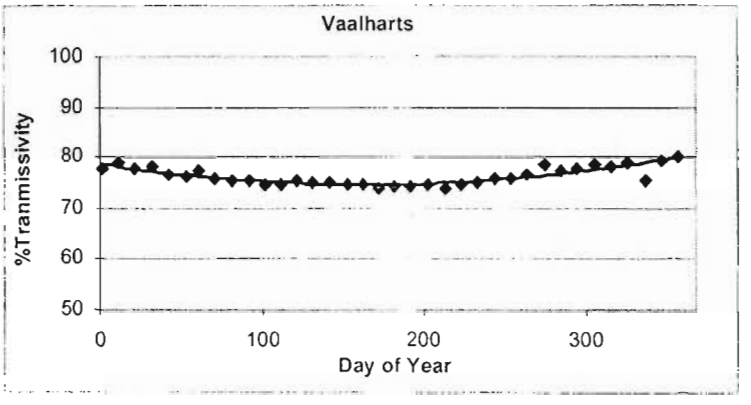

Figure 8.10 A typical maximum transmittance curve at Vaalhartz in the North-West province, 1997-2003

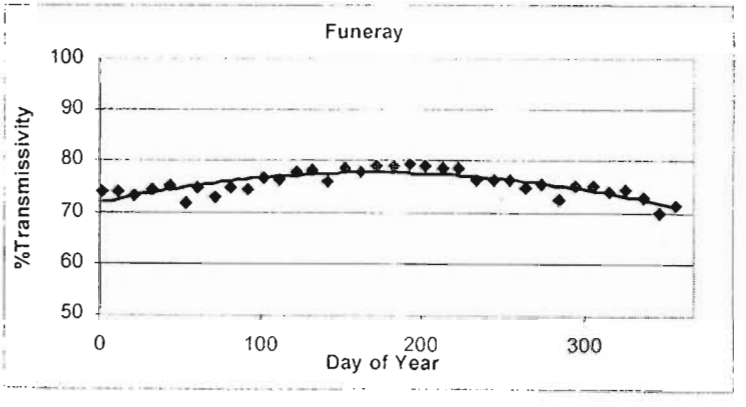

Figure 8.11 A typical maximum transmittance curve experienced at Funeray in the Eastern Cape, 1996-2003

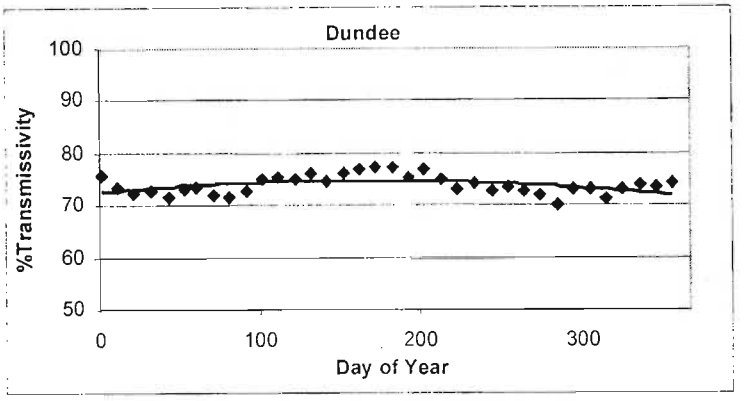

Figure 8.12 A typical maximum transmittance curve experienced at Dundee in KwaZulu-Natal, 1975-1984

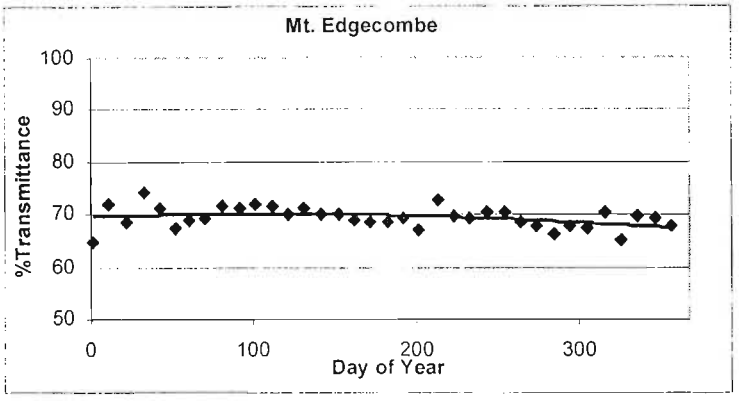

Figure 8.13 A typical maximum transmittance curve experienced at Mt. Edgecombe on the KwaZulu-Natal coast, 1997-2003

Two broad trends become apparent from Figures 8.8 to 8.13. As can be observed, the relationship between transmissivity and day of the year is hyperbolic for most of the country. This hyperbolic relationship flattens out as one moves eastwards and northwards from the Western Cape, where the most defined hyperbolic curves are recorded. Secondly, this relationship eventually becomes parabolic in the more humid eastern locations of the summer rainfall regions. A third, less obvious, trend then become noticeable. If the first two arguments are taken to their logical conclusions, *viz.* that transmittance is reduced in the rainy season, one would expect to find the most parabolic relationships along the humid coastal strip or the Mpumalanga lowveld. This

does not occur, however, as one finds the most defined parabolic relationships in the cooler/moist interior stations at, for example, Funeray. In addition to this, Elgin, which is a winter rainfall station, but is close to the sea, displayed a markedly flatter curve than its closest neighbour, De Tuin. It is for this reason that it is hypothesised that local climate, and more specifically humidity, plays an important role, especially during the winter months when extraterrestrial solar radiation is at a minimum.

8.4.3 Conclusions

It was concluded that, all things being equal, the transmissivity versus day-of-year relationship should be hyperbolic throughout the year and that this hyperbolic relationship is caused by incident solar radiation passing through a greater optical distance during the winter months. That relationship would, therefore, tend to flatten out as one moves towards the equator. Secondly, it was concluded that atmospheric moisture also plays a considerable role in determining the transmissivity regime at a given location. The higher RH experienced in winter in the winter rainfall regions reinforces the hyperbolic relationship, as does the higher humidity experienced during summer in the humid summer regions reinforce the parabolic relationship. In regions where RH is low all year round, e.g. at Vaalhartz or Kenhardt, the latitudinal influences on transmissivity dominate the shape of the curve.

Finally, it was also concluded that observed solar radiation data lacked the quality to accurately determine regional/seasonal maximum transmissivities, because too much data scatter was encountered where a much smoother curve was to be expected. From a detailed perusal of the results it is suggested that variability in instrument calibration is likely to be the main cause of this. For the above reasons it was, therefore, decided to use a single value of atmospheric transmissivity, *viz.* 0.77, throughout the year and throughout the country.

8.5 Solar Radiation Models and Humidity

In Sections 8.3 and 8.4 it was concluded that relative humidity played a significant role in determining the receipt of solar radiation at ground level. In light of these findings, the concept of including a relative humidity term in a solar radiation model is therefore examined. As has been discussed in the opening chapters of this dissertation, considerably fewer weather stations record relative humidity than record temperature and rainfall. The inclusion of relative humidity in a model for solar radiation has, therefore, been a popular yet impractical goal of several researchers.

Cengiz *et al.* (1981) claimed that their solar radiation model had improved the R^2 of estimated values versus observed data from 0.76 to 0.85 by including a minimum daily RH term in it. Clemence (1992) quoted Zucchini (1991), who claimed a cross correlation between sunshine, maximum daily temperature and minimum daily humidity of 0.63 and –0.70 respectively. Owing to the paucity of available RH data the modeller is, therefore, obliged to somehow estimate RH beforehand. In the following sections various attempts are made to include estimated RH, by using the vapour pressure models derived in Chapter 6, in a solar radiation model.

8.5.1 Obtaining the Optimum RH Term

In order to include a RH term in a solar radiation model, one needs to determine which form of RH to use, i.e. minimum daily RH, average daily RH or daily range of RH. Maximum RH was not considered since it is usually associated with minimum temperature conditions or night time.

8.5.2 Methods

In this analysis, estimated solar radiation values from one station, Mount Edgecombe, situated on the humid KwaZulu-Natal coast, were regressed against

observed data. Mount Edgecombe was chosen because of its poor results compared to those of other locations in the solar radiation model analysis (*cf.* Section 8.3.4) This analysis coincided with a further analysis in which an attempt was made to arrive at a new solar radiation model. The new solar radiation model is defined as:

$$Q_t = aQ_{ext}(bT_{mx})c(T_{mx} - T_{mn})d(RH_{Term}) + e$$

where
- $a - e$ = coefficients
- Q_t = incoming solar radiation (MJ/m^2/day)
- Q_{ext} = extraterrestrial solar radiation (MJ/m^2/day)
- T_{mx} = maximum temperature (°C)
- T_{mn} = minimum temperature (°C)
- RH_{Term} = varying form of relative humidity (%).

Minimum daily RH, average daily RH and RH range were estimated using the vapour pressure models and were then used as the RH term. Table 8.6 presents the results of this exercise.

8.5.3 Results and Discussion

Table 8.6 Identification of the RH term most closely related to solar radiation at Mount Edgecombe

RH Term	Slope	Intercept	R^2	RMSE
Minimum RH	0.5313	7.4262	0.54	15.34
Average RH	0.5261	7.7246	0.52	3.59
RH Range	1.1319	0.4852	0.57	9.36
No RH	0.4238	9.3771	0.44	15.67

The slope, intercept R^2 and Residual Mean Square Error refer to the results of the regression analysis, in which the aforementioned model was regressed against observed solar radiation values. The results of this analysis were not

decisive. Employing "average RH" produced the lowest RMSE, while including "RH range" in the model produced the highest R^2 and the closest to the ideal 1:1 line and an intercept of 0.

8.5.4 Conclusions

The RH range analysis, however, produced a considerable number of negative values of estimated solar radiation values, whereas none of the other analyses produced negative values. It was for this reason that it was decided to employ average RH rather than RH range.

8.5.5 Average RH and Solar Radiation Models in Other Climates

In Section 8.5.1 to 8.5.3, data from only one station, *viz.* that of Mt. Edgecombe was investigated in order to determine the optimal RH term to use in a solar radiation model. The objective of the following analysis is to investigate how including an RH term in a solar radiation model would work in other climates within South Africa.

8.5.6 Methods

Having established which RH term to use, the solar radiation model was tested against data from the remaining three weather stations, *viz.* De Vlei in the Western Cape to represent a winter rainfall climate, Vaalhartz in the North-West province to represent a semi-arid climate and Kenhardt in the Northern Cape to represent an arid climate.

8.5.7 Results and Discussion

The results are summarised in Table 8.7. With the exception of De Vlei, it was noted that the model used above, when including the RH term, failed to improve

on, or attain the accuracy of, the Liu and Scott (2001) or even the Bristow and Campbell (1984) models (Tables 8.2 to 8.5).

Table 8.7 Inclusion of an estimated RH term in a solar radiation model at various locations in South Africa

Location	R^2 (RH term included)	R^2 (RH term omitted)	RMSE (RH term included)	RMSE (RH term omitted
De Vlei	0.84	0.72	2.56	4.22
Mt Edgecombe	0.52	0.50	3.59	4.01
Vaalhartz	0.72	0.64	2.82	3.32
Kenhardt	0.74	0.63	2.65	6.25

8.5.8 Conclusions

Because overall there was no improvement, it was decided not to further pursue the explicit involvement of RH in a solar radiation model. The model was, however, unique in that it did display the degree to which involving an RH term in a solar radiation model could improve the estimate of solar radiation.

8.5.9 The Winslow *et al.* (2001) Model and RH

Winslow *et al.* (2001) attempted to include RH indirectly in another derivative of Bristow and Campbell's (1984) model. The Winslow *et al.* (2001) model takes the form:

$$R_s = T_{cf}G[1-0.877(e_s(T_{mn})/e_s(T_{mx}))]$$

where T_{cf} = cloud free atmospheric transmissivity (≠ Clear Sky Index; dimensionless)
= 0.67338 on a rainday (dimensionless)
= 0.774 on a non-rainday (dimensionless)

G = $[1-(H-\pi/4^2)/2H^2]-1$ (h)

H = half-day length (h)

$e_s(T_{mn})$ = saturated vapour pressure at minimum temperature (kPa)

$e_s(T_{mx})$ = saturated vapour pressure at maximum temperature (kPa).

8.5.10 Methods

Mount Edgecombe data were specifically selected since it was the most humid climate of the four test weather stations. Observed solar radiation data was compared with solar radiation values estimated using the Winslow *et al.* (2001) model.

8.5.11 Results and Discussion

The Winslow *et al.* (2001) model provided good results when compared with observed solar radiation data (*cf.* Figure 8.14). It was especially noteworthy that fewer outliers were recorded for the Winslow *et al.* (2001) model when compared to, for example, results from models of Liu and Scott (2001) or Bristow and Campbell (1984).

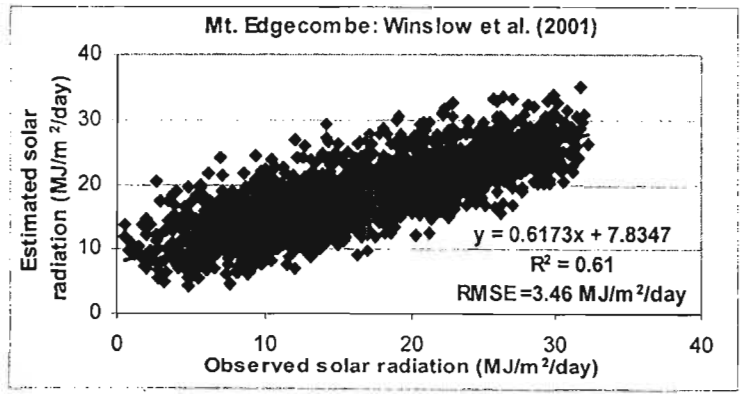

Figure 8.14 The Winslow *et al.* (2001) model compared with observed solar radiation data at Mt. Edgecombe in KwaZulu-Natal

8.5.12 Conclusions

In the literature survey, it was commented upon extensively that using saturated vapour pressure at minimum air temperature failed to provide an accurate

estimate of actual vapour pressure in arid locations (Running *et al.*, 1987; Bristow 1992; Kimball *et al.*, 1997). The ratio of saturated vapour pressure at minimum daily air temperature to saturated vapour pressure at maximum daily temperature in the Winslow *et al.* (2001) model means that this model is also, therefore, subject to the same constraints in arid locations.

8.6 Transferability of Coefficients

In previous sections the Liu and Scott (2001) model comes to the fore as the pre-eminent model at all of the chosen test locations, particularly in the humid locations. The various models were tested against data from already established weather stations. As has been stated in the introduction, politics and financial wherewithal play a role in determining where weather stations are to be located. The context of this dissertation is the estimation of vapour pressure and solar radiation at locations where these data are not being recorded, or where weather station network coverage is sparse.

8.6.1 Methods

The following verification analyses were undertaken in order to transpose "donor weather station" coefficients of the Liu and Scott (2001) model onto rainfall and temperature data from "recipient weather stations" situated in a similar climatic zone. Thereafter, the intention is to compare the output (estimated solar radiation) to recorded solar radiation data.

De Vlei in the Western Cape, (winter rainfall climate), Mount Edgecombe on the KwaZulu-Natal coast (humid coastal climate), Vaalhartz in North-West province (semi-arid climate) and Kenhardt in the Northern Cape (arid climate) were chosen as donor stations. De Vlei's recipient weather stations were Elgin in the Western Cape and Joubertina in the Eastern Cape. Mount Edgecombe's recipient stations were Hluhluwe and Wartburg. Besides being an exercise in the transferability of coefficients, a second objective of the Mt. Edgecombe/

Wartburg/Hluhluwe analyses was to investigate whether one should always choose coefficients of the nearest weather station or whether one should choose coefficients for a weather station located in a comparable climatic zone. Wartburg is located 60 km from the sea and lies at 990 m a.s.l. compared to Hluhluwe which is lies at 35 m a.s.l. and is 6 km from the coast. Mt. Edgecombe itself lies 9 km from the coast.

Kenhardt in the Northern Cape and Vaalhartz in North-West were used interchangeably as donor and recipient weather stations due to the paucity of weather stations in the arid and semi-arid locations. In the Western Cape and KwaZulu-Natal, two weather stations were used in the respective analyses because of the suspected influence of humidity on relationships. Note that Joubertina, although situated in the Eastern Cape was included in the Western Cape analysis.

8.6.2 Results and Discussion

The results are presented in Figures 8.15 to 8.20. As may be observed from Figures 8.15 to 8.20, coefficients are readily transferable between weather stations in regions with similar climates. Joubertina and De Vlei are 388 kilometres apart, yet only a 3% difference in variance was recorded when De Vlei's coefficients were used. The variance did in fact drop dramatically from 0.86 to 0.65 and 0.68 for Elgin and Joubertina. De Vlei's RMSE (established to be 2.06 $MJ/m^2/day$) increased by 1.76 and 2.36 $MJ/m^2/day$ for Elgin and Joubertina respectively.

Both Wartburg and Hluhluwe (respectively 51 and 209 km from the donor station at Mount Edgecombe) experienced a decline of approximately 22% and 5% in variance from that of Mt. Edgecombe with the RMSE increasing by 0.14 and 7.61 $MJ/m^2/day$ for Hluhluwe and Wartburg respectively.

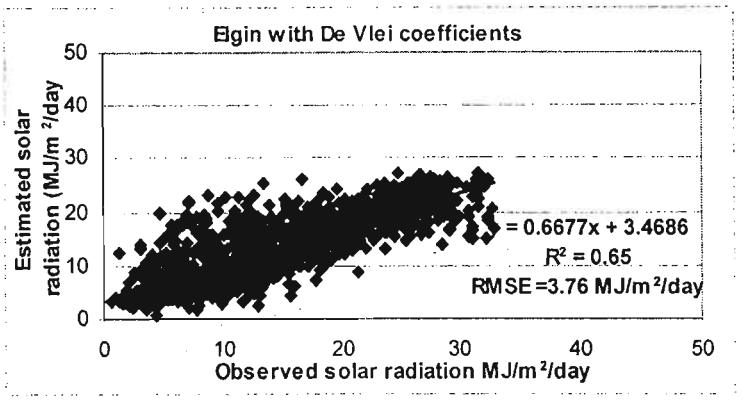

Figure 8.15 The Liu and Scott (2001) model used at Elgin with De Vlei's coefficients

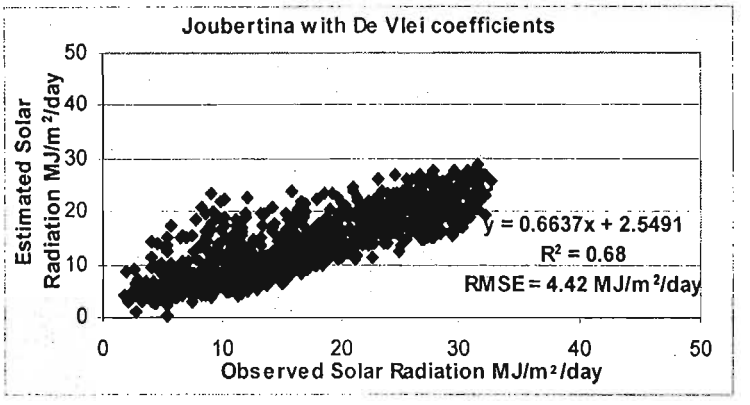

Figure 8.16 The Liu and Scott (2001) model used at Joubertina with De Vlei's coefficients

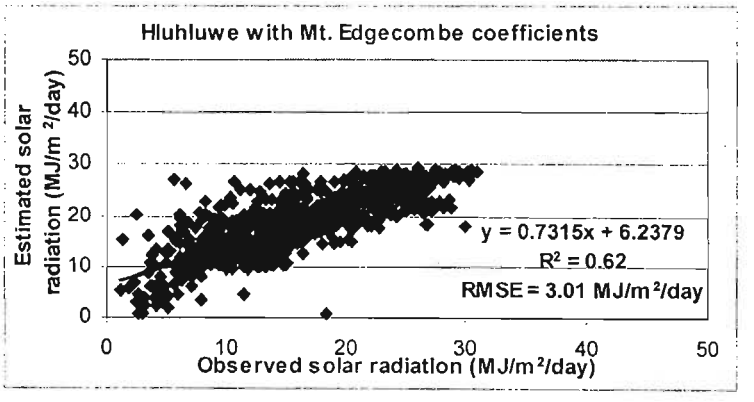

Figure 8.17 The Liu and Scott (2001) model used at Hluhluwe with Mt. Edgecombe's coefficients

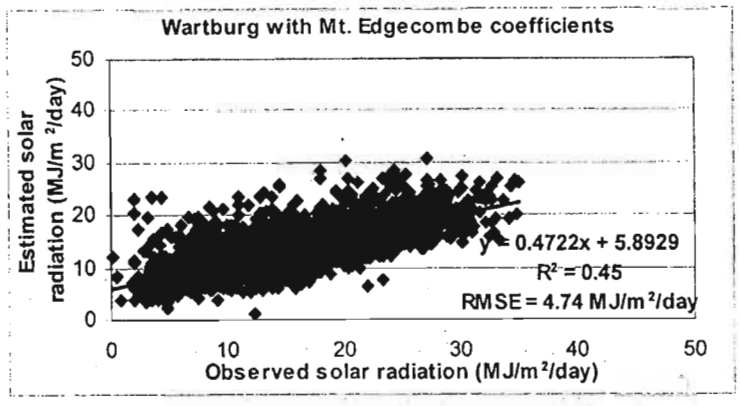

Figure 8.18 The Liu and Scott (2001) model used at Wartburg with Mt. Edgecombe coefficients

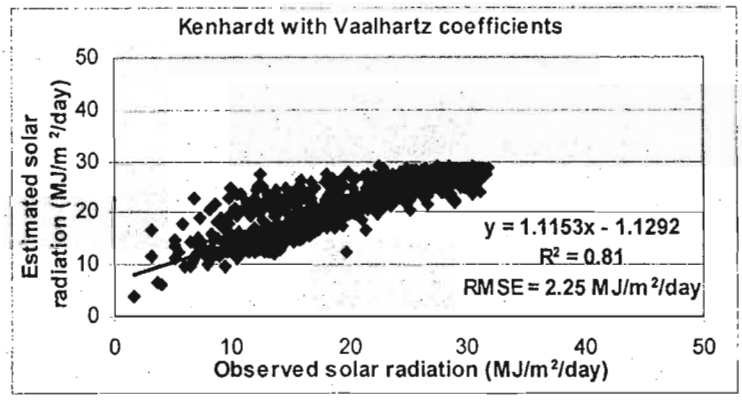

Figure 8.19 The Liu and Scott (2001) model used at Vaalhartz with Kenhardt's coefficients

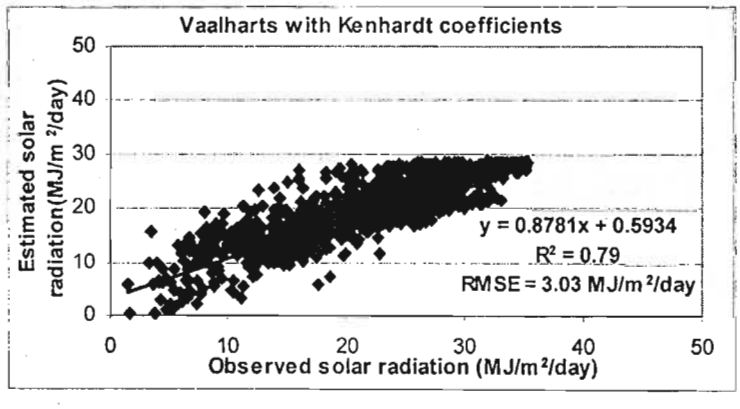

Figure 8.20 The Liu and Scott (2001) model used at Kenhardt with Vaalhartz's coefficients

Vaalhartz in the North-West province and Kenhardt in the Northern Cape produced accurate results despite the fact that a distance of 481 km separates them. It should be noted that Vaalhartz is classified as only semi-arid in character while Kenhardt is classified as arid. This latter fact ignores the recommendation made by Liu and Scott (2001), who stated that coefficients are only readily transferable in an identical/similar climatic zone. It must be stated, however, that Liu and Scott (2001) who were working in Australia, split their subject country into only four sub-regions. It is assumed that each of their climatic zones encompassed a considerable range of climates. It should also be noted that the method used in this analysis of transferring coefficients from nearby weather stations differed from that of Liu and Scott (2001), who obtained an aggregate for each coefficient from several weather stations per climate zone. The reason for this was, again, the relative paucity of data in South Africa particularly in the arid locations.

8.6.3 Conclusions

It was concluded that transferring coefficients from one station to another nearby station within a similar climatic regime produced acceptable results. In the Western Cape and particularly KwaZulu-Natal analyses, it was concluded that in order to minimise the error when transferring coefficients, it was better to choose coefficients from stations within in a similar climatic zone rather than coefficients from a station closest to the point of interest.

8.7 Overall Conclusions

The objective of Chapter 8 were to identify and isolate the best models available for estimating solar radiation using more readily available surrogate data (temperature and rainfall). A second objective was to attempt to improve on a given model's output by including atmospheric moisture status or atmospheric transmissivity, or both.

In this chapter, the Liu and Scott (2001) model comes to the fore as the "best" model available for the estimation of daily solar radiation over South Africa. However the Liu and Scott (2001) model is complicated in that it is first, a multiplicative equation and secondly, that it relies on a three day time step of raindays for each individual measurement of daily solar radiation. For this reason, it does not necessarily make the other models employed in the solar radiation analyses obsolete. In Chapter 9, which follows, maps are produced which employ alternative models to that of Liu and Scott (2001).

The coefficients for the model of Liu and Scott (2001) for 24 weather stations that measure solar radiation are displayed in Table 8.8. As may be observed, all coefficients generally approximate one another and those attained by Liu and Scott (2001). Despite the claim made by Liu and Scott (2001) that coefficient "a" could act as a *de facto* clear sky index, no pattern could be established where one could link coefficient "a" to a given factor, e.g. high altitude stations which would have a high clear sky index, as would stations located in arid regions.

It was also concluded that solar radiation models that rely on air temperature, specifically temperature range, indirectly included relative humidity. Atmospheric moisture status was also a central factor in the maximum transmissivity study (*cf.* Section 8.4), as annual relative humidity regime was considered to strongly affect the maximum transmissivity versus day of year curve at a given location.

Table 8.8 Coefficients of the Liu and Scott (2001) model for 29 weather stations in South Africa

Coefficients Location	a	b	c	d	e	f	g	R^2
Bergfontein	0.726	0.050	1.486	-0.021	-0.061	-0.110	-1.984	0.71
Bleskop	0.783	0.011	1.958	0.052	-0.139	-0.030	-0.834	0.83
Bloemfontein	0.774	0.006	2.209	0.053	-0.141	-0.032	0.043	0.83
Cedara	0.757	0.040	1.583	0.002	-0.153	-0.050	-0.157	0.76
De Tuin	0.774	0.212	1.727	0.558	-0.130	-0.044	-0.186	0.84
De Vlei	0.872	0.226	0.650	0.010	-0.167	-0.082	-2.405	0.86
Dundee	0.665	0.089	2.154	-0.002	-0.149	-0.004	0.829	0.75

Elgin	0.670	0.080	1.258	0.008	-0.142	-0.010	-0.129	0.74
Eston	0.727	0.034	1.530	0.041	-0.165	-0.064	1.417	0.76
Funeray	0.697	0.021	1.800	0.027	-0.184	-0.069	2.111	0.74
Hluhluwe	0.740	0.027	1.649	0.043	-0.140	-0.040	0.695	0.75
Joubertina	0.718	0.029	1.643	0.033	-0.143	-0.066	1.225	0.78
Kenhardt	0.670	0.006	2.400	0.006	-0.200	-0.042	-0.747	0.82
Lilydale	0.650	0.020	1.829	0.015	-0.180	-0.057	-7.200	0.83
Lydenburg	0.547	0.007	2.201	0.035	-0.155	-0.040	5.313	0.50
Mhlati	0.609	0.010	2.12	0.043	-0.147	-0.032	3.098	0.64
Mt. Edgecombe	0.688	0.017	2.361	0.012	-0.186	-0.032	-0.940	0.67
Nelspruit	0.610	0.007	2.272	0.030	-0.141	-0.042	3.107	0.65
Pondoland	0.629	0.022	1.857	0.024	-0.156	-0.034	2.676	0.65
Rustenburg	0.738	0.020	1.654	0.060	-0.102	-0.027	0.787	0.69
St. Lucia	0.770	0.031	0.599	0.043	-0.137	-0.050	-0.301	0.76
Tsolo	0.735	0.022	1.763	0.025	-0.161	-0.049	0.206	0.79
Vaalhartz	0.780	0.033	1.540	0.902	-3.080	-0.536	-2.230	0.84
Wartburg	0.737	0.030	1.632	0.008	-0.143	-0.079	0.769	0.75

CHAPTER 9

MAPPING OF SOLAR RADIATION

In Chapter 8 six models, *viz.* those by Bristow and Campbell (1984), Hargreaves *et al.* (1985), Clemence (1992), Hunt *et al.* (1998), Donatelli and Campbell (1998) and Liu and Scott (2001) were selected from the literature for further analysis. The Liu and Scott (2001) model was identified as the "best" of the models available for estimating solar radiation at ground level in South Africa. Of these six the Liu and Scott (2001) model, however, cannot easily be used in a mapping exercise because it includes the progressive three-day rainday multiplier ($...dR_{j-1} + eR_j + fR_{j+1}$) in its equation. It is this fact, therefore, that limits the Liu and Scott (2001) model to only being a daily solar radiation estimator as opposed to being a monthly mean solar radiation model, which is what is required for this chapter.

9.1 Selection of a Model for Solar Radiation Mapping

The Clemence (1992) model had previously been employed in the construction of solar radiation maps in the South African Atlas of Agrohydrology and - Climatology (Schulze, 1997). As has already been observed in Chapter 8, the Clemence (1992) model produced one of the lowest R^2 of all the models used in the selection process. This meant that for mapping purposes, the selection was restricted to models by Bristow and Campbell (1984), Hargreaves *et al.* (1985), Hunt *et al.* (1998) and Donatelli and Campbell (2001). The selection was further narrowed down by the elimination of the Hargreaves *et al.* (1985) model, which had one of the worst performances when used with Mt. Edgecombe data (*cf.* Table 8.3). Of these remaining models, the Hunt *et al.* (1998) model was chosen ahead of those by Bristow and Campbell (1984) and Donatelli and Campbell (1998). Although these three models produced similar goodness of fit statistics when compared with observed data, those by Bristow and Campbell (1984) and Donatelli and Campbell (1998) both exhibited considerable offsets, i.e. intercepts, (*cf.* Tables 8.2 to 8.5). Figures 9.1 and 9.2 show the distribution of solar

radiation by the Hunt *et al.* (1998) model over South Africa for the months of January (midsummer) and July (midwinter) respectively.

9.2 Interpretation and Discussion

For January, in the more humid regions of the summer rainfall areas, one can observe patches of very high solar radiation areas surrounded by areas of low solar radiation (denoted by patches of red surrounded by patches of blue, *cf.* Figure 9.1). Conversely, one can observe an area of very low daily solar radiation (blue) surrounded by areas of higher solar radiation (red) in the Western Cape. Closer observation revealed that the majority of these locations lay in the escarpment regions of KwaZulu-Natal and Mpumalanga provinces and in the mountainous regions of the Cape interior (Hottentots Holland, in the Stellenbosch district). In the July map (Figure 9.2), the opposite occurs in the same region of the Western Cape, where high values for midwinter of solar radiation are surrounded by much lower values. These regions coincided precisely with the areas of highest recorded rainfall in the country (*cf.* South African Atlas of Agrohydrology and –Climatology, Schulze, 1997).

It was concluded that these are not realistic representations in these particular regions, and that the cause of this was that the second of the two precipitation terms, *viz.* P^2 (which possesses a positive coefficient) in the Hunt *et al.* (1998) model, was dominating the relationship in these regions, thereby inducing extremely the high solar radiation values.

A residual analysis of observed versus estimated values revealed that solar radiation data from particular weather stations had very low negative values (e.g. –10% to –15%) i.e. the observed monthly values were considered to be high.

Text continued on page 125

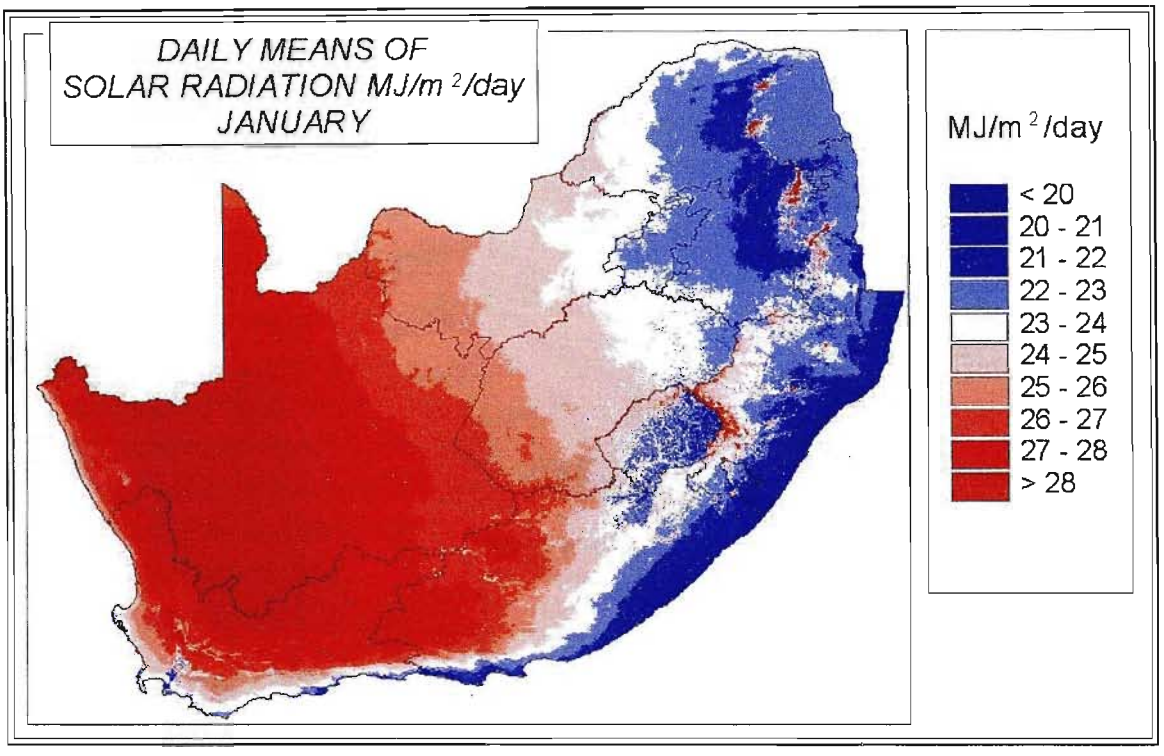

Figure 9.1 Daily mean of solar radiation for South Africa for January

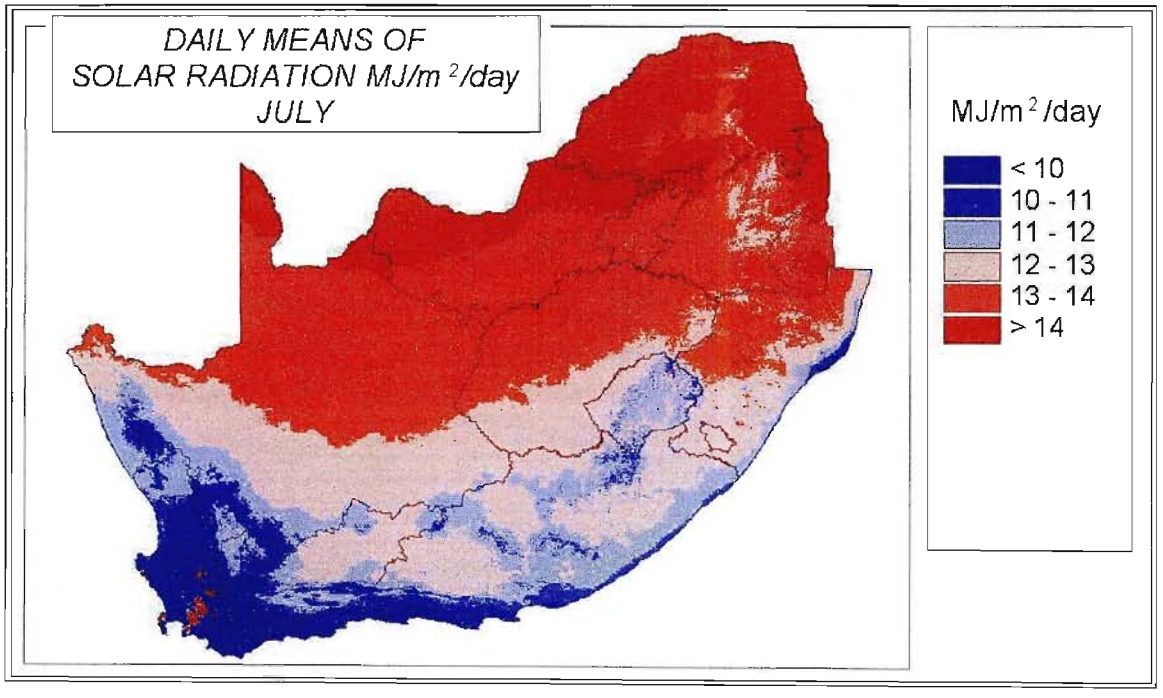

Figure 9.2 Daily mean of solar radiation for South Africa for July

Further investigation revealed that these particular stations were particularly well situated, i.e. no shadowing from surrounding mountain ranges could occur. This indicated that majority of weather stations employed in the solar radiation analyses experienced some degree of shadowing from surrounding high ground.

Two recommendations can be made as a result of this mapping exercise. First, one should identify these stations and find the difference between maximum solar radiation at these stations and other stations of similar latitude and altitude, thereby establishing a correction factor for the latter stations. Having corrected the observed data for aspect and shadowing influences, one should only then proceed to create the solar radiation surfaces. Secondly, concerning the very high solar radiation values in mountainous areas, which resulted from the precipitation term in the Hunt *et al.* (1998) model, two options lend themselves to the researcher/ cartographer. One could ensure that solar radiation data from as many weather stations in these mountainous areas are employed in subsequent mapping exercises. Alternatively, if one is lacking weather station data in these areas, one could employ only models which employ temperature data.

Herewith ends the solar radiation analyses. Further and more general recommendations for solar radiation are stated in the following chapter, Chapter 10, the final chapter in this dissertation.

Problem Statement: In order to estimate daily reference potential evaporation using the Penman-Monteith equation, values of daily vapour pressure and solar radiation are required

Objectives: To review current literature on current models for the estimation of daily vapour pressure and solar radiation, thereafter to employ and improve upon current method and models of estimating vapour pressure and solar radiation

Problem Statement

Broad Objectives	Literature Survey	Methods and Methodologies	Vapour Pressure Estimation	Solar Radiation Estimation	Conclusions and Recommendations
Specific Objectives	i) Introduction Chapter 1 ii) Definitions relating to vapour pressure and solar radiation Chapter 2 iii) Review literature on current methods of estimating daily vapour pressure. Chapter 3 iv) Review literature on current methods of estimating daily solar radiation. Chapter 3	i) Methods and methodologies employed in Chapters 6 to 9 Chapter 4	i) Characterisation of the vapour pressure regime in South Africa. Chapter 5 ii) Development of new models and methodologies of estimating vapour pressure. Chapter 6 iii) Verification of new methods. Chapter 7 iv) Vapour pressure relative humidity and vapour pressure maps Chapter 7	i) Factors affecting solar radiation at ground level Chapter 8 ii) Development of new models and methodologies of estimating solar radiation. Chapter 8 iii) Verification of new methods. Chapter 9 iv) Solar radiation maps Chapter 9	i) Conclusions and recommendations for future research Chapter 10

Chapter 10

CONCLUSIONS AND RECOMMENDATIONS

Techniques for estimating two different climatic elements in South Africa, *viz.* vapour pressure and solar radiation, have been evaluated in this dissertation. Both variables are key inputs for the Penman-Monteith equation, which is currently recognised internationally as the standard reference for the estimation of potential evaporation. Because of their differences, the general conclusions on the estimation of vapour pressure and solar radiation, and recommendations for future research, are presented separately.

10.1 Vapour Pressure

Up until the present time, relatively little research has been conducted on the subject of the estimation of daily vapour pressure. The estimation of daily vapour pressure thus remains an elusive goal. The method described by Bristow (1992) remains the single most important one of estimating vapour pressure on a daily basis. However, as described in the verification chapter (Chapter 6), averaged daily vapour pressure for an entire month was a more achievable goal. It was also shown that this single value per month could be employed to estimate relative humidity and vapour pressure deficit.

10.1.1 Conclusions

It was concluded that over South Africa geographical location and seasonality play the greatest roles in determining the vapour pressure at any given location. The most significant cause of "within-month", i.e. the daily, variation in vapour pressure was found to be air masses. The context of this dissertation is to derive techniques to estimate daily vapour pressure from simple and readily available climatic surrogates such as daily temperature and rainfall. Determining characteristics on air masses would require considerably more complex

information on wind direction, wind speed and relative humidity. Since such information is not readily available, air masses as a variable were therefore omitted from the eventual vapour pressure model. Since air masses were omitted, it was concluded that only monthly means of daily vapour pressure could be estimated explicitly from invariate and variate factors. From this monthly vapour pressure model, as well as a model by Bristow (1992), highly acceptable daily values of vapour pressure could, however, be obtained.

10.1.2 Recommendations

Despite previous conclusions on the strong role of changes in daily vapour pressure resulting from characteristics of prevailing air masses, it was hypothesised that vapour pressure could nevertheless be estimated using only temperature data as a variable, in addition to other invariates. Water in liquid or vapour form acts as a "heat sink". This can be observed by the fact that lower vapour pressures encountered in the arid regions are associated with higher daily temperature ranges. It is suggested, therefore, that in future the minimum possible vapour pressure for a specific month be calculated, thereafter an attempt be made to associate daily temperature range with the difference between vapour pressure on that specific day and mimimum possible vapour pressure. In theory this should be an inverse relationship.

10.1.3 Vapour Pressure Data Quality Control: Recommendations

Some 90% of the data used in the vapour pressure sections of this dissertation were obtained from the South African Weather Service, with the remaining 10% obtained from the ARC-ISCW. Approximately 36 % of the data obtained had to be excluded as it was suspected to be incorrect. It is recommended that databank managers draw day-to-day profiles of uncorrected vapour pressure for the entire record at each weather station, as displayed in Figure 10.1. This allows one to be able to observe immediately which data should be treated with caution.

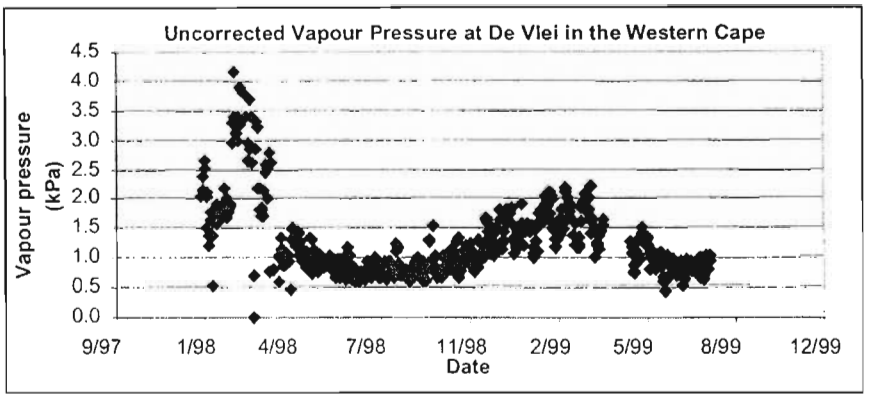

Figure 10.1 An example of how to determine data integrity of vapour pressure and, therefore, RH data by graphical display, with data recorded after April 1998 being considered acceptable

A second method of quality control for vapour pressure data would be to employ a "nearest station" check, especially if one becomes suspicious of extreme individual values. The theory behind a "nearest station" check is that extreme events do not happen in isolation. The influence of air masses (a macroclimatic factor) on daily vapour pressure, alluded to earlier in this chapter, and illustrated in Chapter 6, indicates that this element lends itself to estimation by using the "nearest station" check. Although the "nearest station" check was not applied in this dissertation, Xia *et al.* (1999), who researched methods of estimating missing vapour pressure values along with those of several other climate elements in Bavaria, Germany, recommended using the either the "nearest station" method or a multiple regression model for estimating missing vapour pressure data.

10.2 Solar Radiation

Unlike the estimation of vapour pressure, the estimation of solar radiation is an older and, therefore, a more established science. The reasons for this have been explained in previous chapters. The focus in this study was therefore on comparisons of recently formulated solar radiation models with observed data.

10.2.1 Conclusions

It was concluded that the Liu and Scott (2001) model was the best model of the six tested for the estimation of daily solar radiation. It was also concluded that the Bristow and Campbell (1984) "component" of the equation (i.e. that part which used only temperature data) also indirectly accounted for the influence of atmospheric moisture. In spite of these positive findings, the problem of negative estimated values of solar radiation remains. Negative estimated solar radiation values appeared to be particularly acute during the cooler winter months, when low extraterrestrial solar radiation was combined with days on which very small temperature ranges were experienced. Several options of dealing with this problem present themselves for future research. From empirical observations one can set the temperature range to a minimum of 4° C during the autumn and spring months, with this value changing to 7° C during the colder winter months. Alternatively, one could set negative estimated values to a default value, for example 20% of the extraterrestrial solar radiation on that day, since diffuse radiation on a cloudy day ranges from 16% to 25% of extraterrestrial solar radiation (Savage, 2003; pers. com)

From the atmospheric transmissivity analyses, it was concluded that much of the South African data lacked the resolution to establish accurately what the maximum transmissivity should be at individual locations, and how it may vary intra-annually. In the Western Cape, considerable variance in maximum transmissivity was noticed. It is hypothesised that this was due to some of the weather stations being situated in valleys. Certain stations would, therefore, be shaded for a part of the day, leading to a reduced exposure to incoming solar radiation. It was also concluded that with all other factors being held constant, the natural relationship between day of the year and maximum transmissivity curve should be hyperbolic for most of the country, with this curve flattening out as one moves towards the tropical regions of South Africa. Where this curve becomes parabolic, it was concluded that this was, first, the result of the

location's being in the summer rainfall areas and, secondly, that it was due to the influence of localised RH regimes. The higher the average daily RH in the summer rainfall areas, the more parabolic this curve became.

10.2.2 Recommendations

While the Liu and Scott (2001) model produced the best results overall of the models tested, the Winslow *et al.* (2001) model deserves further study. Despite the Winslow *et al.* (2001) model's producing one of the poorest slopes (0.62, *cf.* Figure 8.18) when comparing estimated solar radiation values to observed solar radiation data, this model nevertheless produced the fewest outliers. It also produced the second highest variance accounted for, *viz.* 0.61 (*cf.* Figure 8.18), as opposed to the 0.64 of the Liu and Scott (2001) model. It is the experience of the author that the most influential coefficient on the slope of the observed/estimated regression is the first coefficient. In the case of the Winslow *et al.* (2001) model, this coefficient, defined as, cloud free atmospheric transmissivity, T_{cf}, is set to 0.673 on a rainday and 0.774 on a non-rainday. It is suggested that these values could be altered for each major climate zone of South Africa, following further research. The ratio of saturated vapour pressure at minimum temperature to saturated vapour pressure at maximum temperature is, however, going to be problematic in the arid regions. The reason for this would be that dew point temperatures are often never attained at night-time. Any further research into the Winslow *et al.* (2001) model would have to be coupled with further attempts to more accurately estimate dew point temperatures in arid locations.

10.2.3 Solar Radiation Data Quality Control: Recommendations

Calibration errors were suspected in many of the data sets used. Instrument variability clearly played a role in data quality. The Cedara and Dundee data sets, for example, produced a markedly different profile for older than for more recent data. The pyranometers used at Cedara and Dundee were of the

thermoelectric variety whereas the pyranometers used at the AGROMET (rural) weather stations of the ARC-ISCW were of the photovoltaic type. Figures 10.2 and 10.3 illustrate the different profiles from the respective instruments.

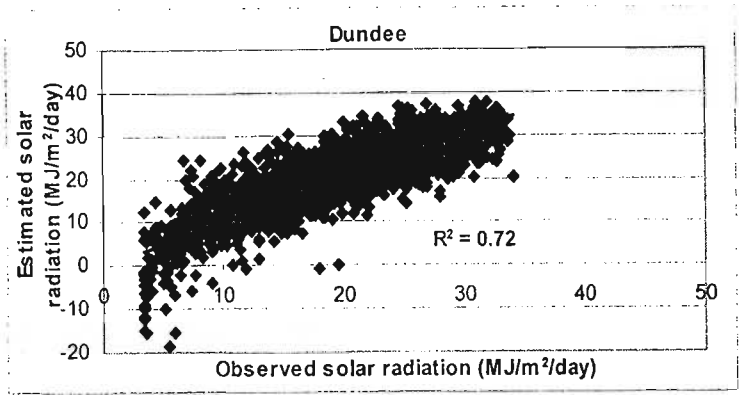

Figure 10.2 An example of the profile of estimated versus observed solar radiation for Dundee, where a thermoelectric sensor was employed

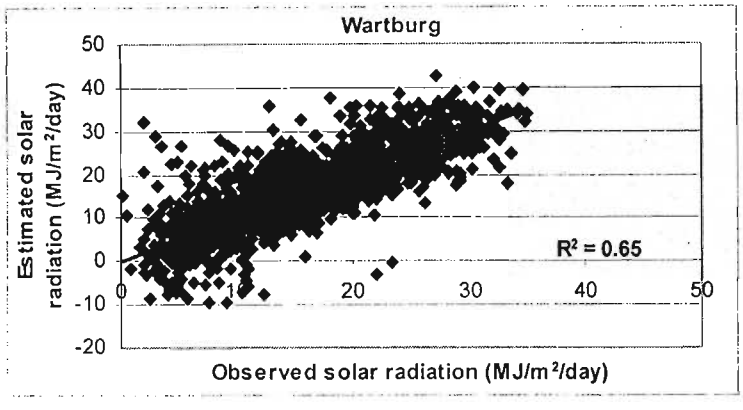

Figure 10.3 An example of the profile of estimated versus observed solar radiation for Wartburg, where a photovoltaic sensor was employed

As may be observed from Figures 10.2 and 10.3, the thermoelectric sensor only records to a minimum solar radiation value of approximately 3 MJ/m^2/day (Figure 10.2) whereas the photovoltaic sensor records any solar radiation value above zero (*cf.* Figure 10.3). This means that in analyses such as those undertaken in the solar radiation sections of this dissertation, considerably greater scatter is associated with data from the photovoltaic sensors. This problem could be partially offset if databank managers set solar radiation values to a minimum value of, for example, 3 MJ/m^2/day.

It is also recommended that databank managers produce a profile for the entire solar radiation record, along with a profile of the extraterrestrial solar radiation, in the same manner as recommended for uncorrected vapour pressure. This method should allow users to obtain immediate visualisation as to which data points are to be treated with caution. An example of such a profile is shown for De Aar, a semi arid location, in Figure 10.4. In this case the entire record was omitted from further analyses because of excessively high solar radiation observations in the summers of 1995/96 and 1999/2000 (some values in excess of extraterrestrial solar radiation) compared with excessively low readings recorded in the summers 2000/01 and 2001/02 when maximum solar radiation was only 30 MJ/m^2/day, i.e. ~66% of the extraterrestrial solar radiation, a value far to low for a semi-arid and frequently cloudless location.

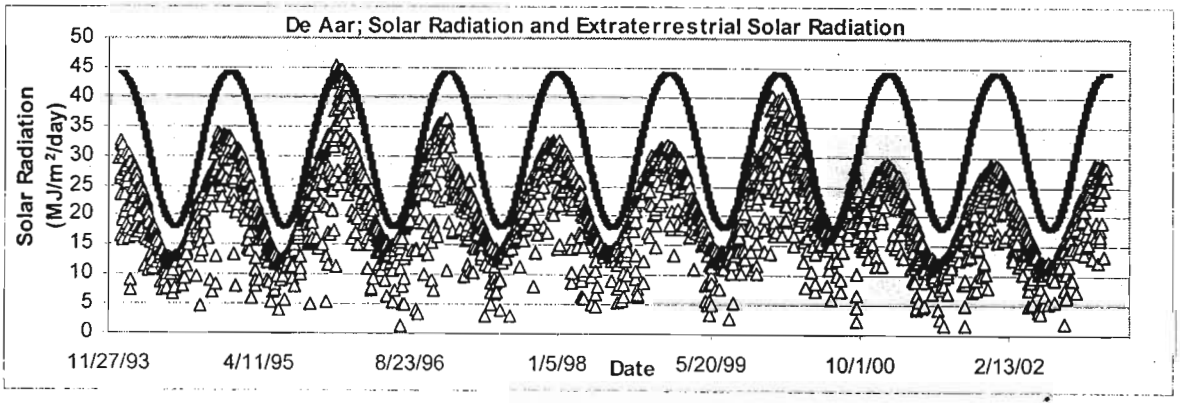

Figure 10.4 An example of profiles of solar radiation in comparison with extraterrestrial solar radiation at De Aar in the Northern Cape

10.3 General Conclusions

At present, relatively few data exist in South Africa for vapour pressure and solar radiation. Both elements are, however, required for use in the Penman-Monteith equation, the currently internationally accepted standard reference for the estimation of potential evaporation. It is, therefore, necessary to estimate values of vapour pressure and solar radiation from more readily available data such as temperature and rainfall.

As was stated in the introductory chapter of this dissertation, the context of this dissertation is to improve on the standard method of estimating vapour pressure, (i.e. Bristow, 1992) in order to estimate vapour pressure deficit, a component in the Penman-Monteith equation. In the preceding chapters, it was determined that relative humidity and vapour pressure deficit could be estimated with confidence by holding vapour pressure constant for an entire month and that this method performed better in arid than humid locations in South Africa. Monthly means of daily vapour pressure were estimated by separate monthly multiple regression models for each month of the year by using geographic information along with temperature data.

The literature survey indicated that, considerable research has been undertaken on the subject of estimating solar radiation at ground level. Of all the methods chosen, the Liu and Scott (2001) model was established to be the most reliable throughout South Africa. It was also established that the long-standing goal of researchers of somehow including atmospheric moisture in a solar radiation model has already been partially realised by the Bristow and Campbell (1984) model, which itself formed the basis of the majority of subsequent attempts by researchers to model solar radiation, the Liu and Scott, 2001 model included.

The estimation of two elements, vapour pressure and solar radiation, has been improved upon, and the Penman-Monteith equation can thus now be more confidently applied throughout South Africa at daily time steps. Of these two elements it is vapour pressure, which, because of a paucity of research to date on the subject, lends itself to expansive research in the future.

REFERENCES

Australian Bureau of Meteorology, 2002. Available from <http://www.bom.gov.au/sat> [Accessed 21/10/02].

Bezuidenhout C.N., 2002. Using the Nearest Neighbour Method to substitute missing daily solar radiation data. South African Journal of Plant and Soil, 19, 195-200.

Bristow K.L., 1992. Prediction of daily mean vapour density from daily minimum air temperature. Agricultural and Forest Meteorology, 59, 309-317.

Bristow K.L. and Campbell G.S., 1984. On the relationship between incoming solar radiation and daily maximum and minimum temperature. Agricultural and Forest Meteorology, 31, 159-166.

Bristow K.L., Campbell G.S., Papendick R.I. and Elliott L.F., 1986. Simulation of heat and moisture transfer through a surface residue–soil system. Agricultural and Forest Meteorology, 36, 193-214.

Boisvert J.B., Hayhoe H.N. and Dube P.A., 1990. Improving the estimation of global solar radiation across Canada. Agricultural and Forest Meteorology, 52, 275- 286.

Castellvi F., Stockle C.O., Perez P.J. and Ibanez M., 1997. Comparison of methods for applying the Priestley-Taylor equation at a regional scale. Hydrological Processes, 15, 1609-1620.

Cengiz, H.S., Gregory J.M., and Sebaugh J.L., 1981. Solar radiation prediction from other climatic variables. Transactions of the American Society of Agricultrual Engineers, 24, 1269-1272.

Clemence B.S.E., 1992. An attempt at estimating solar radiation at South African sites, which measure air temperature only. South African Journal of Plant and Soil, 9, 40-42.

De Jong R. and Stewart D.W., 1993. Estimating global solar radiation from common meteorological observations in western Canada. Canadian Journal of Plant Science, 73, 509-518.

Donatelli M. and Campbell G.S., 1998. A simple model to estimate global solar radiation. Proceedings of Fifth Congress of the European Society of Agronomy. Nitra, Slovakia, 133-134.

Hunt L.A., Kuchar L. and Swanton C.J., 1998. Estimation of solar radiation for use in crop modelling. Agricultural and Forest Meteorology, 91, 293-300.

Iziomon M.G. and Mayer H., 2002. Characterisation of the shortwave radiation regime for locations at different altitudes in South West Germany. Climate Research, 20, 203-209.

Kimball H. H., 1927. Measurement of solar radiation Intensity and determination of the depletion by the atmosphere. Monthly Weather Review, 55, 155-169.

Kimball J.S., Running S.W. and Nemani R., 1997. An improved method of estimating surface humidity from daily minimum temperature. Agricultural and Forest Meteorology, 85, 87-89.

Liu D. L. and Scott B.J., 2001. Estimation of solar radiation in Australia from rainfall and temperature observations. Agricultural and Forest Meteorology, 106, 41-59.

McCaskill M.R., 1990a. Prediction of solar radiation from rain day information using regionally stable coefficients. Agricultural and Forest Meteorology, 51, 247-255.

McCaskill M.R., 1990b. An efficient method for generation of full climatological records from daily rainfall. Australian Journal of Agricultural Research, 41, 595-602.

McGee O.S., 1971. Atmospheric Water Vapour Transport over South Africa. PhD Thesis, Department of Geography, University of Natal, Pietermaritzburg. pp 216.

Meek D. W., 1997. Estimation of the maximum possible daily global solar radiation. Agricultural and Forest Meteorology, 87, 223 -241.

Meinke H., Carberry P.S., McCaskill M.R., Hills M.A. McLeod I., 1994. Evaluation of radiation and temperature data generators in the Australian sub-tropics using crop simulation models. Agricultural and Forest Meteorology, 72, 295-316.

NASA, 2002. Available from <http://earthobservatory.nasa.gov/Library/Aerosols> [Accessed 23/09/2002].

National Renewable Energy Laboratory, 2002. Available from http://www.nrel.gov/education/erulf/> [Accessed 12/09/2002].

Revfeim K.J.A., 1997. On the relationship between radiation and mean daily sunshine. Agricultural and Forest Meteorology, 86, 183-191.

Running S.W., Nemani R.R. and Hungerford R.D., 1987. Extrapolation of synoptic meteorological data in mountainous terrain and its uses for simulating

forest evapotranspiration and photosynthesis. Canadian Journal of Forestry Research, 17, 472-483.

Sadler E.J. and Evans D.E., 1989. Vapour pressure deficit calculations and their effect on the combination equation. Agricultural and Forest Meteorology, 49, 55-80.

Savage M.J., 2003. Personal communication: University of KwaZulu-Natal, KwaZulu-Natal, South Africa, 14/4/2003.

Satturland D.R. and Means J.E., 1978. Estimating solar radiation under variable cloud conditions. Forest Science, 24, 363 -373.

Schulze R.E., 1974. Catchment Evaporation in the Natal Drakensberg. PhD thesis, University of Natal, Pietermaritzburg. pp244.

Schulze R.E., 1997. Section 3: Solar Radiation, South African Atlas of Agrohydrology and -Climatology. Water Research Commission, Pretoria, Report TT82/96. pp 276.

Steel R.G.D. and Torrie J.H., 1981. Principles and Procedures of Statistics: A Biometrical Approach. Napier C. and Maisel J.W. Second Edition, Volume1, Chapter 3. 39-66, McGraw-Hill International Editions.

Tesfamicheal B., 2001. Satellite images of Eritrea: Available from online seminar of Solar Radiation and Resource Mapping for Eritrea, <http://eappc48.lbl.gov/papers> [Accessed 7/09/2002].

Thornton P.E. and Running S.W., 1998. An improved algorithm for estimating incident daily solar radiation, from measurements for temperature, humidity and precipitation. Agricultural and Forest Meteorology, 93, 211-228.

Thornton P.E., Hasenauer H. and White A. M., 2000. Simultaneous estimation of daily solar radiation and humidity from observed temperature and precipitation: An application over complex terrain in Austria. Agricultural and Forest Meteorology, 104, 255-271.

Van Buskirk R., 2002. Personal communication: University of Asmara, Eritrea. 11/09/2002.

Winslow J.C. Hunt E.R. Piper S.C. (2001). A globally applicable model of daily solar irradiance estimated from air temperature and precipitation data. Ecological Modelling, 143, 227-243.

Xia Y., Fabian P., Stohl A. and Winterhalter M., (1999). Forest climatology: Estimation of missing values for Bavaria, Germany. Agricultural and Forest Meteorology, 96, 131-144.

Zucchini W., 1991. Quoted by Clemence, B.S.E. (1992). Department of Statistical Services, University of Cape Town.

Appendix 1: Maximum transmissivity curves recorded at weather stations used in Chapters 8 and 9

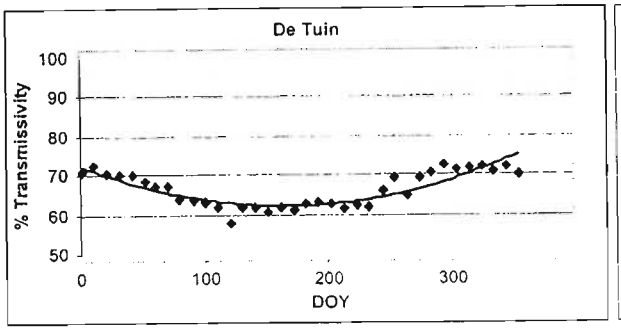

App 1.1 Maximum transmissivity curve at De Tuin in the Western Cape

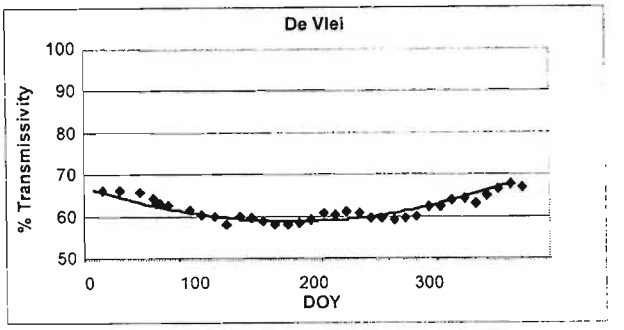

App 1.2 Maximum transmissivity curve at De Vlei in the Western Cape

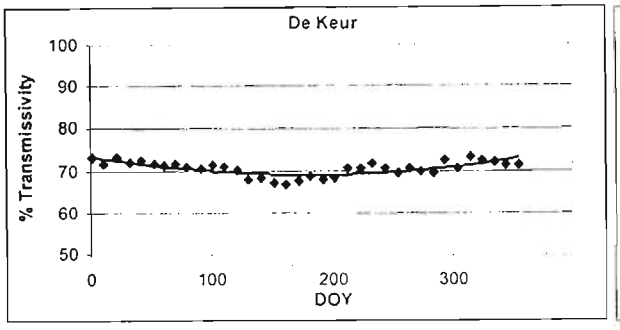

App 1.3 Maximum transmissivity curve at De Keur in the Western Cape

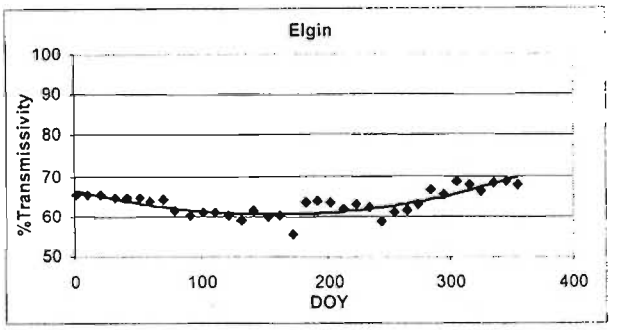

App 1.4 Maximum transmissivity curve at Elgin in the Western Cape

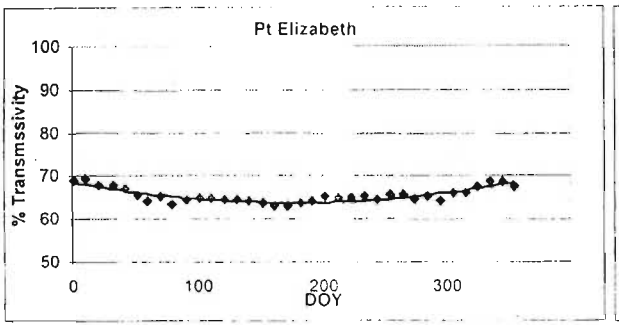

App 1.5 Maximum transmissivity curve at Port Elizabeth in the Eastern Cape

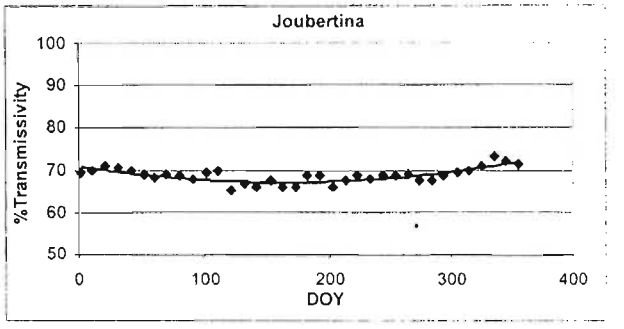

App 1.6 Maximum transmissivity curve at Joubertina in the Eastern Cape

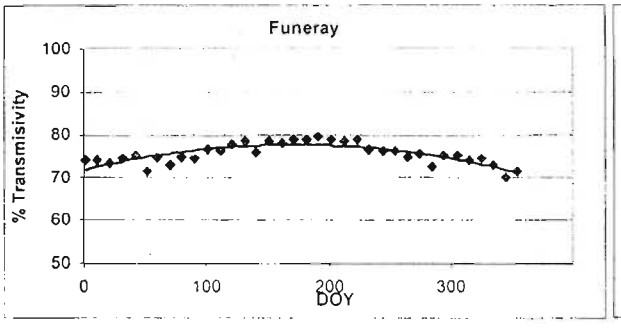

App 1.7 Maximum transmissivity curve at Funeray in the Eastern Cape

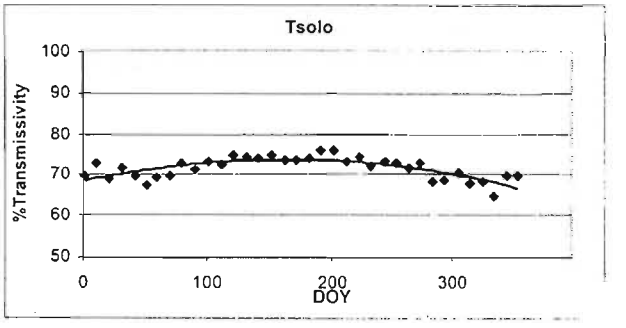

App 1.8 Maximum transmissivity curve at Tsolo in the Eastern Cape

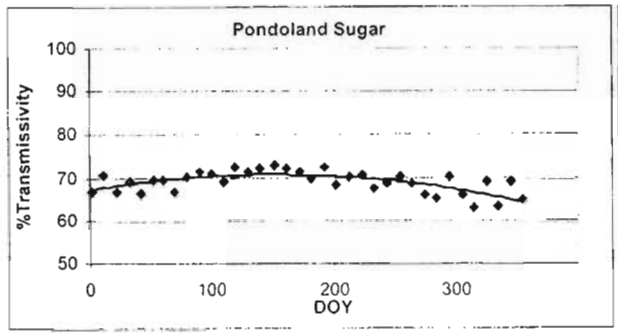

App 1.9 Maximum transmissivity curve at Pondoland in the Eastern Cape

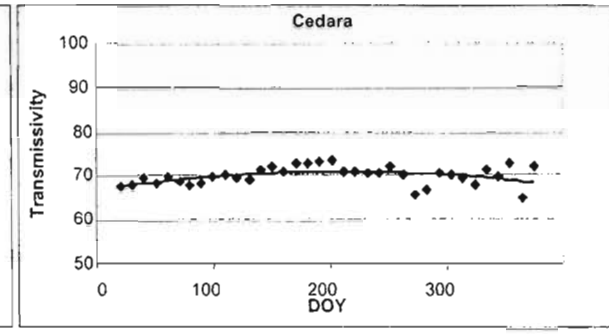

App 1.10 Maximum transmissivity curve at Cedara in the KwaZulu-Natal

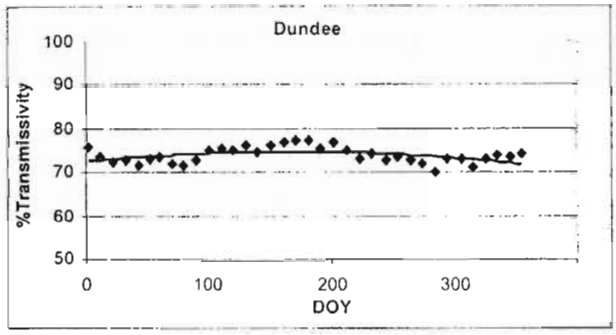

App 1.11 Maximum transmissivity curve at Dundee in the Kwa-Zulu Natal

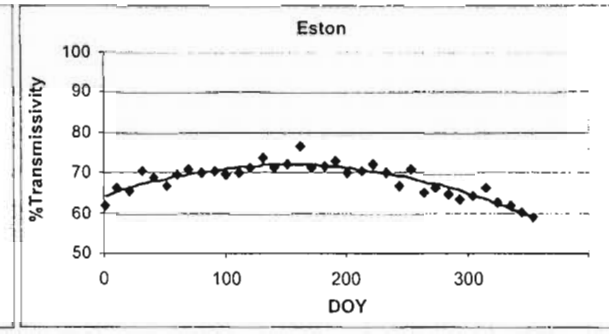

App 1.12 Maximum transmissivity curve at Eston in KwaZulu-Natal

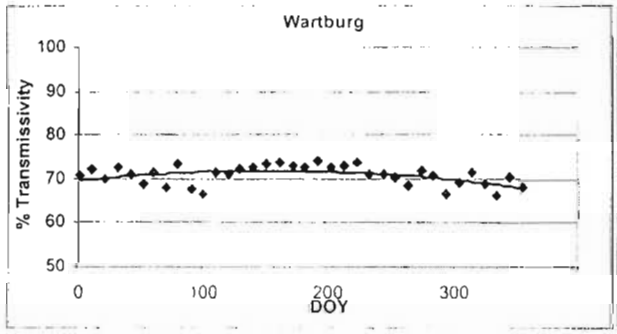

App 1.13 Maximum transmissivity curve at Wartburg in Kwa-Zulu Natal

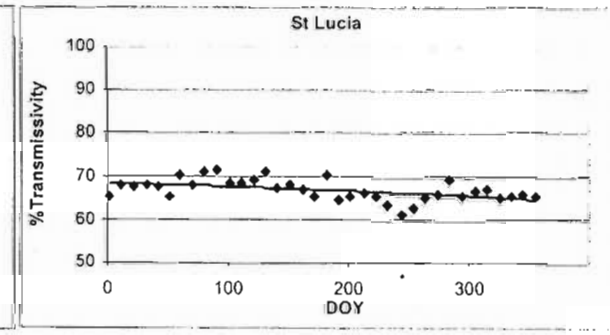

App 1.14 Maximum transmissivity curve at St. Lucia in Kwa-Zulu Natal

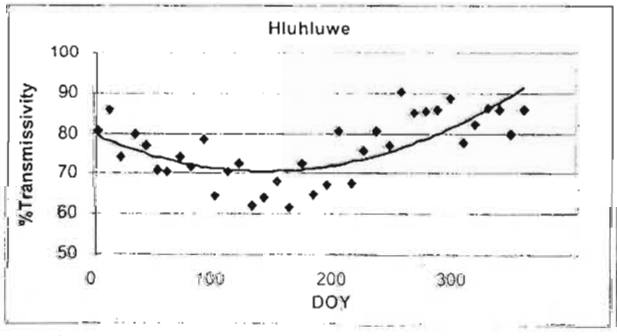

App. 1.15 Maximum transmissivity curve at Hluhluwe in KwaZulu-Natal

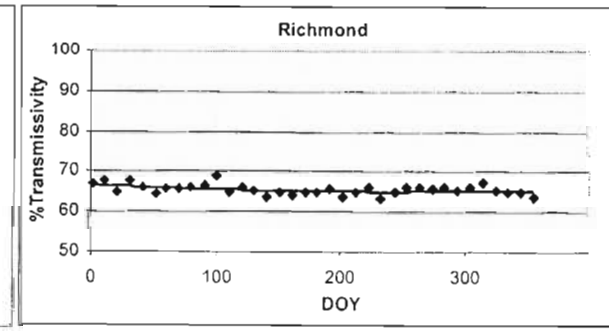

App 1.16 Maximum transmissivity curve at Richmond in KwaZulu-Natal

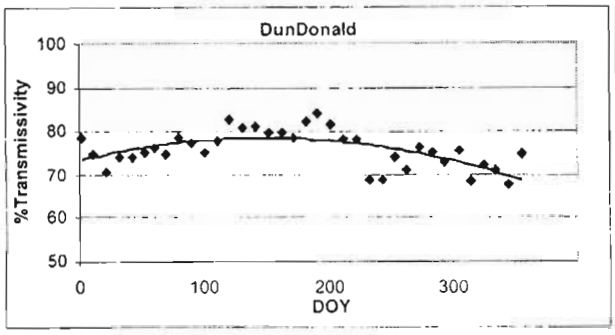

App 1.17 Maximum transmissivity curve at Dundonald in Mpumalanga

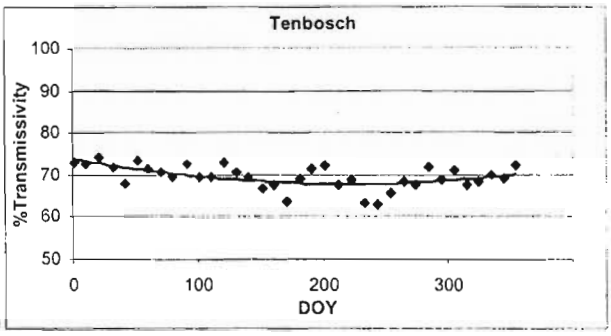

App 1.18 Maximum transmissivity curve at Tenbosch in Mpumalanga

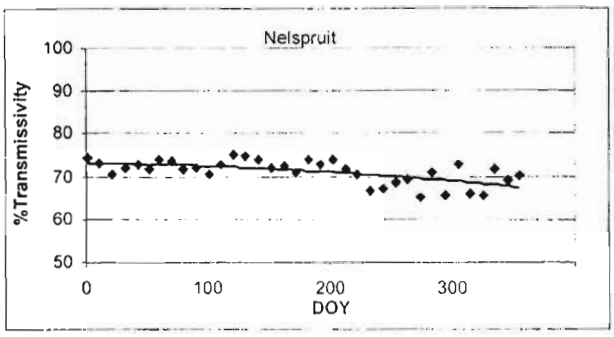

App 1.19 Maximum transmissivity curve at Nelpruit in Mpumalanga

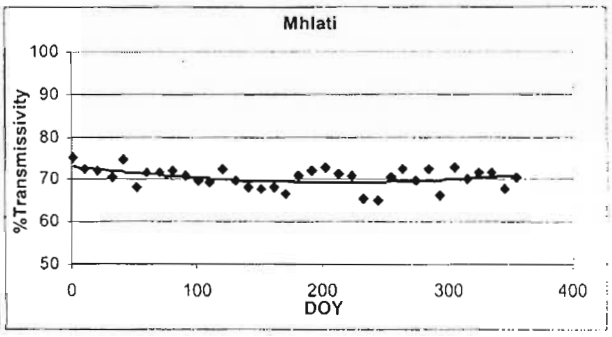

App 1.20 Maximum transmissivity curve at Mhlati in Mpumalanga

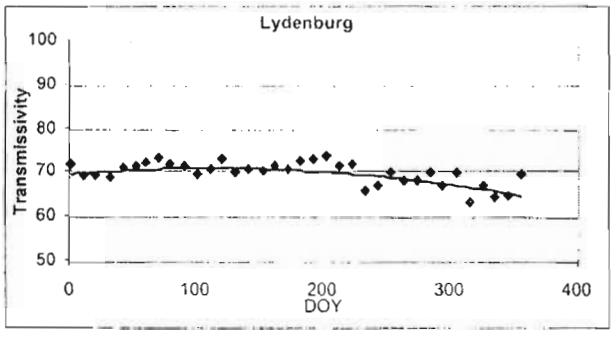

App 1.21 Maximum transmissivity curve at Lydenburg in Mpumalanga

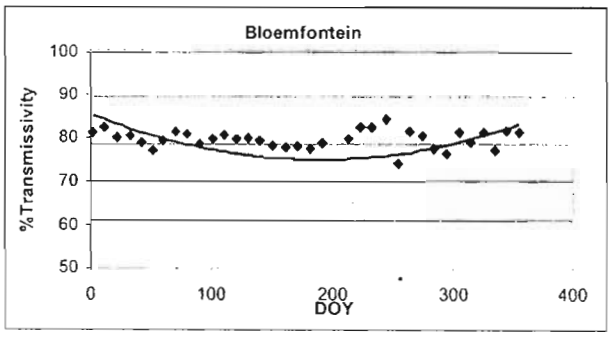

App 1.22 Maximum transmissivity curve at Bloemfontein in Free State

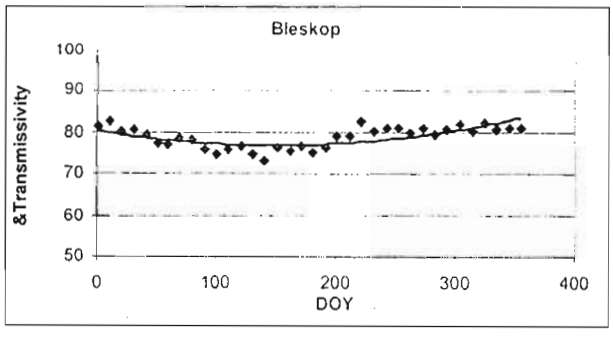

App 1.23 Maximum transmissivity curve at Bleskop in the Northern Cape

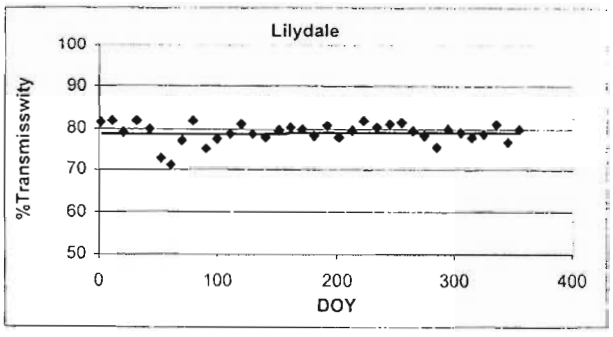

App 1.24 Maximum transmissivity curve at Lilydale in Free State

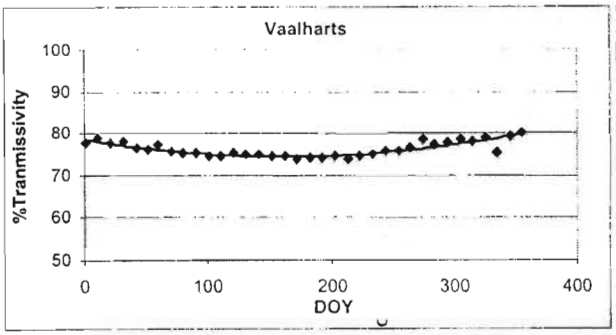

App 1.25 Maximum transmissivity curve at Vaalhartz in North-West province

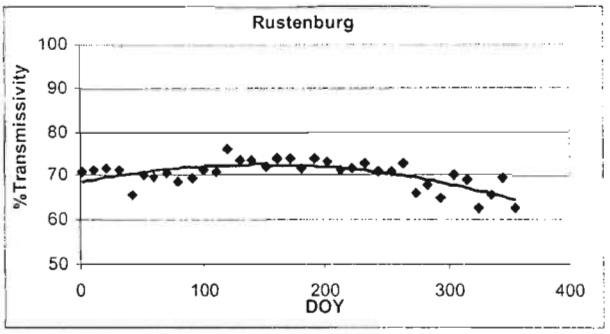

App 1.26 Maximum transmissivity curve at Rustenberg in North-West province

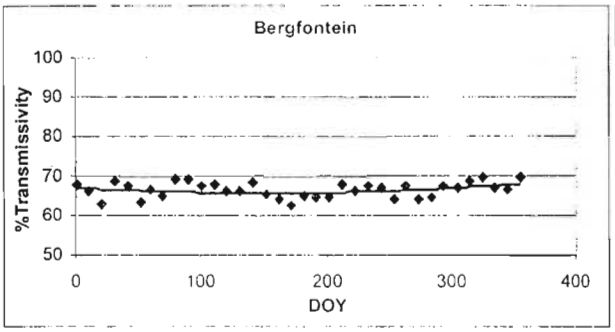

App 1.27 Maximum transmissivity curve at Bergfontein in Limpopo

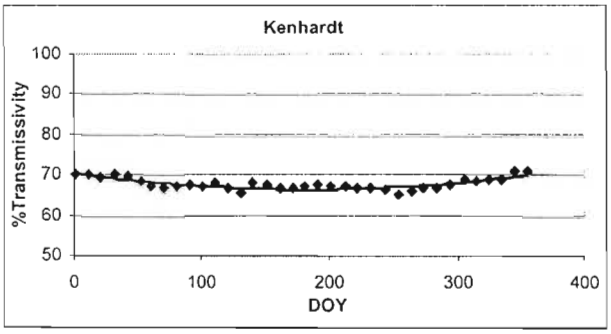

App 1.28 Maximum transmissivity curve at Kenhardt in Northern Cape

Appendix 2: Further Verifications of the Vapour Pressure Models in other Provinces of South Africa

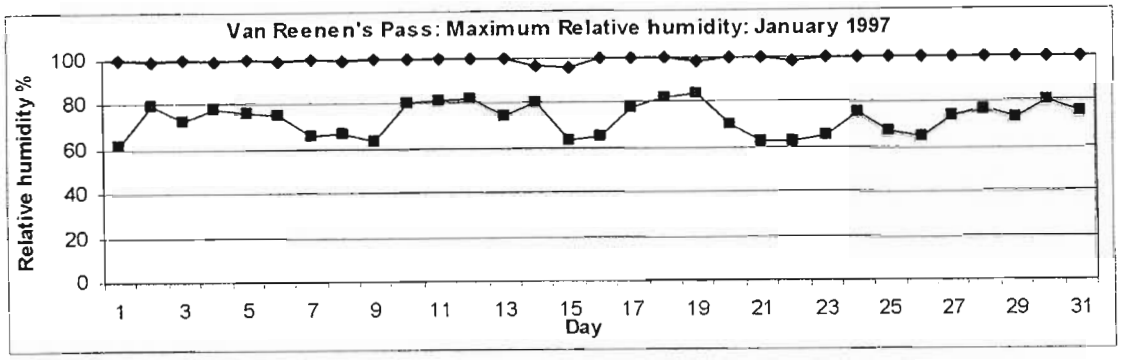

App 2.1 Comparison between January observed daily maximum RH(—♦—) and daily maximum RH estimated using the vapour pressure model (—■—) at Van Reenen's Pass, Free State province

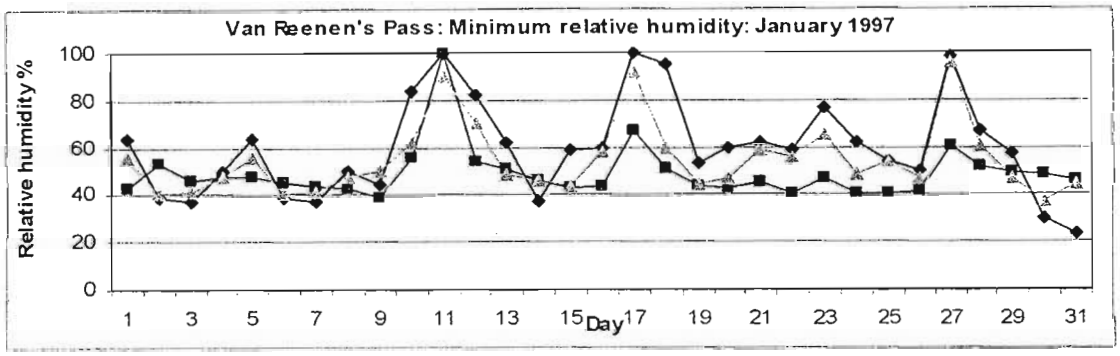

App 2.2 Comparison between January observed daily minimum RH (—♦—) and daily minimum RH estimated using the vapour pressure model (—■—) and Bristow's (1992) model (—△—) at Van Reenen's Pass, Free State province

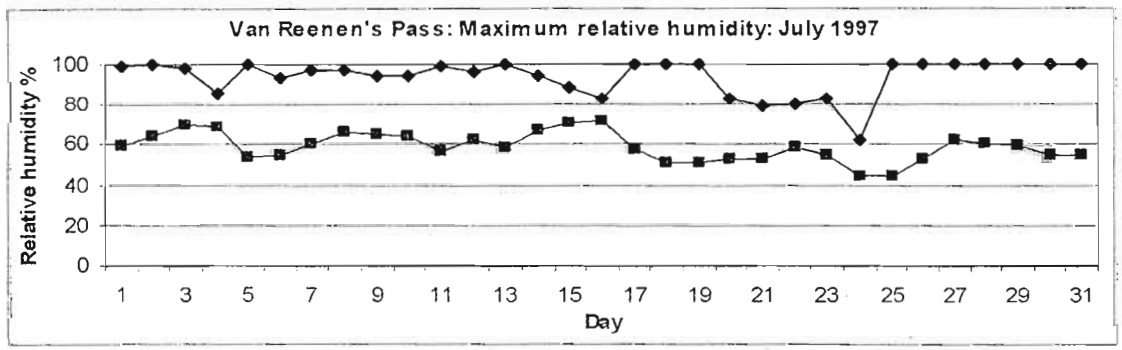

App 2.3 Comparison between July observed daily maximum RH (—♦—) and daily maximum RH estimated using the vapour pressure model (—■—) at Van Reenen's Pass, Free State province

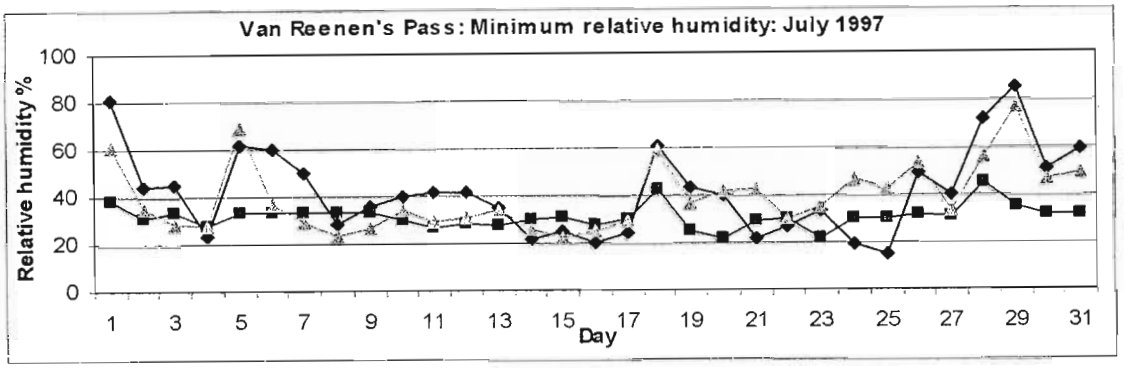

App 2.4 Comparison between July observed daily minimum RH (—◆—) and daily minimum RH estimated using the vapour pressure model (—■—) and Bristow's (1992) model (—▲—) at Van Reenen's Pass, Free State province

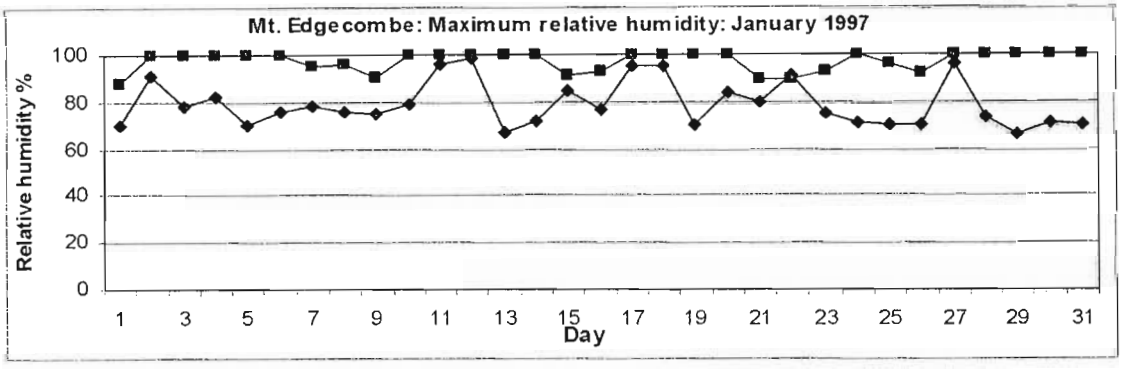

App 2.5 Comparison between January observed daily maximum RH (—◆—) and daily maximum RH estimated using the vapour pressure model (—■—) at Mt. Edgecombe, KwaZulu-Natal

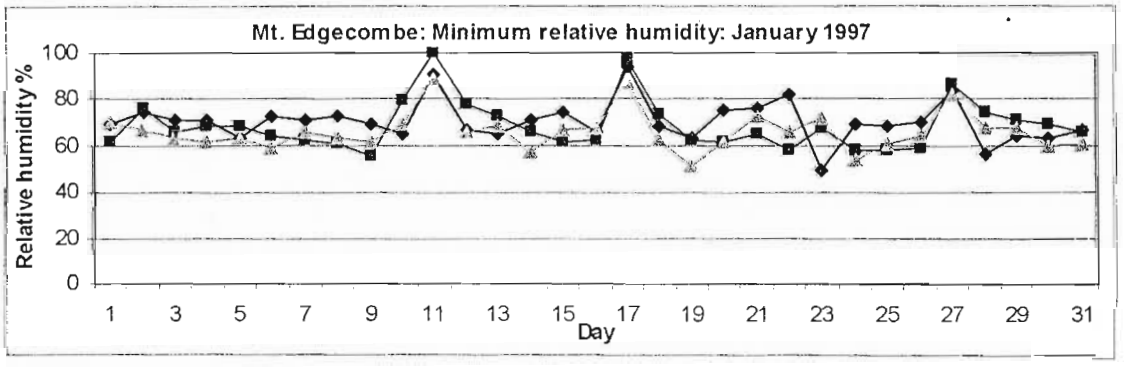

App 2.6 Comparison between January observed daily minimum RH (—◆—) and daily minimum RH estimated using the vapour pressure model (—■—) and Bristow's (1992) model (—▲—) at Mt. Edgecombe, KwaZulu-Natal

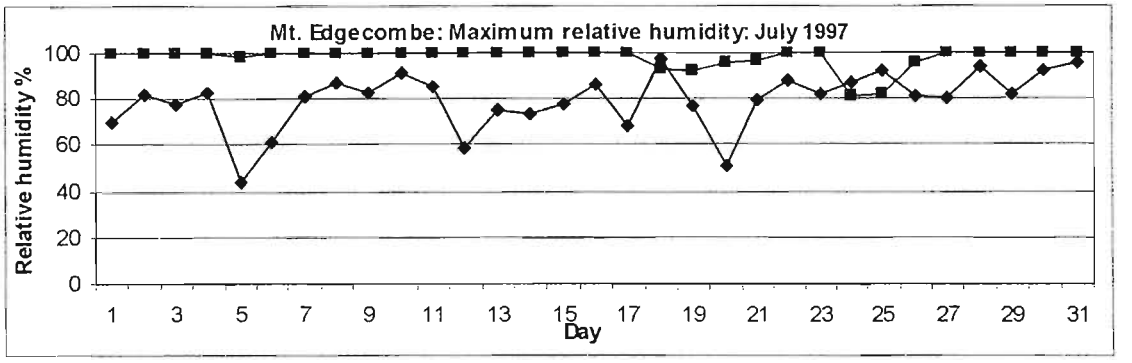

App 2.7 Comparison between July observed daily maximum RH (—♦—) and daily minimum RH estimated using the vapour pressure model (—■—) and Bristow's (1992) model (—▲—) at Mt. Edgecombe, KwaZulu-Natal

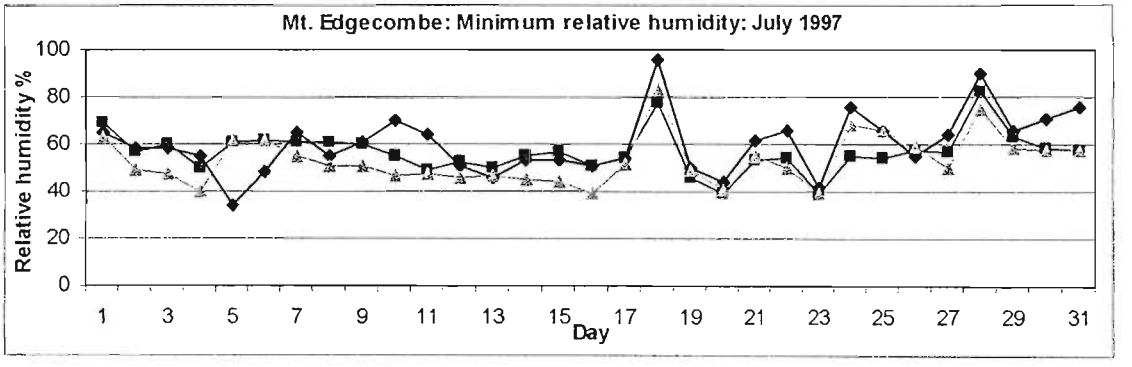

App 2.8 Comparison between July observed daily minimum RH (—♦—) and daily minimum RH estimated using the vapour pressure model (—■—) and Bristow's (1992) model (—▲—) at Mt. Edgecombe, KwaZulu-Natal

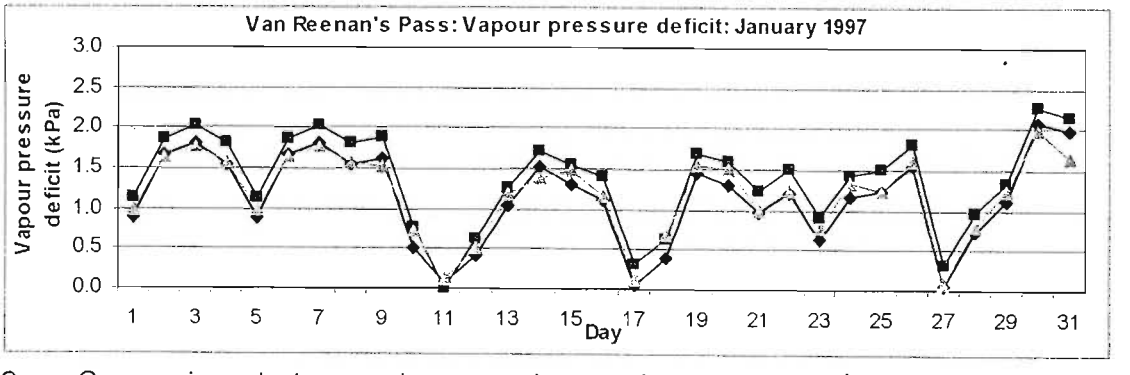

App 2.9 Comparison between January observed daily VPD (—♦—) with daily VPD estimated using the monthly vapour pressure models (—■—) and Bristow's (1992) model (—▲—) at Van Reenen's Pass, Free State province

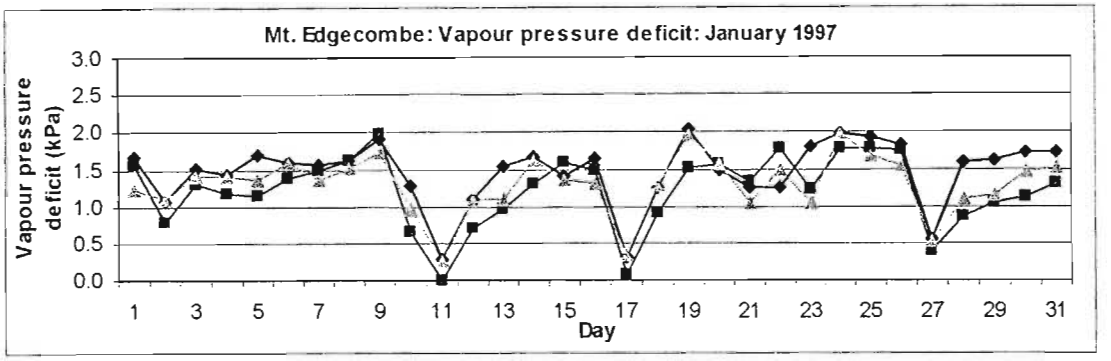

App 2.10 Comparison between January observed daily VPD (—♦—) with daily VPD estimated using the monthly vapour pressure models (—■—) and Bristow's (1992) model (—▲—) at Mt. Edgecombe in KwaZulu-Natal

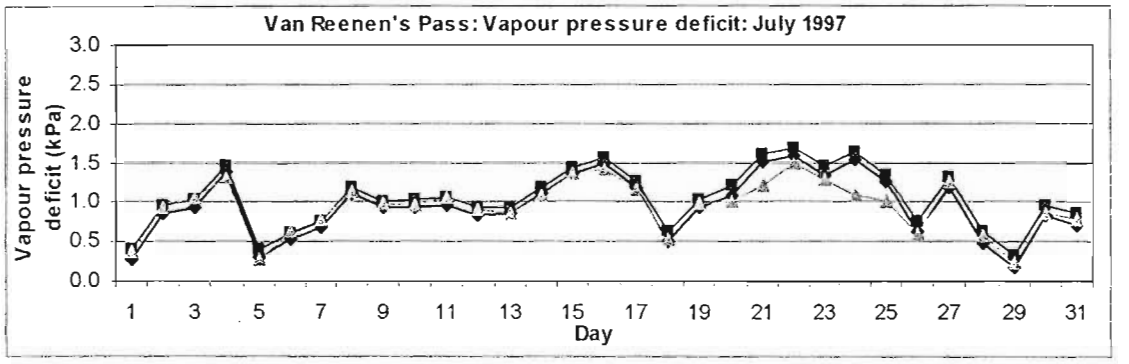

App 2.11 Comparison between July observed daily VPD (—♦—) with daily VPD estimated using the monthly vapour pressure models (—■—) and Bristow's (1992) model (—▲—) at Van Reenen's Pass, Free State province

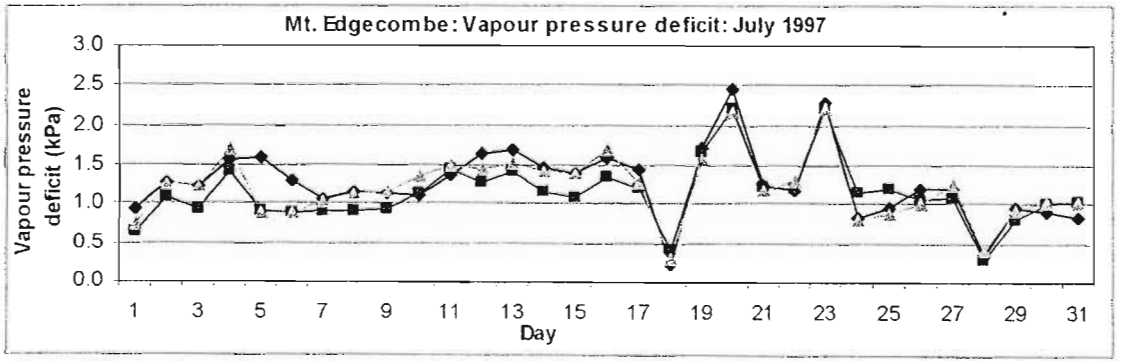

App 2.12 Comparison between July observed daily VPD (—♦—) with daily VPD estimated using the monthly vapour pressure models (—■—) and Bristow's (1992) model (—▲—) at Mt. Edgecombe, KwaZulu-Natal.